UNIVERSITEIT VAN PRETORIA
UNIVERSITY OF PRETORIA
YUNIBESITHI YA PRETORIA

SCALABLE DUAL FLUIDISED BED SYSTEM FOR FAST PYROLYSIS OF WOODY BIOMASS

by

A.B.L. Grobler

Dissertation submitted in partial fulfilment of the requirements for the degree

Master in Chemical Engineering

in the Department of Chemical Engineering

Faculty of Engineering, Built Environment and Information Technology

University of Pretoria

Pretoria

South Africa

September 2014

Supervisor: Professor M.D. Heydenrych

CVD800

DECLARATION

I declare that this dissertation is my own unaided work. It is being submitted for the Degree of Master in Engineering at the University of Pretoria. It has not been submitted before for any degree or examination to any other university.

(Signature of Candidate)

On this 5TH day of September year 2014

SCALABLE DUAL FLUIDISED BED SYSTEM FOR FAST PYROLYSIS OF WOODY BIOMASS

ABSTRACT

Pyrolysis of biomass is the thermochemical conversion process whereby the long lignocellulosic polymers in biomass are cracked into several higher-value products such as bio-oil, bio-char and combustible non-condensable gases (NCG). Fast pyrolysis in particular is aimed at maximising the yield of crude liquid bio-oil, with the production of bio-char and NCG as co-products. Since a large quantity of under-utilised biomass is produced in the forestry sector annually, as by-product from harvesting, this sector has shown particular interest in this process. Furthermore, the continuing drive for renewable and sustainable energy production, particularly of drop-in liquid biofuels, has urged the development of such technology on a commercial scale. The main purpose of this investigation was to evaluate the technical feasibility and performance of the scalable dual fluidised bed (DFB) reactor system designed and constructed at the University of Pretoria by Swart in 2012. The sub-objectives of this study were as follows:

- Biomass pre-treatment equipment was implemented to ensure that the physical characteristics of the biomass feedstock meet the pyrolysis process requirements.
- The scalable DFB reactor system, including all sub-systems and ancillary equipment, was commissioned to ensure satisfactory operation of the complete system.
- Continuous, steady-state experimental runs were conducted to produce fast pyrolysis products in the scalable DFB reactor system.
- The fast pyrolysis products were quantified and characterised to evaluate the technical feasibility of the DFB reactor system.
- A material and energy balance was conducted over the pyrolysis fluidised bed (PFB) reactor to quantify its performance.

Eucalyptus grandis raw material, as received from Sappi Southern Africa's Ngodwana mill, was successfully converted to bio-oil, bio-char and NCG in the scalable DFB reactor system. Fast pyrolysis was conducted at a pyrolysis temperature of 500 °C, a vapour residence time of 4 s and a sawdust feed rate of 2.0 kg/h. The PFB reactor temperature could be controlled easily, at the desired setpoint (500 °C), by continuously circulating hot solids between the two bubbling fluidised beds. The excellent temperature control of the PFB reactor makes the DFB system a suitable reactor system for the fast pyrolysis of biomass on a commercial scale.

At these PFB reactor conditions the yield of fast pyrolysis products, on a dry feedstock basis, was determined as 36.3, 14.0 and 49.7 weight % for bio-oil, NCG and bio-char respectively. High-value process heat, in the form of hot flue gas (450–500 °C), was produced in the combustion fluidised bed

(CFB) reactor as co-product from the DFB reactor system. Therefore, it can be concluded that the conversion of lignocellulosic biomass, through the process of fast pyrolysis, is technically feasible in the scalable DFB reactor system.

Although the crude liquid bio-oil contained highly oxygenated compounds (including organic acids, water, alcohols, esters, sugars, aldehydes, ketones, furans, pyrans and phenolics) it may be utilised for heat generation when co-fired with conventional fossil fuels, including heavy furnace oil. However, the scalable DFB reactor system allows for integrated catalytic fast pyrolysis, which would enable catalytic cracking of the biomass feedstock, and the subsequent pyrolysis vapours, to selectively produce deoxygenated bio-oil compounds, compatible with conventional refinery streams.

The DFB reactor system allowed easy separation of bio-char from the pyrolysis vapours by means of the bio-char cyclone. The bio-char had a high heating value of only 17.0 MJ/kg because of an unexpectedly high inorganic content of 54.4 weight % on a dry basis. However, 77.0 weight % of the inorganics were identified as entrained silica sand fines. Notwithstanding the entrained silica fines, the bio-char carbon content was determined as approximately 55 weight % on a dry basis, which would result in a high heating value of approximately 29 MJ/kg. Combustible NCG (including carbon monoxide, methane, ethane, ethylene, acetylene and propene) were produced as co-product from the fast pyrolysis of *E. grandis* sawdust in the DFB reactor system. The high heating value of the NCG was estimated at 7.3 MJ/kg or 8.3 MJ/Nm^3. Furthermore, it was demonstrated that both the solid bio-char residue and NCG could be combusted in the CFB reactor to supplement its energy demand.

At the sawdust feed rate of 2 000 g/h and silica sand circulation rate of 50 kg/h, the production rate of pyrolysis products was estimated at 687.8, 265.2 and 940.0 g/h for bio-oil, NCG and bio-char respectively. However, only 13.0 g/h of bio-char was collected from the bio-char cyclone, with the balance (i.e. 927.0 g/h) understood to have been transferred to the CFB with the silica sand heat carrier. The recycle rate of the NCG was determined as 7 689.7 g/h. The total energy input from the feedstock and recycled NCG was determined as 150 W, while the energy supplied to the PFB by means of the hot silica sand was determined as 3 889 W. The pyrolysis reaction energy demand, at the feed rate of 2 000 g/h, was determined as 1 000 W. The pyrolysis reactor freeboard temperature was found to be much lower than the fluidised bed temperature (± 195 °C vs. ± 500 °C) as a result of heat loss. Therefore, the energy output from the pyrolysis products was determined as only 344 W. The overall heat loss from the PFB reactor was estimated at a very high 2 696 W, which implies that approximately 69% of the total energy supplied to this reactor by means of the hot silica sand was dissipated to the surrounding atmosphere. From a heat loss evaluation, it was concluded that the biomass throughput could be increased by as much as five to ten times by mitigating the heat loss.

Several process inefficiencies and limitations were identified during the commissioning and operation of the DFB reactor system, which compromised the overall performance. In order to mitigate or eliminate these inefficiencies and limitations, the following future work is recommended:

- Installation of adequate insulation material on the PFB and CFB reactors, the bio-oil container, quencher and demister.
- Redesigning the bio-oil recovery and collection system to reduce the pressure drop in the NCG recirculation loop, thereby increasing the superficial gas velocity of the PFB reactor and subsequently reducing the vapour residence time to < 3 s.
- Investigation of the performance of the scalable DFB reactor system at a higher biomass sawdust throughput.
- Investigation and implementation of heat integration synergies, especially the use of hot flue gases generated in the CFB reactor, to dry and/or pre-heat the biomass feedstock, pre-heat the combustion air or pre-heat the recycled NCG used to fluidise the PFB reactor.
- Installation and commissioning of an electrostatic precipitator for recovery of entrained pyrolysis condensables from the bio-oil recovery and collection system, and subsequent clean-up of the NCG.
- Utilisation of an alternative solvent for bio-oil recovery and collection during process operation as the ethylene glycol utilised in this investigation interfered with the characterisation of the liquid bio-oil.
- Investigation of integrated catalytic fast pyrolysis in the scalable DFB reactor system by replacing the silica sand fluidised bed material with a viable solid catalyst as heat carrier.
- Investigation of the pyrolysis of alternative biomass feedstocks, available within South Africa, in the DFB reactor system, including forestry slash, sawmill residue, bark, municipal waste and sugarcane bagasse.
- A commercial-scale DFB reactor system should be designed to evaluate its technical feasibility and economic viability.

ACKNOWLEDGEMENTS

The author would like to acknowledge Sappi Limited and the Paper Manufacturers Association of South Africa (PAMSA) for providing the financial support for this research project. A special word of thanks is extended to my project supervisor, Professor Mike Heydenrych, for his guidance and support throughout the project. Thank you to all the industrial mentors – Stephen Brent, Mike Nash, Dr Sanet Minnaar, Dr Charlie Clarke, Dr Akwesi Boateng and Neil Goldberg – for sharing their valuable knowledge and experience.

Thank you to Umit Postma, Ryan Merckel, Berdine Coetzee, L'Zanne Jansen van Rensburg, Gerard Puts and Dr Heinrich Badenhorst for their unceasing assistance with the laboratory analyses necessary for the research project. I would also like to extend a word of thanks to all my family, friends and colleagues for their continuing support and encouragement throughout the entire duration of my studies. Finally, I would like to praise my heavenly Father for giving me the strength, knowledge and understanding, and directing me every step of the way.

CONTENTS

		Page
ABSTRACT		i
ACKNOWLEDGEMENTS		iv
LIST OF FIGURES		v
LIST OF TABLES		vii
LIST OF ABBREVIATIONS		viii
1	INTRODUCTION	1-1
1.1	Background	1-1
1.2	Problem and Objective Statement	1-2
1.3	Methodology	1-2
1.4	Scope	1-3
1.5	Importance of the Research	1-3
2	LITERATURE REVIEW	2-1
2.1	Biomass	2-1
2.1.1	Overview	2-1
2.1.2	Availability	2-1
2.1.3	Biomass Preparation	2-1
2.2	Thermochemical Conversion of Biomass	2-2
2.2.1	Overview	2-2
2.2.2	Pyrolysis	2-3
2.2.3	Fast Pyrolysis Requirements	2-4
2.2.4	Fast Pyrolysis Reactor Configurations	2-5
2.3	Fast Pyrolysis Products and Applications	2-6
2.3.1	Bio-oil	2-6
2.3.2	Bio-char	2-8
2.3.3	Non-condensable Gases	2-10
2.4	Fast Pyrolysis Performance-dependent Parameters	2-12
2.4.1	Reactor Temperature	2-12
2.4.2	Vapour Residence Time	2-13

2.4.3 Biomass Particle Size and Heating Rate 2-13
2.5 Conclusions 2-14
3 DUAL FLUIDISED BED REACTOR SYSTEM 3-1
3.1 Introduction 3-1
3.2 Process Overview 3-1
3.3 Combustion Reactor 3-3
3.4 Biomass Feed System 3-4
3.5 Pyrolysis Reactor 3-5
3.6 Bio-oil Recovery and Collection System 3-6
3.7 Distributed Control System 3-7
4 PROCESS OPERATION AND CHARACTERISATION 4-1
4.1 Introduction 4-1
4.2 Feedstock Handling 4-1
4.2.1 Biomass Drying 4-2
4.2.2 Biomass Grinding and Screening 4-3
4.2.3 Biomass Feed System 4-5
4.2.4 Biomass Characterisation 4-5
4.3 Combustion Fluidised Bed Reactor 4-7
4.3.1 Preparation and Start-up 4-7
4.3.2 Process Operation 4-9
4.4 Pyrolysis Fluidised Bed Reactor 4-12
4.4.1 Commissioning 4-12
4.4.2 Process Start-up and Operation 4-14
4.5 Bio-oil Recovery and Collection System 4-20
4.6 Pyrolysis Material and Energy Balance 4-24
5 RESULTS AND DISCUSSION 5-1
5.1 Introduction 5-1
5.2 Pyrolysis Product Distribution 5-1
5.3 Pyrolysis Material and Energy Balance 5-3
5.3.1 Material Balance Results 5-3
5.3.2 Energy Balance Results 5-5

5.3.3 Heat Loss Evaluation 5-5
5.4 Pyrolysis Product Characterisation 5-9
5.4.1 Bio-oil 5-9
5.4.2 Bio-char 5-12
5.4.3 Non-condensable Gases 5-14
5.5 Summary of Pyrolysis Experimental Runs 5-16
6 CONCLUSIONS AND RECOMMENDATIONS 6-1
6.1 Biomass Feedstock Handling 6-1
6.2 Process Commissioning 6-1
6.3 Process Operation and Performance 6-4
6.4 Fast Pyrolysis Product Characterisation 6-5
6.5 Recommendations for Future Work 6-7
REFERENCES x
APPENDIX A PIPING AND INSTRUMENTATION DIAGRAM xiv
APPENDIX B DISTRIBUTED CONTROL SYSTEM xv

LIST OF FIGURES

Figure 2.1: Two-stage biomass pyrolysis model 2-4

Figure 2.2: Typical bubbling fluidised bed pyrolysis reactor (Sadaka & Boateng, 2009) 2-5

Figure 2.3: Crude pyrolysis oil 2-6

Figure 2.4: Illustration of bio-char as co-product from fast pyrolysis 2-9

Figure 2.5: Bio-char as a carbon-sequestering and GHG-mitigating agent (Postma, 2012) 2-9

Figure 2.6: Utilisation of NCG for supplying process heat to the endothermic pyrolysis process 2-10

Figure 2.7: Summary of applications for fast pyrolysis products (Crocker, 2010: 174) 2-11

Figure 2.8: Variation in fast pyrolysis product yield with reactor temperature (Boateng, 2011) 2-12

Figure 2.9: Variation in fast pyrolysis product yield with particle size (Shen et al., 2009) 2-13

Figure 3.1: Process flow diagram of dual fluidised bed reactor system 3-2

Figure 3.2: Combustion fluidised bed reactor 3-4

Figure 3.3: Pneumatic biomass feed system 3-5

Figure 3.4: Pyrolysis fluidised bed reactor 3-5

Figure 3.5: Bio-oil recovery and collection system 3-7

Figure 4.1: Biomass pre-treatment process 4-1

Figure 4.2: Biomass feedstock as received 4-2

Figure 4.3: Air/sun drying of biomass woodchips 4-2

Figure 4.4: Influence of air/sun drying of biomass woodchips 4-3

Figure 4.5: Eccentric motor-driven sieve, fitted with 2 mm mesh screen 4-4

Figure 4.6: Retch SM100 cutting mill, fitted with 2 mm mesh screen 4-4

Figure 4.7: Vibrating tertiary screen 4-4

Figure 4.8: Calibration of biomass feed screw conveyor 4-5

Figure 4.9: Calibration of sand transfer screw conveyor 4-8

Figure 4.10: Combustion unit during start-up conditions 4-8

Figure 4.11: Combustion unit during fluidisation conditions 4-9

Figure 4.12: CFB reactor temperatures from a typical steady-state experimental run 4-10

Figure 4.13: CFB reactor operating parameters from a typical steady-state experimental run 4-11

Figure 4.14: Automatic control of PFB temperature 4-13

Figure 4.15: Pyrolysis unit during start-up conditions 4-15

Figure 4.16: PFB reactor temperatures from a typical experimental run 4-16

Figure 4.17: PFB reactor operating parameters from a typical steady-state experimental run 4-17

Figure 4.18: Combustion of bio-char particles in the CFB 4-18

Figure 4.19: Bio-char samples collected from the bio-char cyclone 4-18

Figure 4.20: NCG collected in FlexiFoil® sample bags 4-19

Figure 4.21: Brownish-yellow pyrolysis vapour entering the bio-oil quencher (RHS) 4-21

Figure 4.22: Bio-oil/ethylene glycol mixture from hydrocyclone 4-21

Figure 4.23: Bio-oil/ethylene glycol mixture in bio-oil container 4-21

Figure 4.24: Spent NCG cartridge filter element 4-22

Figure 4.25: Bio-oil quencher operation from a typical experimental run 4-23

Figure 4.26: Bio-oil cooler operation from a typical experimental run 4-23

Figure 4.27: System boundary for pyrolysis reactor material and energy balance 4-25

Figure 5.1: Pyrolysis reactor heat transfer resistance network 5-6

Figure 5.2: Pyrolysis reactor surface temperature profile 5-6

Figure 5.3: Combustion reactor heat transfer resistance network 5-7

Figure 5.4: Combustion reactor surface temperature profile 5-7

Figure 5.5: Vapour entraining from liquid recovery system (LHS) 5-15

LIST OF TABLES

Table 2.1: Estimation of biomass availability in South Africa (Postma, 2012) 2-2

Table 2.2: Product yields and applications from the thermochemical conversion of biomass (Bridgwater, 2012) 2-3

Table 2.3: Typical properties of crude pyrolysis liquids (Sadaka & Boateng, 2009) 2-8

Table 3.1: List of equipment in the dual fluidised bed reactor system 3-3

Table 3.2: Feedback controller variables for the pyrolysis process control system 3-8

Table 3.3: Measuring instruments used in the scalable pyrolysis system 3-9

Table 4.1: TGA method for the proximate analysis of biomass 4-6

Table 4.2: Proximate and ultimate composition of *E. grandis* raw material 4-6

Table 4.3: Lignocellulosic composition and physical properties of *E. grandis* raw material 4-7

Table 4.4: Combustion fluidised bed operating parameters 4-9

Table 4.5: Silica sand entrainment from the DFB reactor system 4-11

Table 4.6: Results from commissioning of PFB reactor 4-13

Table 4.7: Pyrolysis fluidised bed operating parameters 4-16

Table 4.8: GC-MS method for characterisation of NCG 4-19

Table 4.9: GC column specifications for characterisation of NCG 4-19

Table 4.10: Operating parameters of the bio-oil recovery system 4-22

Table 4.11: GC-MS method for identification of bio-oil constituents 4-24

Table 5.1: Fast pyrolysis product yields 5-2

Table 5.2: Material balance over fast pyrolysis reactor 5-4

Table 5.3: Energy balance over fast pyrolysis reactor 5-5

Table 5.4: Comparison of actual vs. predicted pyrolysis unit heat loss and biomass throughput 5-8

Table 5.5: Identification of *E. grandis* bio-oil components by GC-MS analysis 5-10

Table 5.6: Properties and composition of bio-char co-product 5-13

Table 5.7: Properties and composition of NCG co-product 5-15

Table 5.8: Operating parameters, and material and energy balance of fast pyrolysis runs 5-17

LIST OF ABBREVIATIONS

CFB	combustion fluidised bed
d.b.	dry basis
DCS	distributed control system
DFB	dual fluidised bed
GC	gas chromatograph/chromatography
GHG	greenhouse gas
HHV	high heating value
LPG	liquefied petroleum gas
MS	mass spectrometer/spectrometry
NCG	non-condensable gases
PFB	pyrolysis fluidised bed
P&ID	piping and instrumentation diagram
SGV	superficial gas velocity
TGA	thermogravimetric analyser/analysis
VFD	variable frequency drive
VRT	vapour residence time

1 INTRODUCTION

1.1 Background

The continuing drive for renewable liquid transportation fuels derives from various factors. Firstly, there are the growing environmental concerns about greenhouse gas (GHG) emissions from fossil-based fuels, and secondly about the long-term availability of these resources (Crocker, 2010: 1). The ever-increasing demand for liquid fuels, combined with volatile price increases, strict legislation on GHG mitigation and decreasing supply, has evoked rapid growth within the biofuels industry (Crocker, 2010: 2). Biomass, as a renewable source of energy, can be utilised for the production of renewable liquid fuels. As a raw material, biomass can be produced sustainably and it is a near-universal feedstock. Therefore, biomass is considered the renewable energy source with the highest potential to contribute to the global energy demand (Crocker, 2010: 146).

Various thermal, mechanical and biological technologies have been identified for the conversion of biomass into renewable energy-dense products, each with its own advantages and disadvantages. According to Crocker (2010: 149), thermal conversion technologies are expected to offer the greatest contribution to the global energy solution in the short term. This is due to their flexibility, improved efficiency, environmental acceptance and also the possibility of integration into existing biomass processing facilities in the pulp, paper and forestry sector (Crocker, 2010: 149). Pyrolysis of biomass is the thermochemical conversion of lignocellulosic material, in the absence of oxygen, to produce several higher-value products such as crude liquid bio-oil, solid bio-char and combustible producer gas (Bridgwater, 2012). Pyrolysis of biomass is a versatile process because these three products may be produced in varying proportions depending on the process conditions. Also, pyrolysis is a rather robust process due to its capability of processing various feedstocks. The crude liquid bio-oil has application in both the energy and chemicals industries, but most research is focused on upgrading the bio-oil to renewable drop-in liquid biofuels (Demirbas, 2006).

This research project was conducted at the University of Pretoria, South Africa, in collaboration with Sappi, the Paper Manufacturers Association of South Africa (PAMSA), and the Department of Agriculture in the United States. This investigation follows from a previous study which dealt with the design, modelling and construction of a scalable dual fluidised bed (DFB) reactor system for the pyrolysis of woody biomass (Swart, 2012). In 2009–2010 a cold-flow concept unit of the dual fluidised bed system was built and tested at the Agricultural Research Service in Wyndmoor, Pennsylvania, US. It was concluded that the novel, scalable solids transport mechanism employed in the dual fluidised bed design is suitable for the biomass pyrolysis process. In 2011–2012, a scalable dual fluidised bed pyrolysis system was constructed at the University of Pretoria, South Africa.

1.2 Problem and Objective Statement

A large quantity of underutilised lignocellulosic biomass is produced annually as by-product from forestry, sawmills, pulp and paper mills, municipal waste and agricultural operations in South Africa (Brent, 2011). These underutilised biomass resources are readily available as feedstock for pyrolysis to produce higher-value products. This initiated the design, modelling and construction of a scalable DFB reactor system, as conducted by Swart (2012), to facilitate the conversion of lignocellulosic biomass by the process of pyrolysis. Although the scalable DFB reactor system had been designed and constructed, little attention had been given to the commissioning, operation and performance of the system.

The main purpose of this investigation was to evaluate the technical feasibility and performance of the scalable DFB reactor system designed and constructed at the University of Pretoria. In order to realise the main purpose of this study, several sub-objectives were considered, as follows:

- Biomass raw material handling equipment must be implemented to ensure that the physical characteristics (i.e. moisture and particle size) of the biomass feedstock meet the pyrolysis process requirements.
- The scalable DFB reactor system, including all sub-systems and ancillary equipment, must be commissioned to ensure satisfactory operation of the complete system.
- Continuous, steady-state experimental runs must be conducted to produce fast pyrolysis products in the scalable DFB reactor system.
- The fast pyrolysis products must be quantified and characterised in order to evaluate the technical feasibility of the DFB reactor system.
- A material and energy balance must be conducted over the pyrolysis fluidised bed reactor in order to quantify its performance.

1.3 Methodology

This research project continued from a previous study which dealt with the design, modelling and construction of a scalable DFB reactor system for the pyrolysis of woody biomass (Swart, 2012). The current research project was divided into several phases, as outlined below, in order to achieve the objectives of this investigation.

1. A thorough study was conducted of the process design and model, as well as the design and construction considerations, in order to understand the operability of the complete system.
2. A literature study of the important operating parameters and process conditions was conducted in order to understand the effects of these parameters on the pyrolysis system performance.
3. All necessary ancillary equipment and instruments were installed to assist with process preparation, start-up, operation and shutdown.

4. A complete distributed control system (DCS) was developed in order to operate, monitor and control the pyrolysis process safely and effectively.
5. Equipment for handling the raw biomass material was evaluated to ensure that the physical characteristics (i.e. moisture and particle size) of the biomass feedstock meet the pyrolysis process requirements.
6. A process start-up, operation and shutdown procedure was developed to enable safe and effective operation of the DFB reactor system.
7. All main unit operations and sub-systems of the DFB reactor system were commissioned to enable operation of the complete pyrolysis system. Since only cold commissioning of the novel solids transport mechanism employed in the DFB reactor system was conducted by Swart (2012), hot commissioning was conducted to ensure feasible operation.
8. Continuous, steady-state experimental runs of the complete DFB reactor system were conducted to convert the lignocellulosic biomass feedstock into pyrolysis products.
9. A total material and energy balance over the pyrolysis reactor was conducted, based on the process operating information, in order to quantify the performance.
10. All process and operational inefficiencies and/or limitations suspected of influencing the performance of the DFB reactor system were identified as reasonably as possible.
11. Analysis and characterisation of the pyrolysis products and biomass feedstock were also conducted.

1.4 Scope

This investigation follows from a previous study which dealt with the design, modelling and construction of a scalable DFB reactor system for the fast pyrolysis of woody biomass (Swart, 2012). The scope of this research included commissioning of the DFB reactor system, production and characterisation of fast pyrolysis products and quantification of pyrolysis performance by conducting a material and energy balance over the pyrolysis fluidised bed reactor.

1.5 Importance of the Research

The growing concern about the environmental impact of fossil-fuel-based energy, as well as its sustainability, has provoked most countries to pursue alternative, renewable and sustainable energy sources (Zhang, Xu & Champagne, 2010). Pyrolysis of biomass has been identified as a versatile and feasible conversion technology for the sustainable production of energy and high-value chemicals from a renewable resource (Demirbas, 2006).

The South African forestry sector and the pulp and paper industry have shown particular interest in pyrolysis technology since a large quantity of under-utilised biomass is produced annually as a by-product from their operations (Brent, 2011). Converting this biomass into energy-dense products, for energy production, would provide them with the opportunity to enter the rapidly growing biofuels

market and to broaden their focus beyond traditional wood products. The pyrolysis of biomass offers several other advantages:

- It would add value to an under-utilised material stream that many industries regard as waste.
- There would be a decreased environmental impact and carbon footprint through the utilisation of alternative and renewable resources.
- The use of biomass-derived fuels may significantly reduce the world's dependence on fossil-based fuels.
- The crude bio-oil from pyrolysis can be upgraded to drop-in liquid transportation fuels and also refined to speciality chemicals of high commercial value.
- The bio-char can be used as a solid fuel, or for soil amendment and nutrient replacement when fed back to the plantation floors in the forestry sector.
- The process is considered carbon-negative when the carbon-rich bio-char is fed back to the forestry floors, thereby capturing and removing carbon from the atmosphere.
- The process would result in the production of high-value heat in the form of hot flue-gas as well as valuable producer gas as co-product.

A novel, scalable DFB pyrolysis system was designed and constructed in an attempt to demonstrate that these advantages could be realised on a commercial scale (Swart, 2012). Furthermore, according to Postma (2012), the development of such technology on a commercial scale has the potential to contribute significantly to South Africa's energy demands. This research project aims to evaluate the technical feasibility and performance of the scalable DFB reactor system developed at the University of Pretoria for the pyrolysis of lignocellulosic biomass.

2 LITERATURE REVIEW

2.1 Biomass

2.1.1 Overview

Biomass is biologically produced material derived from living, or recently living, organisms that consists mainly of carbon, hydrogen and oxygen (Fengel & Wegener, 2003: 26). Woody biomass, obtained from woody plants, is one of the largest biomass energy sources used to produce second-generation biofuels (Meincken, 2011). It consists mainly of lignocellulosic biomass which is not edible and therefore does not pose a threat to food security as is the case with crops used for first-generation biofuels (e.g. sugarcane and maize). The term *lignocellulose* refers to biomass composed of cellulose, hemicellulose and lignin (Meincken, 2011) as macromolecular components and other substances with low molecular weight such as extractives and ash (Fengel & Wegener, 2003: 26). The proportions and chemical composition of these components vary among different hardwood and softwood species and ultimately influence the characteristics of the products produced from these raw materials (Fengel & Wegener, 2003: 26).

2.1.2 Availability

A large quantity of under-utilised lignocellulosic biomass is produced annually as a by-product from forestry, sawmills, pulp and paper mills, municipal waste and agricultural operations in South Africa (Brent, 2011). Under-utilised lignocellulosic biomass is considered a low-value waste for many of these and other industries. These by-products – slash, cuttings, sawdust, branches, bark and leaves – can be converted into different forms of energy using different conversion technologies (Faaij, 2006). There is therefore a strong drive in South Africa to convert this under-utilised commodity into valuable products (Meincken, 2011). Table 2.1 shows the estimated availability of these under-utilised resources in South Africa. Forestry residues and corn stover contribute the largest fraction in the forestry and pulp, and agricultural sectors respectively. Table 2.1 highlights the potential for converting these renewable and sustainable resources into various bioenergy products.

2.1.3 Biomass Preparation

The lignocellulosic biomass, available in various forms, shapes and sizes, may have to undergo pre-treatment in order to be processed into useful products (Meincken, 2011). The extent of pre-treatment depends not only on the nature of the feedstock, but also on the type of conversion technology employed. The most common biomass pre-treatments include chipping, milling (fine grinding), screening, pelletising and drying, all of which are energy-intensive and costly processes. However, the efficiency of these conversion technologies may be increased significantly through the application of the correct biomass pre-treatment steps or a combination thereof (Meincken, 2011).

Table 2.1: Estimation of biomass availability in South Africa (Postma, 2012)

Biomass type	Mt/year
Forestry logging residues	6.7
Sawmill operations	2.1
Pulp industry	1.0
Total (Forestry & Pulp)	**9.8**
Corn stover	10.7
Wheat straw	2.0
Sunflower stalks	0.6
Sugarcane bagasse	5.5
Total (Agricultural)[a]	**18.8**

[a] Based on 5 years of data from the Department of Agriculture, Forestry & Fisheries, South Africa

2.2 Thermochemical Conversion of Biomass

2.2.1 Overview

Thermochemical conversion processes are used to convert biomass into energy-dense products of high commercial value (Bridgwater, 2012). The nature of the biomass feedstock (moisture, particle size and composition) plays an integral part in selecting the appropriate conversion technology. However, in most cases these biomass properties can be altered, to suit a particular conversion process, via biomass pre-treatment. The four major thermochemical processes for converting biomass are combustion, torrefecation, pyrolysis and gasification (Brent, 2011). These thermochemical processes are temperature dependent and lead to the formation of four important products, namely heat, bio-char, bio-oil and synthesis gas (syngas).

The combustion of biomass is an exothermic process, which requires the presence of oxygen to produce heat. Torrefecation, pyrolysis and gasification are endothermic processes which all produce bio-oil, bio-char and syngas, but in varying proportions. These endothermic processes require either an oxygen-free or an oxygen-limited environment in order to be sustained. The operating temperature and product yields of the three endothermic processes differentiate them from one another. Table 2.2 shows the typical operating temperature, product yields and applications of the four major thermochemical processes for converting biomass (Brent, 2011).

2.2.2 Pyrolysis

Pyrolysis of biomass is the thermochemical conversion of lignocellulosic material, in the absence of oxygen, into a solid bio-char and pyrolysis vapour (Demirbas, 2006). The pyrolysis vapour is quenched to remove the condensable fraction known as crude bio-oil or pyrolysis oil. The non-condensable fraction is known as pyrolysis gases, producer gas, syngas or simply NCG. Pyrolysis is an endothermic process which requires elevated temperatures to crack the long lignocellulosic polymers present in the biomass.

Table 2.2: Product yields and applications from the thermochemical conversion of biomass (Bridgwater, 2012)

Conversion process	Temperature	Main products (wt % d.b.)	Applications
Torrefecation	200–320 °C	Bio-char (80%) Syngas (20%)	Boiler fuel & charcoal
Pyrolysis	400–600 °C	Bio-oil (30 – 75%) Bio-char (12 – 35%) Syngas (13 – 35%)	Production of high-value fuels & chemicals
Gasification	750–900 °C	Syngas (85%) Bio-char (10%) Bio-oil (5%)	Fuel gas & liquid hydrocarbons (Fischer-Tropsch)
Combustion	> 900 °C	Heat	Steam & electricity

The pyrolysis of biomass is typically modelled by a two-stage pyrolysis model, which is presented in Figure 2.1 (Papadikis, Gu & Bridgwater, 2009). The two-stage model suggests that woody biomass is converted into three products, namely char, tar and gas (primary reaction). The model also accounts for moisture in the woody biomass to be converted into water vapour, which affects the energy requirement of the pyrolysis reactor. The char product from the primary reaction is a solid residue known as bio-char. The tar and gas products from the primary reaction include the condensable and non-condensable compounds, referring to bio-oil and producer gas respectively. The objective of fast pyrolysis is to minimise the vapour residence time in order to suppress further decomposition of tar into char and gas (secondary reaction), thereby maximising the liquid product yield.

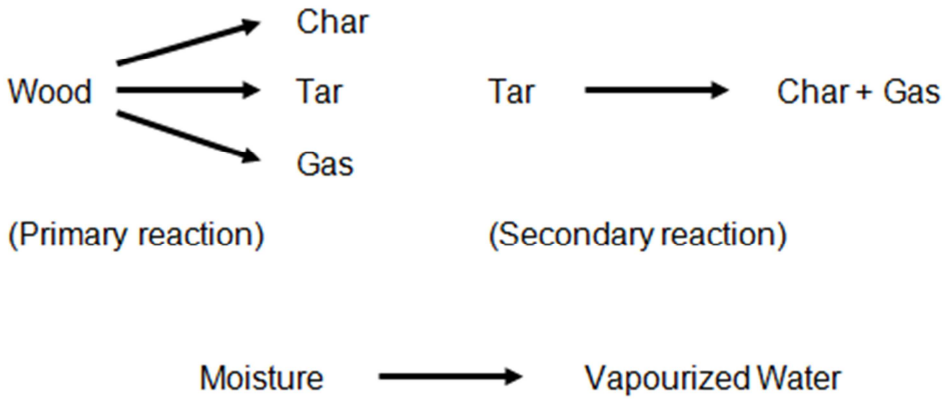

Figure 2.1: Two-stage biomass pyrolysis model

2.2.3 Fast Pyrolysis Requirements

Fast pyrolysis in particular is aimed at maximising the crude liquid bio-oil yield, as the main product, while inhibiting the formation of bio-char and producer gas as co-products. Currently, the main focus of pyrolysis research is on fast pyrolysis for liquid production because the liquid may be used for energy, chemicals or as an energy carrier (Crocker, 2010: 149). Also, the liquid bio-oil product is more convenient to store and transport compared with the bulky biomass from which it is derived. In order to maximise the production of liquid bio-oil during fast pyrolysis, the following process parameters must be adhered to (Bridgwater, 2012):

1. A carefully controlled pyrolysis reactor temperature in excess of 450 °C as well as a vapour phase temperature of around 350–400 °C – it is evident from Table 2.2 that a lower reaction temperature favours bio-char formation
2. Very high biomass particle heating rates at the reaction interface – this is normally the rate-limiting step in the fast pyrolysis reaction and necessitates fine grinding of the biomass feedstock to a particle size less of than 2–3 mm
3. A short pyrolysis vapour residence time (VRT) of typically less than 2–3 seconds – this is of paramount importance to prevent secondary reactions of tars into bio-char and gases of lower molecular weight as demonstrated in Figure 2.1
4. Rapid removal of solid bio-char and ash from the hot pyrolysis vapours – it has been found that both bio-char and ash have a catalytic effect on pyrolysis vapour cracking to gases with low molecular weight (Crocker, 2010: 151)
5. Drying of the biomass feedstock, typically to a moisture content of less than 10%, in order to minimise the water in the liquid bio-oil product
6. Rapid cooling/quenching of pyrolysis vapours to generate the crude liquid bio-oil product

2.2.4 Fast Pyrolysis Reactor Configurations

Most research and development (R&D) on fast pyrolysis technology has focused on the reactor configuration, which is the heart of the process (Crocker, 2010: 151). Numerous fast pyrolysis reactor configurations have been studied and developed over the years, each with its own advantages and limitations. Bridgwater (2012) has compiled a comprehensive list of fast pyrolysis reactors which introduces and explains the various configurations. Some of the more typical designs are as follows: bubbling fluidised beds, circulating and transported fluidised beds, rotating cones and ablative reactors (Bridgwater, 2012). Other, less common, reaction systems are the following types: entrained flow, vacuum, screw and auger kilns, fixed beds, microwave and hydro-pyrolysis. Regardless of the reactor configuration employed, in order to ensure satisfactory and efficient operation of the fast pyrolysis reactor, the requirements in Section 2.2.3 must be met. Fluidised bed reactors are the most common fast pyrolysis reactors in both industry and R&D (Joubert, 2013). Fluidised beds have the advantage of being a well-developed and well-understood technology for the fast pyrolysis of woody biomass. They also offer the advantage of being simpler to design, construct and operate compared with other reactor types, as well as being scalable to a commercial-scale unit (Bridgwater, 2012). Bubbling fluidised beds in particular have an additional advantage over circulating and transported fluidised beds in that they allow easy bio-char separation via typical gas-solid separators. Bubbling fluidised beds provide good gas-solid contact, which permits very efficient heat and mass transfer, as well as good temperature control (Sadaka & Boateng, 2009). Figure 2.2 illustrates a typical bubbling fluidised bed pyrolysis reactor.

In a bubbling fluidised bed reactor, the heat required to drive the endothermic pyrolysis reactions can be supplied in a variety of ways. Bridgwater (2012) provides an overview of the main methods for supplying the necessary heat. Typically in fluidised bed reactors, a heated sand medium (i.e. hot solids) is employed directly to heat the biomass feedstock to the reaction temperature very rapidly. The biomass decomposition products (i.e. solid char, gas and vapour) are entrained from the fluidised bed reactor by the conveying fluidising gas, as illustrated in Figure 2.2.

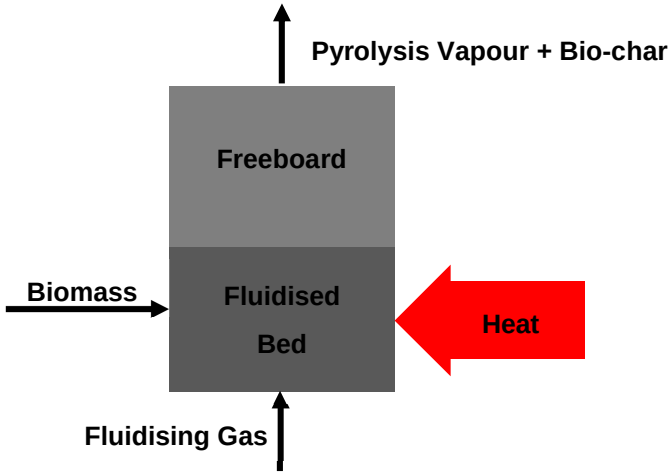

Figure 2.2: Typical bubbling fluidised bed pyrolysis reactor (Sadaka & Boateng, 2009)

The scalable DFB fast pyrolysis system at the University of Pretoria employs a bubbling fluidised bed-type reactor for the conversion of biomass to pyrolysis products. Swart (2012) has provided a detailed design of the bubbling fluidised bed fast pyrolysis reactor, as well as the design and construction considerations.

2.3 Fast Pyrolysis Products and Applications

Fast pyrolysis of biomass is the thermochemical cracking of long lignocellulosic polymers, in the absence of oxygen, into solid bio-char, crude liquid bio-oil and non-condensable gases (Demirbas, 2006). The three major constituents of lignocellulosic biomass are cellulose, hemicellulose and lignin. Therefore, the major pyrolysis products of woody biomass are derived from these three components in varying proportions (Kim, Kim, Lee et al., 2013).

2.3.1 Bio-oil

The condensable fraction of pyrolysis vapour is a viscous, dark brown liquid that resembles fossil crude oil, as can be seen in Figure 2.3. This condensable fraction is known as pyrolysis oil, bio-oil or crude bio-oil (Sadaka & Boateng, 2009). Crude pyrolysis liquid is produced as the main product of fast pyrolysis at yields typically between 30 and 75 weight % dry basis (wt % d.b.), depending on the feedstock characteristics and process conditions (Bridgwater, 2012).

Figure 2.3: Crude pyrolysis oil

(*Source:* http://bioweb.sungrant.org/General/Biopower/
Technologies/Pyrolysis/Pyrolysis+Oil/Pyrolysis+Oil.htm)

Crude pyrolysis liquid consists of a very complex mixture of oxygenated hydrocarbons with a substantial amount of water from the pyrolysis reaction, known as pyrolytic water, as well as from the biomass feedstock (Crocker, 2010: 164). Other compounds that are typically found in pyrolysis liquid include: organic acids, alcohols, esters, sugars, aldehydes, ketones, hydrocarbons, furans, pyrans, phenolics and extractives, as well as a whole range of other carbohydrate and lignin degradation

products (Oasmaa, Solantausta, Arpiainen et al., 2010). It has been reported that pyrolysis liquid may have more than 300 chemical components, making its characterisation extremely difficult and complex (Kim et al., 2013). Crude bio-oil tends to be polar, and therefore immiscible with fossil-based fuels, due to the presence of a vast amount of oxygenated compounds (Sadaka & Boateng, 2009). The elemental composition of pyrolysis liquid is very similar to that of the original biomass feedstock from which it derives (Sadaka & Boateng, 2009). This explains why the high heating value (HHV) of the resultant pyrolysis liquid is comparable to that of the parent biomass. The HHV of pyrolysis liquid is relatively low, about half that of fossil crude, due to its high oxygen and water content (Sadaka & Boateng, 2009). Compared with fossil crude, pyrolysis liquid contains less nitrogen and sulphur, which results in lower NOx and SOx gas emissions during its combustion.

Crude bio-oil is acidic, due to the presence of organic acids. This makes the pyrolysis liquid highly corrosive and unstable, which translates to some difficulties when considering storage and transportation requirements (Sadaka & Boateng, 2009). Its dynamic viscosity also adds to transportation challenges, since pumping through pipelines may become increasingly more difficult as its viscosity increases as a result of secondary reactions (Crocker, 2010: 169). Bio-oil handling and transportation characteristics may be improved by the use of suitable solvents (Bridgwater, 2012). Depending on the efficiency of the solids (i.e. bio-char and ash) removal system, the crude pyrolysis liquid may also contain bio-char and ash. These have been found to have an unwanted catalytic effect on pyrolysis liquid degradation (Crocker, 2010: 151). Table 2.3 presents typical physical and chemical properties of crude pyrolysis liquids. Note that the property ranges are fairly conservative because these properties are strongly dependent on the feedstock characteristics and processing conditions.

Despite the aforementioned shortcomings, bio-oil from fast pyrolysis has a lot of potential to be utilised in its crude or upgraded form. Typical applications of crude bio-oil include combustion for heat generation, co-firing with conventional fuels, and low-grade fuel in robust diesel engines (Crocker, 2010: 174–177). Numerous catalytic and chemical biomass/bio-oil upgrading technologies have been studied and developed to produce drop-in liquid transportation fuels such as petrol, diesel and kerosene. Bridgwater (2012), Crocker (2010) and Butler, Devlin, Meier et al. (2011) provide extensive reviews on effective and feasible bio-oil upgrading technologies. These technologies are aimed at deoxygenating the crude liquid bio-oil in order to increase its HHV and hydrocarbon fuel miscibility (Bridgwater, 2012). According to Bridgwater (2012) and Butler et al. (2011), bio-oil deoxygenation can be accomplished by either integrated catalytic (in situ) pyrolysis or by a close decoupled operation. Furthermore, according to Lin & Huber (2009), the main deoxygenation mechanism is rejection of oxygen as H_2O or CO_2. The deoxygenated bio-oil product is compatible with fossil fuel refinery streams, and can be refined to transportation-grade fuels in a conventional petroleum refinery (Bridgwater, 2012). According to Bridgwater (2012), typical catalysts employed for catalytic upgrading of crude liquid bio-oil include zeolites (e.g. ZSM-5, HZSM-5), metal oxides (e.g. CuO, ZnO) and precious metals (e.g. Pt, Pd).

Table 2.3: Typical properties of crude pyrolysis liquids (Sadaka & Boateng, 2009)

Physical property	Typical value
Moisture content	15–30%
Specific gravity	1.1–1.2
pH	2.8–4.0
Viscosity (40 °C, 25% water)	25–100 cP
HHV	16–26 MJ/kg
Elemental analysis	
C	55–64%
H	5–8%
O	27–40%
N	0.05–1%
Ash	0.03–0.3%

2.3.2 Bio-char

The solid residue from biomass degradation by fast pyrolysis is known as bio-char. Figure 2.4 provides an illustration of bio-char from biomass fast pyrolysis. The bio-char is produced as a co-product of fast pyrolysis at yields typically between 12 and 35 wt % d.b., depending on the feedstock characteristics and process conditions (Kim et al., 2013).

Bio-char consists mainly of carbon, hydrogen and inorganic metals. The carbon content in bio-char can be as high as 80–90 wt % d.b., which can be sequestered permanently in soil (Kim et al., 2013). Pyrolysis is considered a carbon-negative process since bio-char, as a carbon-sequestering agent, captures and removes CO_2 from the atmosphere. Bio-char also acts as a GHG-mitigating agent through the removal of atmospheric CO_2. This process is illustrated in Figure 2.5. Bio-char has a high calorific value, due to its high carbon content, which makes it an attractive solid fuel. It has a typical high heating value of approximately 20–30 MJ/kg, which makes it comparable to high-grade coal (Kim et al., 2013). Bio-char, as a solid fuel, has been tested extensively in typical charcoal applications such as pellets and briquettes (Kim et al., 2013).

Figure 2.4: Illustration of bio-char as co-product from fast pyrolysis

(*Source:* http://bioweb.sungrant.org/General/Biopower/
Technologies/Pyrolysis/Pyrolysis+Oil/Pyrolysis+Oil.htm)

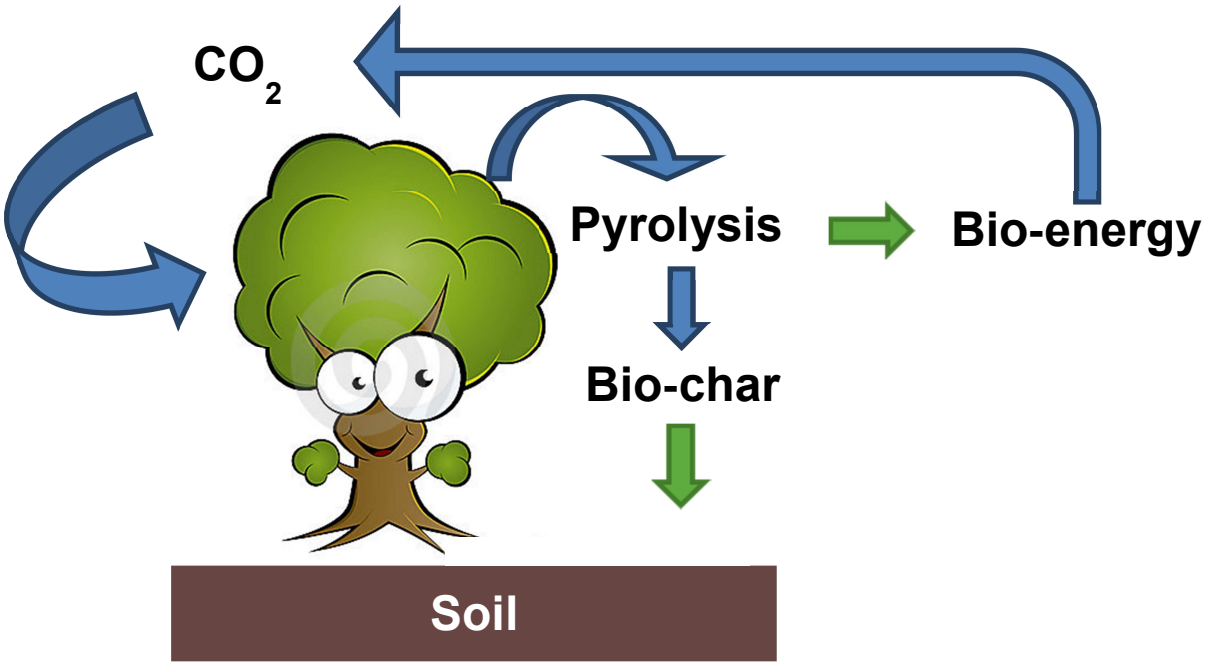

Figure 2.5: Bio-char as a carbon-sequestering and GHG-mitigating agent (Postma, 2012)

The inorganic fraction of bio-char contains mainly potassium, phosphorous, calcium, magnesium and sodium, which are important plant mineral nutrients (Kim et al., 2013). The proportion of inorganic material in the bio-char is strongly dependent on the ash content of the original biomass feedstock (Crocker, 2010: 151). Therefore, bio-char can be used as a fertiliser in soil amendment and nutrient-replacement applications to enhance soil quality and plantation productivity (Kim et al., 2013). In order to utilise these bio-char nutrients, the fast pyrolysis process must allow separation of bio-char as a co-product. The rapid and efficient separation of bio-char and ash from pyrolysis vapour is an important prerequisite for fast pyrolysis since these solids have a vapour-cracking effect which reduces the crude pyrolysis liquid yield (Crocker, 2010: 151).

2.3.3 Non-condensable Gases

The non-condensable fraction of pyrolysis vapour, also referred to as syngas, producer gas or simply NCG, is produced as a co-product of fast pyrolysis at yields typically between 13 and 35 wt % d.b., depending on the feedstock characteristics and process conditions (Bridgwater, 2012). NCG typically contains numerous permanent gases, including CO_2, CO, H_2, CH_4, C_2H4 and C_3H_6, but other C_2, C_3 and C_{4+} hydrocarbons may also be present (Wright, Daugaard, Satrio et al., 2010). Although CO_2 may constitute a large proportion of the NCG, most of the other components are combustibles which constitute a fuel gas with a low-to-medium calorific value, with a typical HHV of 6–8 MJ/kg (Boateng, 2011).

The NCG can be utilised as a fuel gas to supplement the energy requirement of the endothermic pyrolysis process, as illustrated in Figure 2.6 (Bridgwater, 2012). It may also be combusted to produce high-value process heat in order to generate steam and/or electricity, pre-heat the fluidising gas (if a fluidised bed is employed) or dry the biomass feedstock (Crocker, 2010: 174). Utilising the NCG as a fuel gas within the pyrolysis system improves the overall efficiency by reducing the demand for external fuel sources to drive the endothermic process. The possibility also exists for producing liquid fuels from the non-condensable syngas via conventional Fischer-Tropsch gas-to-liquids conversion technology.

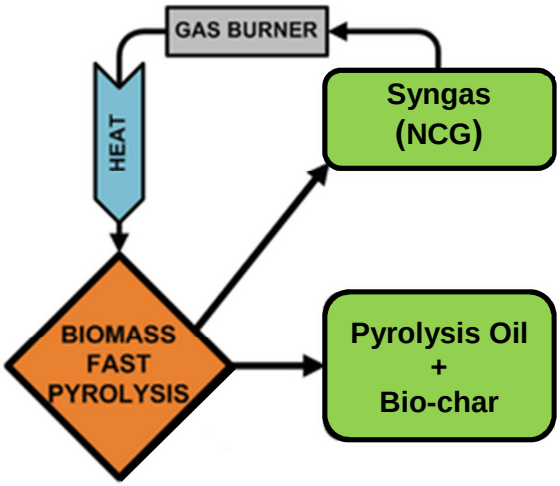

Figure 2.6: Utilisation of NCG for supplying process heat to the endothermic pyrolysis process

Fast pyrolysis of lignocellulosic biomass results in the formation of three distinctly different products, namely pyrolysis oil as the main product, and bio-char and syngas as co-products. Each of these pyrolysis products has unique properties and features which make it suitable for a particular application(s). Figure 2.7 summarises the general applications of fast pyrolysis products (Crocker, 2010: 174–179).

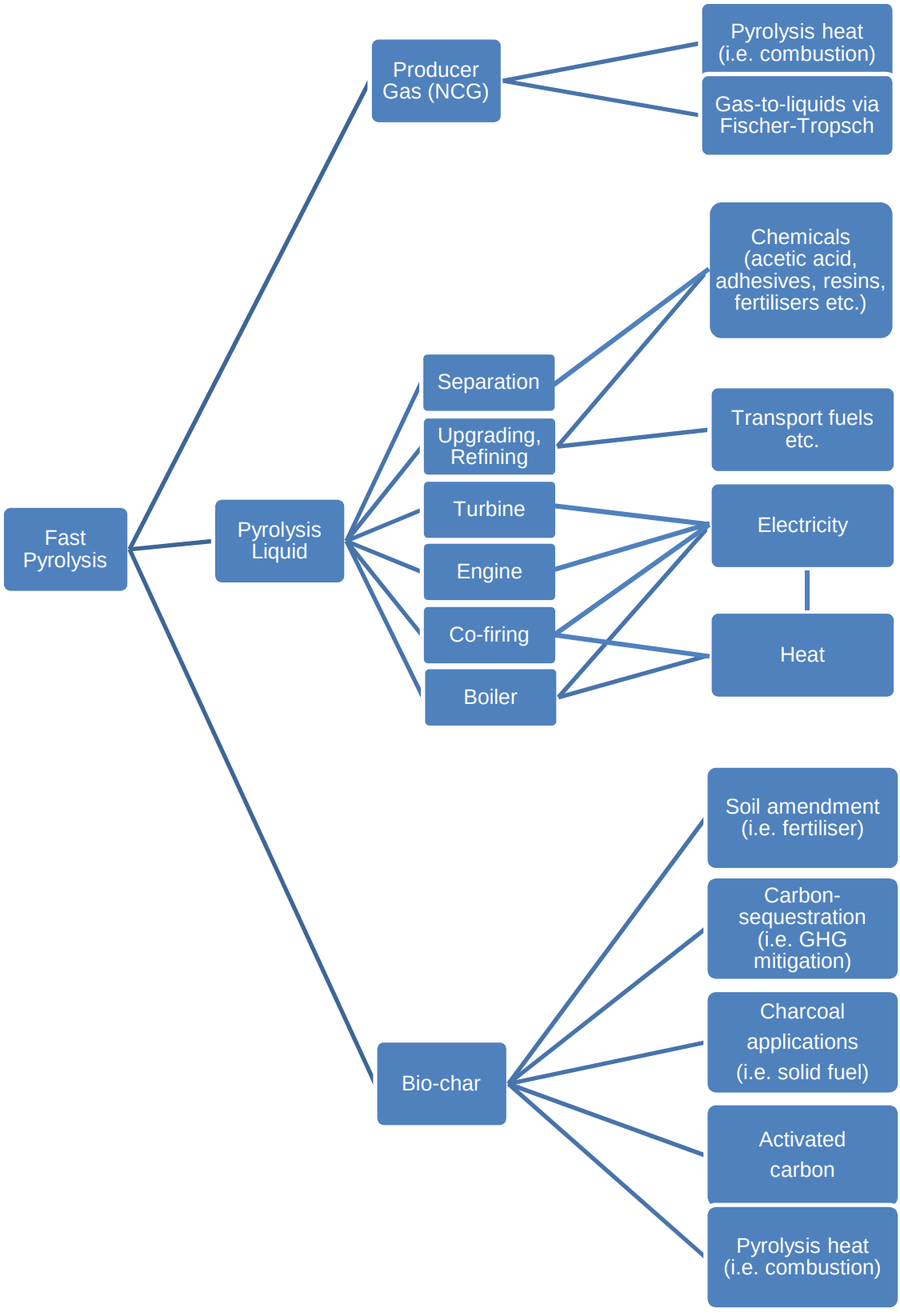

Figure 2.7: Summary of applications for fast pyrolysis products (Crocker, 2010: 174)

2.4 Fast Pyrolysis Performance-dependent Parameters

The yield and composition of fast pyrolysis products, and therefore system performance, depend strongly on several operating parameters (Joubert, 2013). Numerous performance-dependent parameters have been investigated to quantify their influence on fast pyrolysis product yields and composition (Oasmaa et al., 2010; Kim et al., 2013; DeSisto, Hill, Beis et al., 2010; Joubert, 2013; Boateng, 2011). The operating parameters that have been reported to have the most profound influence on fast pyrolysis reactor performance include reactor temperature, pyrolysis vapour residence time, feedstock heating rate and particle size (Bridgwater, 2012; Joubert, 2013).

2.4.1 Reactor Temperature

The pyrolysis reactor temperature has been demonstrated to be the operating parameter with the most influence on pyrolysis product distribution (DeSisto et al., 2010; Joubert, 2013; Boateng, 2011; Bridgwater, 2012; Joubert, 2013). In general, fast pyrolysis is conducted at a reactor temperature between 400 and 600 °C, although lower temperatures have been reported (Raveendran, Ganesh & Khilar, 1996). The high biomass particle heating rate required for fast pyrolysis necessitates operation at elevated temperatures, within this range. The pyrolysis liquid yield can vary as much as 30–75 wt % d.b. over this pyrolysis temperature range (Bridgwater, 2012). Pyrolysis reactor temperatures < 400 °C favour the production of bio-char, whereas reactor temperatures > 600 °C favour the formation of NCG (Bridgwater, 2012). Therefore, the final pyrolysis product distribution can be changed or optimised by altering the temperature of the fast pyrolysis reactor. DeSisto et al. (2010) have also illustrated that the pyrolysis reactor temperature influences the composition of the crude bio-oil and therefore its quality. Figure 2.8 demonstrates the influence of reactor temperature on product yields of corn stover fast pyrolysis (Boateng, 2011).

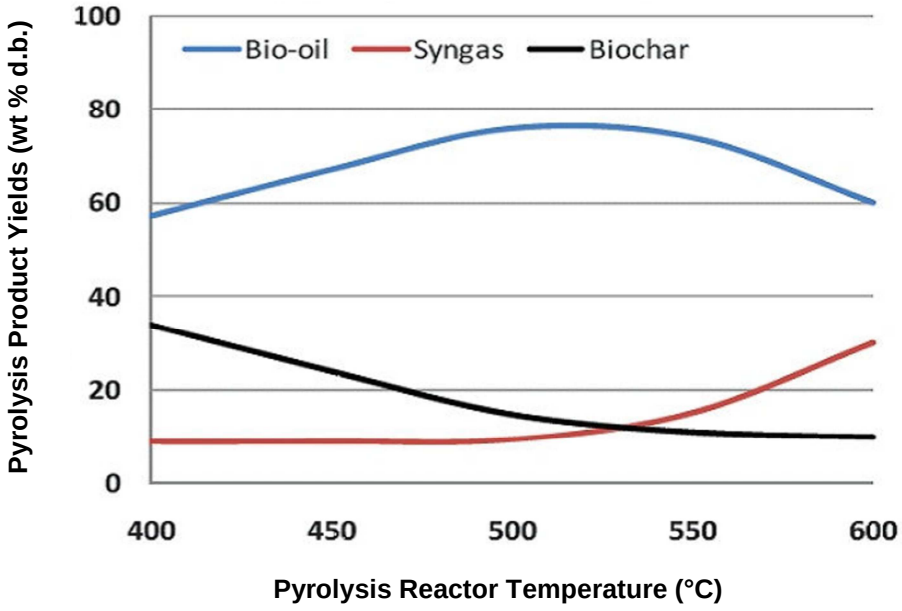

Figure 2.8: Variation in fast pyrolysis product yield with reactor temperature (Boateng, 2011)

2.4.2 Vapour Residence Time

The degree of thermal degradation of pyrolysis vapours is strongly dependent on the vapour residence time (VRT). Since fast pyrolysis is aimed at maximising the liquid bio-oil product, it is of the utmost importance to ensure that the VRT is below 2–3 seconds to prevent secondary reactions of tars producing bio-char and gases of lower molecular weight (Bridgwater, 2012).

2.4.3 Biomass Particle Size and Heating Rate

The biomass particle heating rate has been identified as the limiting step in the fast pyrolysis reaction rate (Boateng, 2011; Bridgwater, 2012). The particle heating rate is strongly dependent on the size of the biomass particle, the pyrolysis reactor temperature and the heat-transfer medium used to heat the biomass particle (Joubert, 2013). The biomass particle heating rate can therefore be manipulated by altering any of the abovementioned parameters. It has been established that the biomass particle size affects not only the fast pyrolysis bio-oil yield, but also the bio-oil composition (Shen, Wang & Garcia-Perez, 2009). Shen et al. (2009) demonstrated that the bio-oil yield decreases with an increase in biomass particle size, but only to a certain extent. They found that the decrease in bio-oil yield was insignificant as the particle size was increased beyond 1.5 mm (Shen et al., 2009). Figure 2.9 demonstrates the influence of particle size on product yields of oil mallee woody biomass fast pyrolysis (Shen et al., 2009).

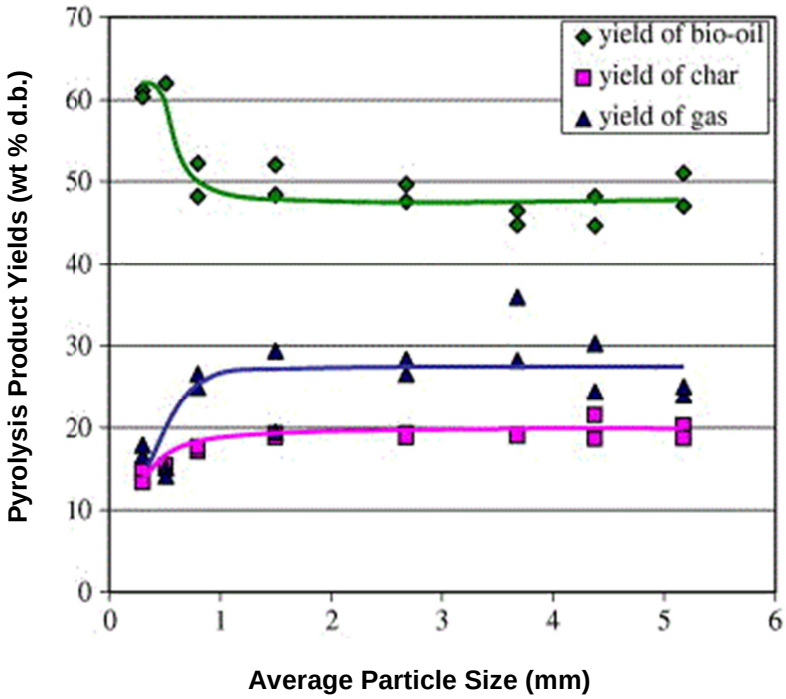

Figure 2.9: Variation in fast pyrolysis product yield with particle size (Shen et al., 2009)

2.5 Conclusions

Woody biomass, consisting mainly of lignocellulosic constituents, namely lignin, cellulose and hemicellulose, is one of the largest biomass energy sources used to produce second-generation biofuels (Meincken, 2011). A large quantity of under-utilised lignocellulosic biomass is produced annually as a by-product from forestry, sawmills, and pulp and paper mills in South Africa (Brent, 2011). Pyrolysis has been identified as one of the most viable thermochemical conversion processes to convert this under-utilised resource into energy-dense products of high commercial value (Bridgwater, 2012). Fast pyrolysis in particular is currently the main focus of pyrolysis research for the production of liquid bio-oil as the main product, which may be used for energy, chemicals or as an energy carrier (Crocker, 2010: 149). The co-products from fast pyrolysis, namely bio-char and non-condensable gases (NCG), have also been demonstrated to have numerous attractive applications (Crocker, 2010: 174). Fluidised bed reactors were found to be the most common fast pyrolysis reactors in both industry and R&D (Joubert, 2013). Bubbling fluidised beds in particular have additional advantages over other conventional fluidised bed reactors, which makes them the most attractive reactor configuration for larger-scale units (Bridgewater, 2012). Various operating parameters have been identified to affect the performance of these fast pyrolysis units, including reactor temperature, vapour residence time (VRT), and biomass particle size and heating rate (Joubert, 2013). In order to ensure optimal performance of the fast pyrolysis process, these parameters have to be sustained within rigorous control limits.

3 DUAL FLUIDISED BED REACTOR SYSTEM

3.1 Introduction

Pyrolysis of biomass is the thermochemical conversion of lignocellulosic material into several higher-value products such as bio-oil, bio-char and syngas. Pyrolysis is an endothermic process and requires heat to crack the long lignocellulosic polymers to form these products of lower molecular weight. Combustion reactions have been demonstrated to be a viable source of heat to drive these pyrolysis reactions (Swart, 2012). The pyrolysis system therefore consists of two fluidised bed reactors, namely the pyrolysis reactor and the combustion reactor. Dual fluidised bed (DFB) systems have been identified as feasible reactor systems for pyrolysis because they can provide a reliable source of heat for the endothermic process, promoting the high heat transfer rates and short residence times required for optimum liquid yields (Bridgwater, 2012). Although many DFB systems have been investigated for the pyrolysis of biomass, not much has been published on the scaling up to a commercial-scale system.

A scalable combustion-reduction integrated pyrolysis system has been designed, constructed and commissioned at the University of Pretoria, capable of producing these pyrolysis products from woody biomass. The system consists of a combustion fluidised bed reactor (oxidation) for heating sand (the heat-carrying medium) and a pyrolysis fluidised bed reactor (reduction) for the endothermic pyrolysis reactions. This DFB system includes all the ancillary units for biomass feeding, gas-solid separation cyclones for bio-char and ash collection, and a complete downstream bio-oil recovery system. The latter consists of a quencher, a demister, a hydrocyclone and a gas blower for recirculation of non-condensable gases (NCG). A scalable solids-transport system, consisting of an overflow standpipe and a screw conveyor, has also been implemented for the transfer of solids (heat carrier) between the two fluidised beds, creating a circulating system. This section provides an overview of the dual fluidised bed pyrolysis system, including the main unit operations and ancillary equipment. Swart (2012) provides a detailed description of the physical design and construction of these processing units.

3.2 Process Overview

The process flow diagram of the scalable dual fluidised bed reactor system is presented in Figure 3.1. The equipment list, corresponding to the equipment numbers in Figure 3.1, is shown in Table 3.1. The solid heat carrier (i.e. sand) is heated in the combustion fluidised bed (CFB) by means of exothermic combustion reactions. The heat carrier is then transferred to the pyrolysis fluidised bed (PFB) via the overflow standpipe (z-valve), which connects the two fluidised beds. Biomass sawdust is fed to the PFB where it is converted into pyrolysis vapour and bio-char. The colder solids and a fraction of the bio-char are transported back to the CFB, via the sand screw conveyor, thereby creating a circulation system. The fixed sand bed in the overflow standpipe (z-valve) creates a

hydraulic seal which prevents the flow of unwanted oxygen into the PFB, where an oxygen-free environment is essential for the pyrolysis reactions to occur. The bio-char produced in the PFB is removed from the pyrolysis vapour in the bio-char cyclone and collected as a co-product. According to Bridgwater (2012), removal of the solid bio-char from the hot pyrolysis vapours is essential as he established that the bio-char has a catalytic effect on pyrolysis vapour cracking to low-molecular-weight gases. The hot pyrolysis vapours are transferred to the bio-oil recovery and collection system, which rapidly quenches the condensable fraction to form bio-oil.

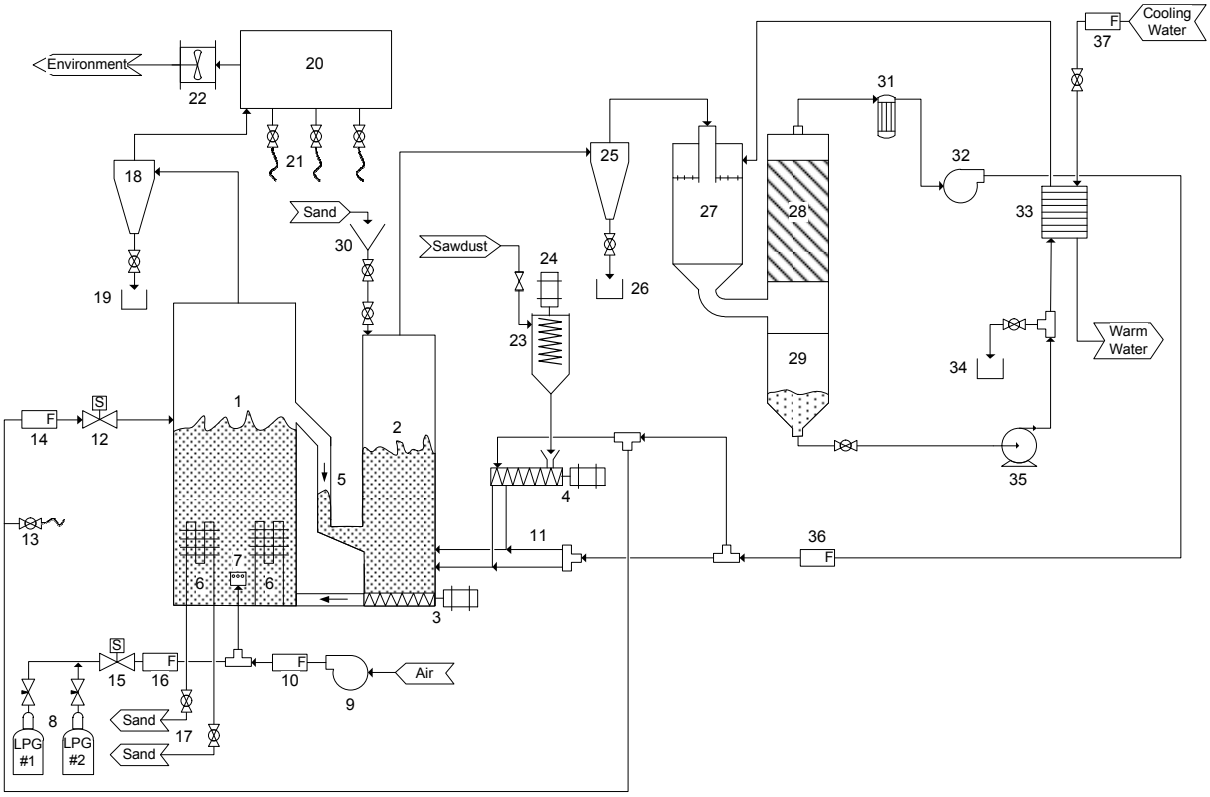

Figure 3.1: Process flow diagram of dual fluidised bed reactor system

The NCG are also separated from the bio-oil in the bio-oil recovery system. They pass through a cartridge filter to remove any entrained bio-oil and/or bio-char. The blower transfers the NCG back to the PFB in order to fluidise the reactor, as well as to provide the necessary oxygen-free environment. A fraction of the NCG, containing several combustibles, is purged to the CFB as a supplementary fuel. As mentioned before, a small fraction of the bio-char from the PFB enters the CFB with the solids, which also supplements the energy demand in the CFB. According to Wright et al. (2010), the NCG and a fraction of the bio-char produced can be combusted to provide the necessary process heat for the pyrolysis reactions in a larger-scale system. A full-scale dual fluidised bed system would therefore be able to operate self-sufficiently without the need for additional fuel sources (Wright et al., 2010). Ash and hot flue gases are produced in the CFB. The ash is removed from the flue gas in the ash cyclone and the remaining flue gas is cooled and diluted in an extraction box before being purged into the atmosphere. The hot flue gases are a source of high-value heat and can be used to pre-heat the combustion air or recycled NCG, and/or to dry the biomass feedstock.

Table 3.1: List of equipment in the dual fluidised bed reactor system

Item No.	Description	Item No.	Description
1	Combustion fluidised bed	20	Extraction/dilution box
2	Pyrolysis fluidised bed	21	Flexible air hoses
3	Sand screw feeder	22	Extraction fan
4	Biomass screw feeder	23	Biomass hopper
5	Overflow standpipe (z-valve)	24	Biomass agitator
6	Electrical heating elements	25	Bio-char cyclone
7	Bubble cap distributor	26	Bio-char container
8	LPG cylinders	27	Quencher
9	Air blower	28	Demister
10	Air flow transmitter	29	Bio-oil cyclone/container
11	Pneumatic biomass feeder	30	Sand replenish hopper
12	NCG purge solenoid valve	31	Cartridge filter
13	NCG sample point	32	NCG blower
14	NCG purge flow transmitter	33	Brass plate heat exchanger
15	LPG solenoid valve	34	Bio-oil container
16	LPG flow indicator	35	Bio-oil pump
17	Sand drains	36	NCG flow transmitter
18	Ash cyclone	37	Water flow transmitter
19	Ash container		

3.3 Combustion Reactor

The process heat carrier, used to provide the energy for the endothermic pyrolysis reactions, is heated in the combustion reactor by means of exothermic combustion reactions. The diagram in Figure 3.2 shows the combustion reactor with its ancillary equipment. The equipment numbers in Figure 3.2 correspond to the equipment descriptions in Table 3.1. The CFB reactor is operated in the bubbling regime to minimise the entrainment of solids from the reactor. Liquefied petroleum gas (LPG) is used as the main fuel in the CFB. Air is fed to the CFB to combust (oxidise) the LPG and to fluidise the combustion reactor. Air from the air blower is mixed with the LPG before being fed to the CFB through the bubble cap distributor. Air is supplied in excess to ensure complete combustion of all the fuel sources in the CFB. Both the air and the LPG flow are measured and monitored to ensure that the air is supplied in excess. A fraction of the pyrolysis bio-char and the purged NCG are also fed to the CFB as supplementary fuels. The bio-char enters the combustion reactor via the sand screw conveyor, while the NCG is fed into the freeboard of the CFB.

The heat carrier is transferred to the PFB by means of an overflow standpipe, also referred to as the z-valve. Swart (2012) provides the detailed design of the z-valve. The entrance of the overflow standpipe is positioned at the splash zone of the CFB. This allows for the heat carrier to spill over into the standpipe and into the PFB. Colder solids and a fraction of the bio-char are transported back to the CFB via the sand screw conveyor, positioned at the bottom of the CFB. Ash and hot flue gas exit the CFB at the top of the reactor. The ash is removed from the hot flue gas in the ash cyclone.

An extraction system, consisting of an extraction fan, an extraction/dilution box and flexible air hoses, is used to extract, cool and dilute the hot flue gas before being discharged to the atmosphere. Both the combustion reactor and the overflow standpipe are insulated with a 25 mm castable refractory lining to minimise heat loss to the surrounding atmosphere. A layer of 15 mm Vermiculite insulating material is installed between the castable refractory and the shell, followed by a 25 mm layer of ceramic fibre wool fitted to the outside of the shell. Two electrical elements are fitted in the CFB to ensure a safe and convenient start-up. Two gate valves are installed at the bottom of the CFB to drain the heat carrier in the event of a process shutdown. A borosilicate-glass peephole is installed at the top of the CFB so that the CFB operation can be monitored visually.

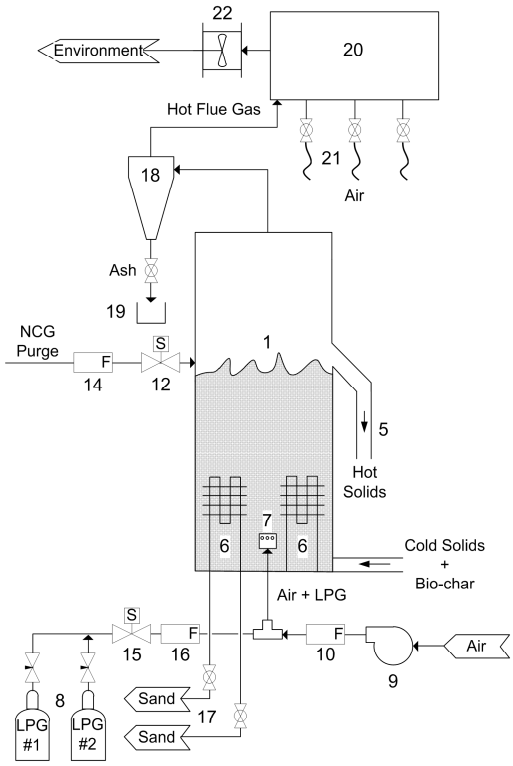

Figure 3.2: Combustion fluidised bed reactor

3.4 Biomass Feed System

A diagram of the biomass feed system is presented in Figure 3.3. The equipment numbers in Figure 3.3 correspond to the equipment descriptions in Table 3.1. Pre-treated biomass sawdust is charged to the biomass hopper. An agitator in the biomass hopper prevents the formation of unwanted clumps and structural bridging, thereby ensuring unrestricted flow of sawdust into the biomass screw feeder. The sawdust is pneumatically conveyed from the biomass screw to the pyrolysis reactor, where it is continuously injected into the bottom of the PFB. The biomass screw feeds sawdust into a distribution unit, where it is vigorously mixed with the pneumatic conveying fluid. NCG, from the gas-cleaning section, are used as the pneumatic conveying fluid. The NCG are also used to fluidise the PFB. The sawdust distribution unit is fitted with sight-glass which allows visual monitoring of its operation. The biomass hopper hangs on three load cells, which are connected to a

weightometer to provide a mass indication of the available or used sawdust. Contrary to biomass feed systems used in other laboratory- and pilot-scale pyrolysis systems (Shen et al., 2009; Joubert, 2013), the pneumatic biomass feed system is easily scaled up to a commercial-scale unit.

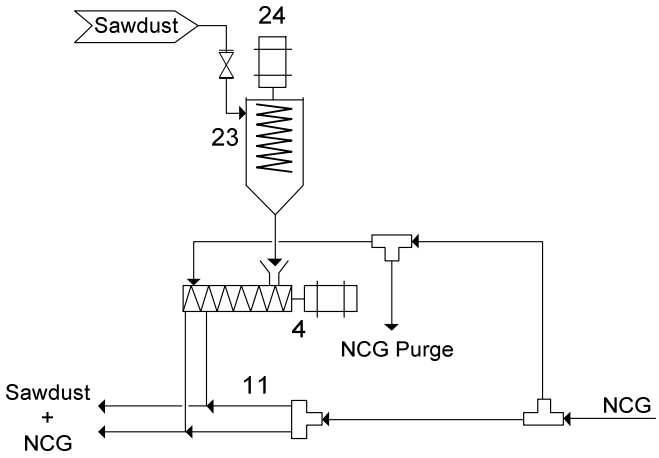

Figure 3.3: Pneumatic biomass feed system

3.5 Pyrolysis Reactor

The process heat required to drive the endothermic pyrolysis reactions is supplied by the hot heat carrier (i.e. sand) from the CFB. The hot solids from the CFB spill over into the overflow standpipe (z-valve) which feeds the hot solids into the pyrolysis reactor. The fixed sand bed in the overflow standpipe (z-valve) creates a hydraulic seal which prevents the flow of unwanted oxygen into the PFB, where an oxygen-free environment is essential for the pyrolysis reactions to occur. A diagram of the pyrolysis reactor with its ancillary equipment is presented in Figure 3.4. The equipment numbers in Figure 3.4 correspond to the equipment descriptions in Table 3.1.

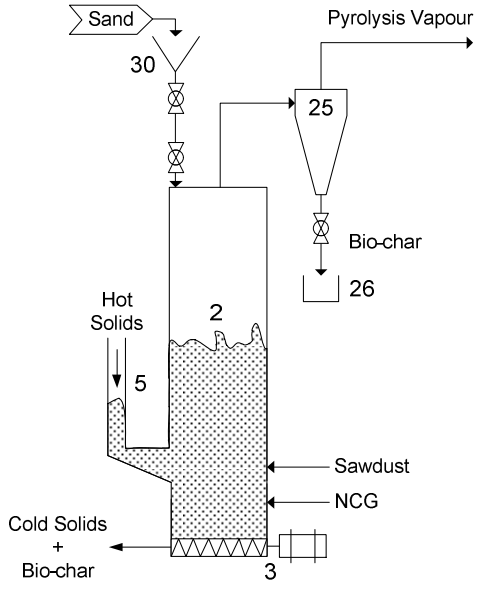

Figure 3.4: Pyrolysis fluidised bed reactor

The pyrolysis fluidised bed reactor is also operated in the bubbling regime in order to minimise the entrainment of heat carrier solids from the reactor. NCG, from the gas-cleaning section, are transferred to the pyrolysis reactor by means of the NCG blower to fluidise the pyrolysis reactor and to provide the necessary oxygen-free environment inside the PFB. A fraction of the NCG is used to inject the biomass sawdust pneumatically into the hot PFB. Inside the PFB, the biomass sawdust is cracked to form pyrolysis vapour and bio-char. The bio-char is entrained with the pyrolysis vapour at the top of the PFB. The bio-char is removed from the pyrolysis vapour in the bio-char cyclone and collected as a co-product. Contrary to other laboratory- and pilot-scale pyrolysis systems (Bridgewater, 2012), the DFB system allows for easy separation and recovery of bio-char as a co-product from pyrolysis. Pyrolysis bio-char has been demonstrated to have numerous attractive and viable applications, especially in the South African forestry sector as a soil amendment and carbon-sequestering agent (Brent, 2011; Bridgwater, 2012; Crocker, 2010). The bio-char separation and recovery system is also easily scaled up to a full-scale unit.

The pyrolysis vapour is transferred to the bio-oil recovery and collection system, where the bio-oil fraction is collected. The colder heat-carrier solids, together with a fraction of the pyrolysis bio-char, are transferred back to the CFB by means of the sand screw conveyor in order to be reheated by exothermic combustion reactions. A double-valve sand-replenish system is installed at the top of the PFB to replace any entrained fluid bed material. The double-valve system allows fluid bed material to be charged with minimal air ingress into the PFB. A borosilicate-glass peephole installed at the top of the PFB allows visual monitoring of the PFB operation. The PFB reactor is insulated with 25 mm of ceramic fibre wool, fitted to the outside of the shell.

3.6 Bio-oil Recovery and Collection System

The bio-oil recovery and collection system consists of a bio-oil quencher (i.e. scrubber), demister, hydrocyclone, bio-oil pump and heat exchanger as shown in Figure 3.5. The equipment numbers in Figure 3.5 correspond to the equipment descriptions in Table 3.1. The hot pyrolysis vapour from the PFB is rapidly quenched in the bio-oil recovery and collection system in order to recover the condensable fraction known as bio-oil. To maximise the liquid bio-oil yield, the condensable fraction (i.e. tars) has to be quenched and isolated quickly to prevent unwanted secondary reactions from occurring, which would convert the vapours into low-molecular-weight NCG (Bridgwater, 2012).

Hot pyrolysis vapour is rapidly cooled with cold bio-oil in the bio-oil quencher. The mixture passes through the hydrocyclone which separates condensable bio-oil from the NCG. The condensed bio-oil collects at the bottom of the hydrocyclone. Some bio-oil is entrained with the NCG into the demister unit. The purpose of the demister unit is to separate the entrained bio-oil from the NCG. The bio-oil removed in the demister unit also collects at the bottom of the hydrocyclone. The bio-oil pump transfers hot bio-oil to the brass plate heat exchanger where it is indirectly cooled with cold water.

The cold bio-oil is circulated back to the quencher where it is sprayed into direct contact with the incoming hot pyrolysis vapour, thereby completing the bio-oil recovery cycle. The liquid bio-oil product is collected at a take-off point located on the bio-oil pump delivery.

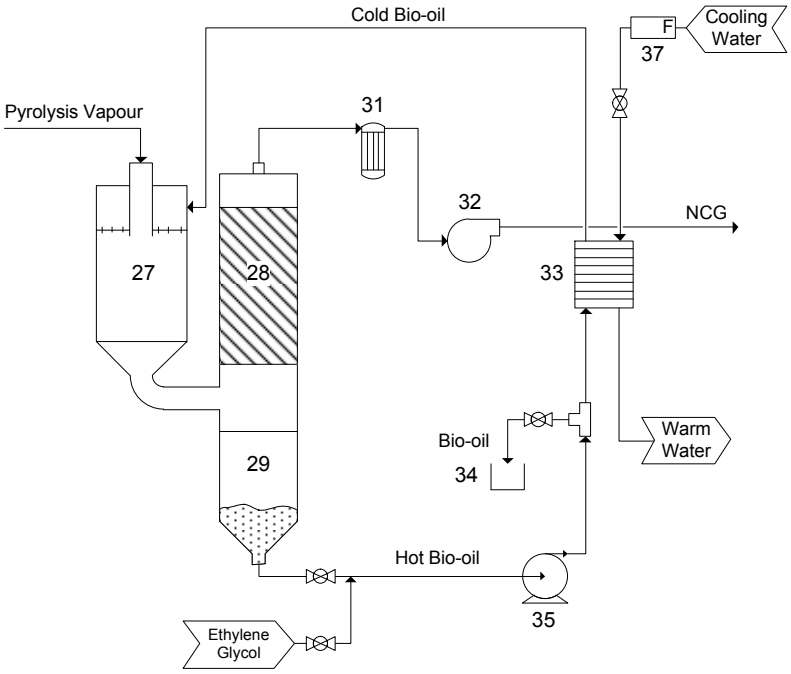

Figure 3.5: Bio-oil recovery and collection system

NCG from the demister unit pass through a 10 µm cartridge filter to remove any entrained liquid bio-oil before they enter the NCG blower. The filter element of the cartridge filter is easily replaced at the end of each experimental run. NCG from the cartridge filter are circulated back to the PFB via the NCG blower. Most of the NCG are used as fluidising and pneumatic conveying fluid in the PFB and sawdust feed system respectively. The remaining NCG are purged from the pyrolysis reactor section to avoid pressurising the PFB. The NCG are purged to the CFB in order to supplement the fuel requirement in the combustion reactor. The bio-oil quencher, hydrocyclone and demister units are constructed from borosilicate-glass so that their operation can be monitored visually. Ethylene glycol was selected as the cooling medium for quenching the hot pyrolysis vapour during start-up.

3.7 Distributed Control System

The control system of the scalable DFB reactor system is shown in the piping and instrumentation diagram (P&ID) in Appendix A. It consists of five feedback controllers, namely TIC 1, TIC 2, PIC 1, PIC 2 and PIC 3. The controlled, measured and manipulated variables, and the control element for each feedback control loop, are presented in Table 3.2. TIC 1 is used to control the CFB reactor temperature by manipulating the LPG flow rate to the combustion reactor. The controller set-point for TIC 1 is set manually by the operator. TIC 2 is used to control the PFB reactor temperature by

manipulating the flow rate of hot sand to the pyrolysis reactor. The set-point for controller TIC 2 is set manually by the operator. PIC 1 controls the air flow rate to the CFB, while PIC 2 controls the NCG flow rate to the PFB by manipulating the air and NCG blower speeds respectively. PIC 3 is used to control the freeboard pressure in the PFB by manipulating the NCG purge flow rate to the CFB.

Table 3.2: Feedback controller variables for the pyrolysis process control system

Controller	Controlled variable	Measured variable	Manipulated variable	Control element
TIC 1	Combustion fluidised bed temperature	Combustion fluidised bed temperature	LPG flow rate to combustion reactor	LPG solenoid valve
TIC 2	Pyrolysis fluidised bed temperature	Pyrolysis fluidised bed temperature	Hot solids flow rate to pyrolysis reactor	Sand screw variable frequency drive
PIC 1	Air flow rate to combustion reactor	Pressure drop over air orifice plate	Air blower speed	Air blower variable frequency drive
PIC 2	NCG flow rate to pyrolysis reactor (incl. purge)	Pressure drop over NCG orifice plate	NCG blower speed	NCG blower variable frequency drive
PIC 3	Freeboard pressure in pyrolysis fluidised bed	Freeboard pressure in pyrolysis fluidised bed	NCG purge flow rate	NCG solenoid valve

A list of the measuring instruments used in the DFB reactor system is given in Table 3.3. These measurements are used not only to monitor the performance of the dual reactor system, but also to ensure the safe operation of all processing equipment. The purpose of each measuring instrument is also shown in Table 3.3. The location of these measuring instruments is shown on the P&ID in Appendix A. The distributed control system (DCS) for the DFB pyrolysis process was developed using LabView™ 2011 Professional Development Software by National Instruments. An illustration of the DCS used for control and data acquisition operations on the pyrolysis system is presented in Appendix B.

The DCS includes controls for the operation of all ancillary equipment, including electrical heating elements, solenoid valves, electric motors and variable frequency drives (VFDs). The DCS also provides indicators for all measured process parameters, including temperatures, pressures, flow rates and valve positions. Indication of equipment status, including motors, valves, controllers and heating elements, is also provided. Estimation of certain process variables, including volumetric flow rates, superficial gas velocities, vapour residence time and fluidised bed heights, is made possible by calculator functions within the DCS. Process performance monitoring is accomplished by trending key process variables by means of graphical indicators in the DCS.

Table 3.3: Measuring instruments used in the scalable pyrolysis system

Item No.	Parameter	Measurement	Type
IT1-01	Temperature	Bottom of combustion fluidised bed	Transmitter
IT1-02	Temperature	Middle of combustion fluidised bed	Transmitter
IT1-03	Temperature	Middle of pyrolysis fluidised bed	Transmitter
IT1-04	Temperature	Middle of pyrolysis fluidised bed	Transmitter
IT1-05	Temperature	Freeboard of pyrolysis fluidised bed	Transmitter
IT1-06	Temperature	Freeboard of combustion fluidised bed	Transmitter
IT1-07	Temperature	Air flow to combustion fluidised bed	Transmitter
IT1-08	Temperature	Total NCG flow from NCG blower	Transmitter
IT1-09	Temperature	Heating element inside combustion reactor	Transmitter
IT3-01	Temperature	NCG from demister	Transmitter
IT3-02	Temperature	Cold water to heat exchanger	Transmitter
IT3-03	Temperature	Warm water from heat exchanger	Transmitter
IT3-04	Temperature	Hot bio-oil from quencher	Transmitter
IT3-05	Temperature	Cold bio-oil to quencher	Transmitter
IT4-01	Temperature	Flue gas/air mixture before extraction fan	Transmitter
IT5-01	Temperature	Surrounding indoor environment	Transmitter
IP1-01	Pressure	Air stream after air orifice plate	Transmitter
IP1-02	Pressure	Air stream before air orifice plate	Transmitter
IP1-03	Pressure	Freeboard of pyrolysis fluidised bed	Transmitter
IP1-04	Pressure	Freeboard of combustion fluidised bed	Transmitter
IP1-05	Pressure	NCG stream after NCG orifice plate	Transmitter
IP1-06	Pressure	NCG stream before NCG orifice plate	Transmitter
IP1-07	Pressure	Bottom of combustion fluidised bed	Transmitter
IP1-08	Pressure	Bottom of pyrolysis fluidised bed	Transmitter
IP1-09	Pressure	LPG delivery pressure	Indicator
IP3-01	Pressure	Bio-oil pump delivery pressure	Transmitter
FT1-01	Flow	NCG purge to combustion reactor	Indicator transmitter
FT3-01	Flow	Cold water to brass plate heat exchanger	Transmitter
FI1-02	Flow	LPG to combustion reactor	Indicator
IM1-01	Mass	Sawdust mass in biomass hopper	Indicator transmitter

4 PROCESS OPERATION AND CHARACTERISATION

4.1 Introduction

Fast pyrolysis of woody biomass is the thermochemical conversion process whereby the long lignocellulosic polymers present in wood are cracked to form liquid bio-oil as the main product. Bio-char and non-condensable gases (NCG) are produced as co-products during fast pyrolysis (Bridgwater, 2012). This section provides an overview of the raw material handling and operational procedures that were followed in this investigation. A brief summary of the hot commissioning of the pyrolysis fluidised bed (PFB) reactor is also presented. The operational process variables (dependent and independent) for each main section of the scalable dual reactor system are presented in this section. These process variables were either determined by direct measurement or calculated from other process parameters. They were controlled, monitored and recorded on the distributed control and data acquisition system, which is detailed in Section 3.7. The analytical methods and instrumentation used for the analysis and characterisation of the pyrolysis feedstock and products are also presented in this section. From the gathered process information, a material and energy balance was conducted to quantify the performance of the pyrolysis reactor; this is presented in Section 4.6. Details pertaining to each unit operation of the scalable dual reactor system, used in this investigation were previously presented in Chapter 3.

4.2 Feedstock Handling

E. grandis hardwood, from Sappi Southern Africa's Ngodwana mill, was used in this investigation as the initial test biomass. The *E. grandis* woodchips were collected from the woodchip screening plant. According to Wright et al. (2012), pre-treatment of the biomass feedstock is essential to ensure optimal performance of the pyrolysis process. A schematic diagram of the biomass pre-treatment process used in this investigation is presented in Figure 4.1.

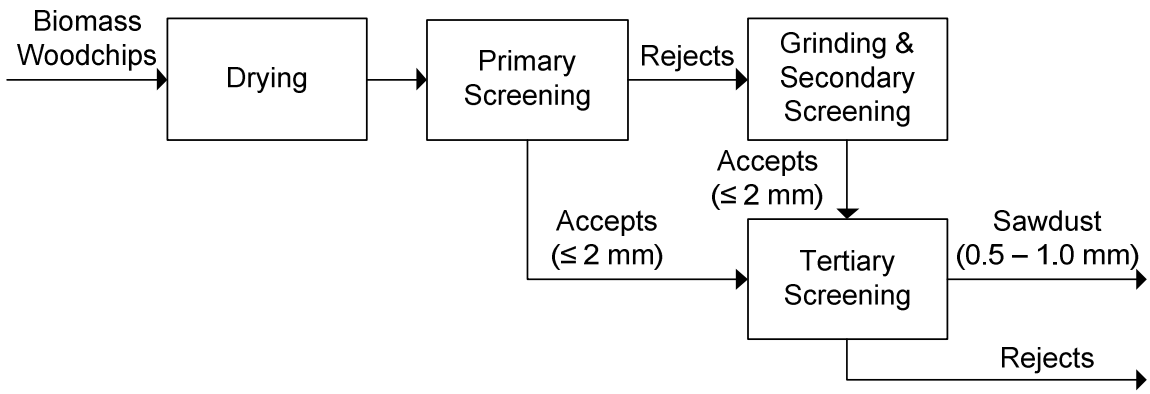

Figure 4.1: Biomass pre-treatment process

4.2.1 Biomass Drying

Biomass drying is an essential pre-treatment step to the pyrolysis process as excess moisture consumes process heat and also contributes to lower process yields (Wright et al., 2012). Biomass feedstock drying also alleviates some processing problems, including blinding of screens during fine grinding or blocking of transfer lines during pneumatic conveying. The moisture content of the biomass woodchips, as received, was extremely variable, as demonstrated in Figure 4.2. In order to prevent processing problems downstream, the raw material was dried to a consistent moisture content. The biomass woodchips were air/sun dried for 6–12 h by distributing the woodchips evenly on a plastic ground sheet, as shown in Figure 4.3. The woodchips were mixed and redistributed frequently to ensure consistent drying. Numerous random grab samples of the air/sun-dried material were collected and analysed after the 6–12 h drying period. Moisture content analysis was conducted on the starting material and on the air/sun-dried woodchips according to the standard TAPPI method (T264 – TAPPI, 1988b). The results from air/sun drying of the biomass feedstock are presented in Figure 4.4.

Figure 4.2: Biomass feedstock as received

Figure 4.3: Air/sun drying of biomass woodchips

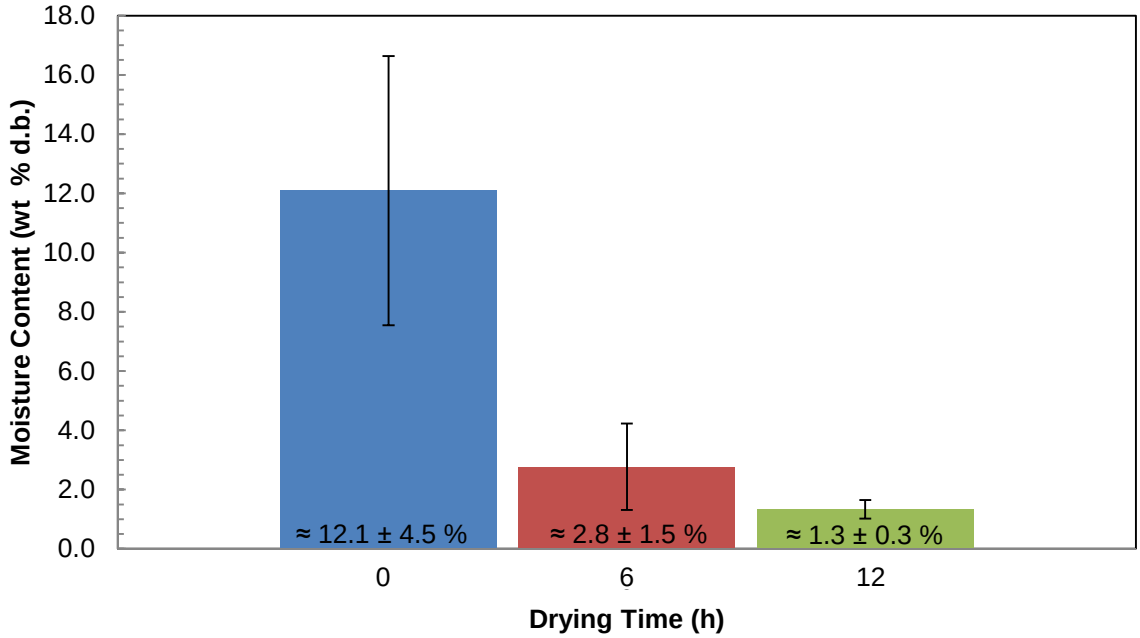

Figure 4.4: Influence of air/sun drying of biomass woodchips

It is evident from Figure 4.4 that the moisture content of the biomass woodchips, as received, was extremely variable and ranged from 7.6–16.6 wt % d.b. After the woodchips had been air/sun dried for 6 h, the average moisture content and standard deviation were reduced to 2.8 and 1.5 wt % d.b. respectively. Air/sun drying for an additional 6 h produced a biomass material with an average moisture content of 1.3 wt % d.b. and standard deviation of 0.3 wt % d.b. It is noticeable that most of the free moisture was removed during the first 6 h of drying while the mass transfer driving force was at its highest. The standard deviation also reduced significantly as the material dried out evenly. However, as the biomass dried, further drying became increasingly more difficult due to the reduced driving force after the initial 6 h drying period. Based on these results, the biomass woodchips, as received, were air/sun dried for only 6 h before further pre-treatment.

4.2.2 Biomass Grinding and Screening

As shown in Figure 4.1, the dried woodchips were subjected to a series of screening and grinding operations to produce a biomass with suitable physical properties for processing in the fast pyrolysis system. The dried woodchips were subjected to an eccentric motor-driven sieve (primary screen), fitted with a 2 mm mesh screen, to remove any oversized material (rejects). The eccentric motor-driven sieve is shown in Figure 4.5. The rejects from the primary screen were charged to a Retch SM100 cutting mill, fitted with a 2 mm mesh screen (secondary screen), to grind the oversized material to a uniform particle size of ≤ 2 mm. The accepts from both the primary and secondary screens were combined and charged to a Filtra Vibracion S.L. vibrating sieve (tertiary screen) to isolate the 0.5–1.0 mm particle size fraction, which was used as the starting material in the DFB reactor system. Figure 4.6 shows the Retch SM100 cutting mill and secondary screen and Figure 4.7

the tertiary screen. According to Shen et al. (2009), the performance of the pyrolysis system is strongly dependent on a high biomass particle heating rate, which necessitates a biomass particle size of ≤ 1.0–1.5 mm (Shen et al., 2009).

Figure 4.5: Eccentric motor-driven sieve, fitted with 2 mm mesh screen

Figure 4.6: Retch SM100 cutting mill, fitted with 2 mm mesh screen

Figure 4.7: Vibrating tertiary screen

4.2.3 Biomass Feed System

Before every process start-up, ± 10 kg of pre-treated biomass sawdust was charged to the biomass hopper. The amount of sawdust used during each experimental run was measured by weighing the biomass material before and after each run. The average sawdust throughput was determined from the weight measurement data. Alternatively, the amount of biomass sawdust consumed was determined from the mass indication on the biomass hopper. Also, as part of the process commissioning, the biomass feed screw was calibrated to determine the sawdust feed rate, based on the speed of the biomass feed screw. The results from the biomass feed screw calibration are presented in Figure 4.8. This relationship was programmed into the DCS to calculate the sawdust throughput, based on the biomass screw speed.

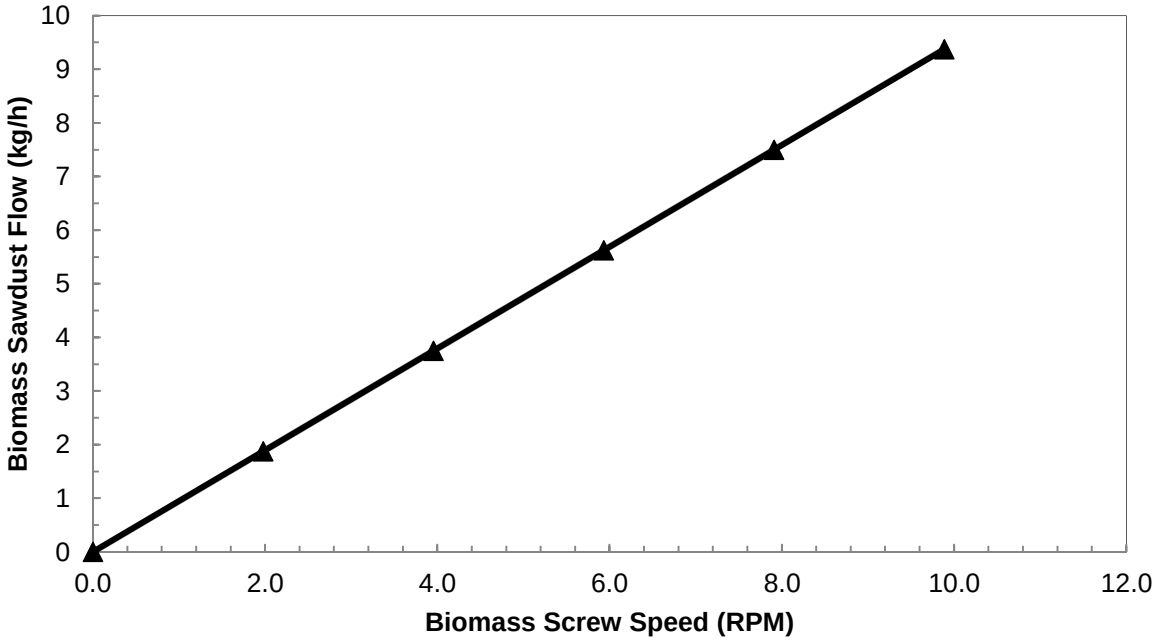

Figure 4.8: Calibration of biomass feed screw conveyor

4.2.4 Biomass Characterisation

Physical and chemical characterisation of the pre-treated biomass sawdust was conducted at the University of Pretoria, the Agricultural Research Council and the Sappi Technology Centre, South Africa. The proximate analysis of the *E. grandis* sawdust was conducted on a PerkinElmer Thermo-gravimetric Analyser (TGA) 4000 at the University of Pretoria. The TGA method used for the proximate analysis is presented in Table 4.1 (Danje, 2011).

The ultimate analysis was conducted on an elemental analyser at the Agricultural Research Council in Pretoria. The lignocellulosic composition was determined at the Sappi Technology Centre, according to standard TAPPI methods (T222, T264, T211 and T249 – TAPPI, 1988a, 1988b, 1985a & 1985b). The high heating value (HHV) of the *E. grandis* sawdust was also determined at the Sappi Technology Centre, on a Leco AC-350 V1.60 Auto Calorimeter.

Table 4.1: TGA method for the proximate analysis of biomass

Sample size	20 mg
Nitrogen flow rate	70 mℓ/min
Temperature range	20–700 °C (N_2 environment)
Heating rate	10 °C/min
Sample hold	7 min @ 700 °C
Gas switch	N_2 to O_2, 15 mℓ/min for 30 min

The results from the proximate and ultimate composition analysis are presented in Table 4.2. The lignocellulosic composition, high heating value and particle size range of the *E. grandis* sawdust are presented in Table 4.3. It should be noted that the moisture content, as determined after the initial air/sun drying for 6 h (± 2.8 wt % d.b.), does not correspond to the moisture content of the actual starting material due to additional processing and handling before the sawdust was charged to the biomass hopper. As mentioned above, the additional processing included particle size reduction (i.e. grinding) and particle size classification (i.e. screening) of the biomass raw material after drying.

Table 4.2: Proximate and ultimate composition of *E. grandis* raw material

Proximate composition	
Moisture	5.4 wt %
Ash	3.5 wt % d.b.
Volatiles	72.7 wt % d.b.
Fixed carbon	21.1 wt % d.b.
Ultimate composition	
Carbon	44.7 wt % d.b.
Hydrogen	5.7 wt % d.b.
Nitrogen	0.5 wt % d.b.
Sulphur	BDL[a]
Oxygen[b]	49.1 wt % d.b.

[a] Below detection limit

[b] by difference

Table 4.3: Lignocellulosic composition and physical properties of *E. grandis* raw material

Lignocellulosic composition	
Extractives	0.3 wt % d.b.
Lignin	31.2 wt % d.b.
α-cellulose	29.3 wt % d.b.
Hemicellulose	35.4 wt % d.b.
Holocellulose	64.8 wt % d.b.
High heating value (HHV)	18.2 MJ/kg
Particle size range	0.5–1.0 mm

4.3 Combustion Fluidised Bed Reactor

4.3.1 Preparation and Start-up

The scalable DFB reactor system detailed in Chapter 3 was utilised for the fast pyrolysis of *E. grandis* sawdust in this investigation. The dual reactor system consists of the combustion fluidised bed (CFB) and the pyrolysis fluidised bed (PFB). Both fluidised bed reactors were operated in the bubbling fluidisation regime. Fused silicon oxide (silica sand) was used as the solid heat carrier and fluidised bed material in both reactors. The fused silica used in this investigation had a mean particle diameter of 0.5 mm ± 0.05 and a solid density of ± 2 500 kg/m^3, which classifies it as a Geldart B solid in terms of Geldart's classification of fluidised bed material. Although fused silica has a relatively low thermal conductivity (± 1.1 W/m.K), its sand-like fluidisation behaviour allows for easy operation in the bubbling fluidisation regime. The amount of fluidised bed material charged to the reactors was measured by weighing before every process start-up.

Based on the estimated fluid and solid properties, as well as the fluidised bed heights, 15 kg and 5 kg of fused silica were charged to the CFB and PFB respectively. However, for a safer and quicker process start-up of the CFB, the total 20 kg of fused silica was charged to the pyrolysis unit via the sand replenish system before start-up of the DFB reactor system. The sand transfer screw was calibrated to determine the sand transfer rate between reactors, based on the speed of the sand screw conveyor. The results from the sand transfer screw calibration are presented in Figure 4.9. This relationship was programmed into the DCS to calculate the sand transfer rate, based on the screw speed.

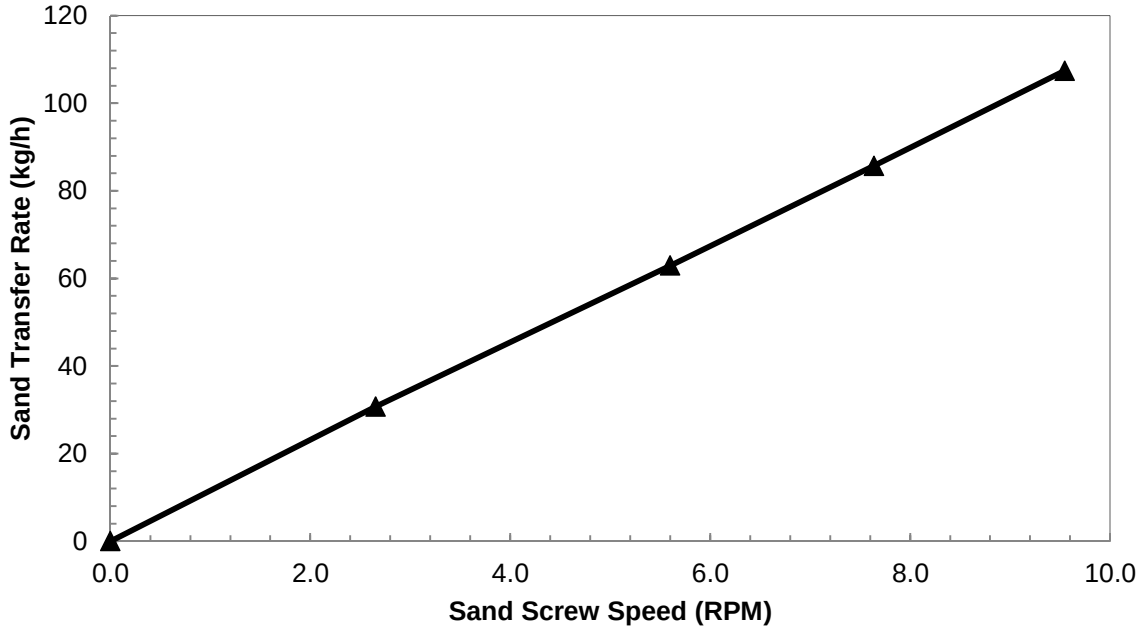

Figure 4.9: Calibration of sand transfer screw conveyor

The fused silica was heated in the combustion unit by means of LPG combustion reactions. The total 20 kg of silica sand was charged to the pyrolysis unit via the sand replenish system before process start-up. This allowed the empty combustion unit to be heated up during start-up conditions, by means of two electrical elements, to a temperature above the auto-ignition temperature of LPG (± 450 °C). Thereafter LPG was introduced into the combustion unit, followed by combustion air. Alternatively, the LPG was ignited in the combustion unit by a piezoelectric igniter installed at the bubble cap distributor. The flue gas extraction system was put into operation before the LPG and air mixture was introduced into the combustion reactor. The cold silica sand in the pyrolysis unit was transferred to the combustion unit, by means of the sand screw conveyor, as soon as a healthy flame was sustained in the combustion reactor. The condition of the combustion unit flame was monitored visually via the borosilicate-glass peephole at the top of the unit, as illustrated in Figure 4.10.

Figure 4.10: Combustion unit during start-up conditions

4.3.2 Process Operation

As the combustion unit started to fill up with sand, the flow rate of the LPG and air were increased proportionally to initiate bubbling fluidisation of the sand bed. At that point, hot sand started to spill over into the pyrolysis unit via the overflow standpipe (z-valve) as shown in Figure 4.11. The sand was continuously heated and circulated until both reactors had reached their desired temperature operating point. The combustion reactor temperature was controlled automatically or manually by manipulating the position of the LPG solenoid valve.

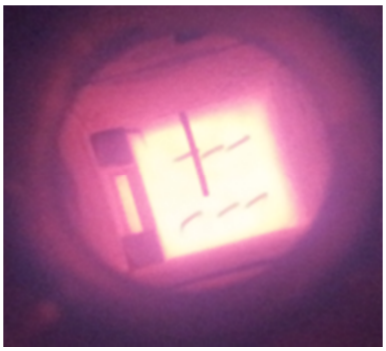

Figure 4.11: Combustion unit during fluidisation conditions

The operating parameters of the CFB reactor are presented in Table 4.4. These parameters, as well as other process variables, were monitored and recorded throughout each experimental run by means of the distributed control and data acquisition system detailed in Section 3.7. The operating parameters reported here are averages from the steady-state operation of the CFB reactor. Note that the CFB reactor temperatures are reported as ranges since the CFB reactor was controlled manually throughout the experimental runs.

Table 4.4: Combustion fluidised bed operating parameters

Operating parameter	Combustion reactor	Source
Bed temperature	670–700 °C	Measurement
Outlet temperature	450–500 °C	Measurement
Air flow [a]	300 ℓ/min	Calculated from air orifice pressure drop
SGV [a]	0.4 m/s	Calculated from volumetric air flow and CFB cross-sectional area
Min. fluidisation velocity	0.2 m/s	Calculated from empirical formula
LPG flow	15 ℓ/min	Measurement
NCG purge flow	4 ℓ/min	Measurement
Bed height	400 mm	Calculated from CFB pressure drop

[a] At process conditions (i.e. temperature and pressure)

The CFB reactor temperatures from a typical experimental run are presented in Figure 4.12. Shown here are trends of the average CFB, CFB outlet, air inlet and flue gas extraction box temperatures. The CFB temperature, as monitored and recorded on the DCS, is an average from three thermocouples within the fluidised bed. It is evident from Figure 4.12 and Table 4.4 that the flue gas exiting the CFB reactor is significantly cooler than the actual fluidised bed temperature as a result of significant heat loss from the reactor. It was concluded that the high heat loss was caused by inadequate and ineffective insulation of both the fluidised bed and freeboard sections of the CFB reactor. Nonetheless, the flue gas exiting the CFB reactor at ± 450–500 °C is still a viable source of high-value heat that could be utilised in various applications, including drying/pre-heating the biomass feedstock and/or pre-heating of combustion air or recycled NCG. Figure 4.13 gives some of the CFB reactor operating parameters, including air blower speed, air flow and superficial gas velocity (SGV), from a typical steady-state run. Characterisation of the combustion reactor products (i.e. flue gas and ash) was outside the scope of this investigation.

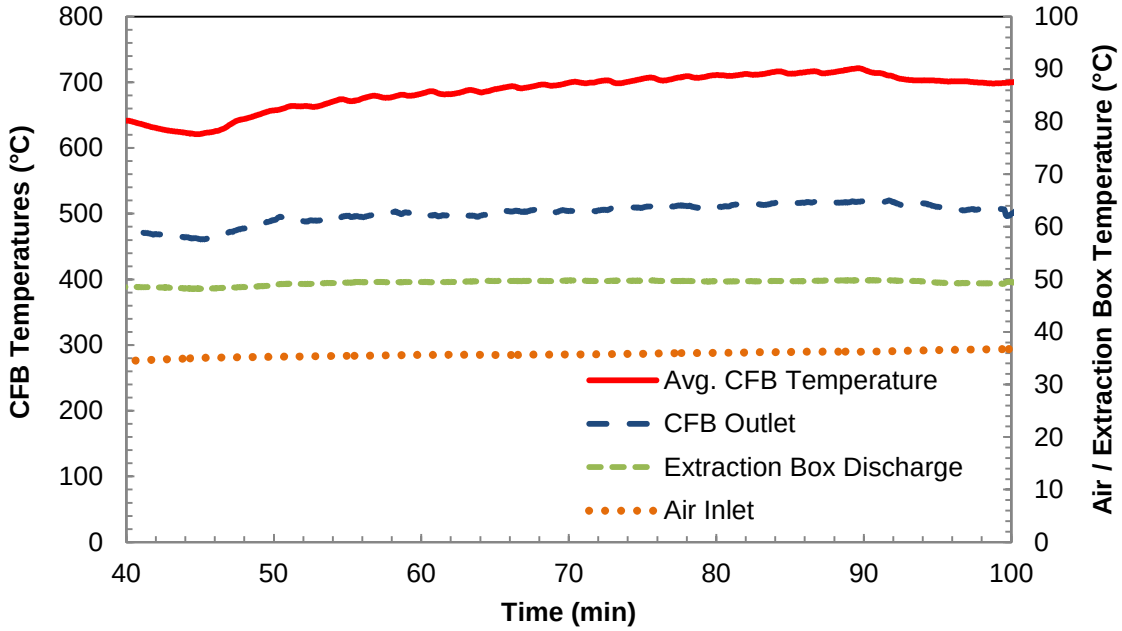

Figure 4.12: CFB reactor temperatures from a typical steady-state experimental run

At the end of each experimental run, the biomass feed screw was stopped to discontinue the fast pyrolysis process. Thereafter, the combustion unit was taken out of operation by closing the LPG solenoid and hand isolation valves. The sand transfer conveyor was stopped to terminate sand circulation. The combustion air blower was also stopped to terminate fluidisation. The sand bed was left to cool overnight, with the extraction system still in operation, before draining the silica sand from the combustion and pyrolysis units. Silica sand remaining in the pyrolysis unit after the shutting down of the dual reactor system was drained through the bottom of the combustion unit by transferring the material to the combustion unit via the sand screw. The total amount of silica sand collected from the combustion and pyrolysis units was measured by weighing and recorded. The ash, and some entrained fluidised bed material, collected from the ash cyclone was also measured by weighing and

recorded at the end of each experimental run. The total amount of sand entrained from the DFB reactor system during its operation was estimated from the weight measurement data, as shown in Table 4.5.

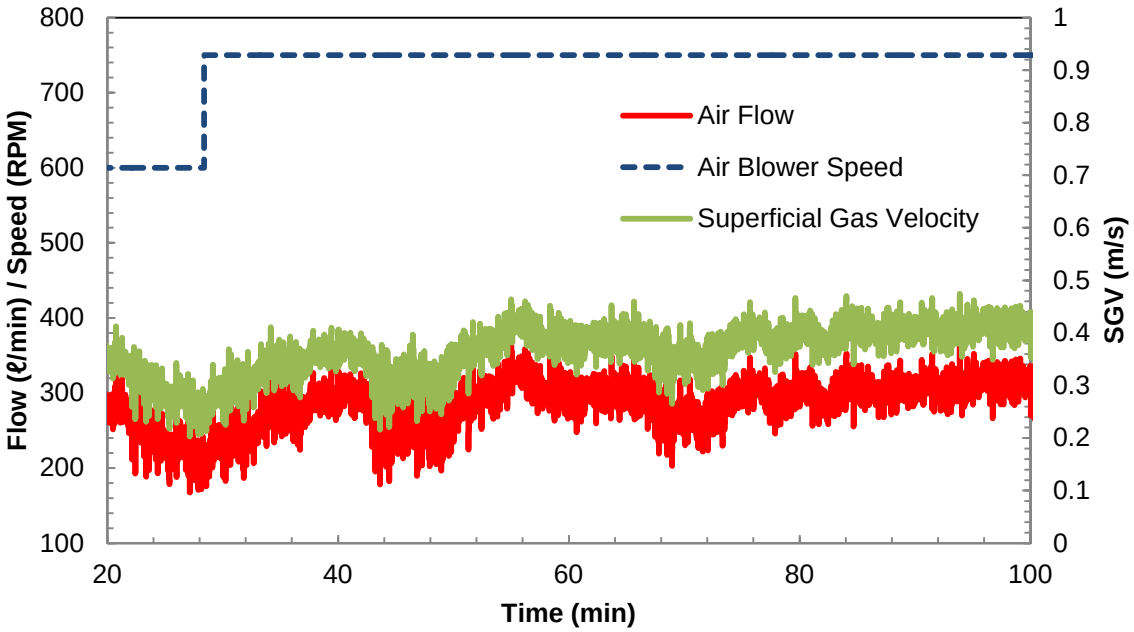

Figure 4.13: CFB reactor operating parameters from a typical steady-state experimental run

Table 4.5: Silica sand entrainment from the DFB reactor system

Parameter	Average value
Total silica sand charged (kg)	20
Silica sand charged to combustion unit (kg)	15
Silica sand charged to pyrolysis unit (kg)	5
Recovered from combustion and pyrolysis unit (kg)	17.8
Entrained from combustion and pyrolysis unit (kg)	2.2
Recovered from ash cyclone (kg)	2.0
Entrained from dual reactor system	0.2
Silica sand loss from combustion and pyrolysis units (wt %)	11%
Total silica sand loss (wt %)	1%

It is clear from the results given in Table 4.5 that a considerable amount (± 11 wt %) of silica sand fluidised bed material was entrained from the two fluidised bed reactors during operation. However, it should be noted that although the silica sand bed material may be subject to some attrition and abrasion in the bubbling fluidised beds, the silica sand used in this investigation was utilised as

received from the supplier and contained a fair amount of fines. The sand fines would inevitably be entrained from the bubbling fluidised beds, especially during start-up conditions. A large fraction of silica sand fines (± 2.0 kg) collected from the ash cyclone at the end of every experimental run provided conclusive evidence of the presence of a large amount of fines in the starting fluidised bed material.

4.4 Pyrolysis Fluidised Bed Reactor

4.4.1 Commissioning

According to Swart (2012), several cold commissioning runs, including that of the CFB, solids transfer mechanism and biomass flow from hopper to pneumatic conveyor, were conducted in order to ensure satisfactory operation of these systems. However, to ensure that the PFB reactor would perform as required during operation, several hot commissioning runs were performed to establish the following: fluidisation of hot solids in the PFB reactor; circulation of hot solids between the PFB and CFB; and control of the PFB temperature. Prior to the hot commissioning runs, the CFB was brought online, as described in Sections 4.3.1 and 4.3.2, in order to heat up the silica sand. The PFB performance was evaluated at different volumetric NCG flow rates. The NCG flow was increased incrementally by increasing the NCG blower speed. While the PFB was being maintained at its desired temperature setpoint (i.e. 500 °C), the influence of NCG flow on fluidisation state, superficial gas velocity, vapour residence time, vapour temperature and NCG feed temperature was monitored and recorded. The fluidisation behaviour of the hot solids bed was observed visually through the top borosilicate sight-glass. Furthermore, biomass sawdust, as described in Section 4.2, was continuously fed to the PFB during the hot commissioning runs. Table 4.6 presents the data from the hot commissioning of the PFB reactor.

At low flow rates of NCG (< 100 ℓ/min), small bubbles were observed at the centre of the PFB as the solids bed moved into a state of minimum fluidisation (i.e. onset of fluidisation). As the NCG blower speed was increased, the higher flow rate of NCG (> 100 ℓ/min) resulted in larger bubbles, which caused the entire bed of solids to take on the appearance of a rapidly boiling liquid (i.e. bubbling fluidisation). As the PFB entered into the bubbling fluidisation regime, hot solids from the overflow standpipe (z-valve) were able to flow freely into the PFB, thereby heating the PFB reactor. It was therefore concluded that the PFB reactor could be operated in the bubbling fluidisation regime by fluidisation with recirculating NCG.

In order to maintain the solids bed in the PFB, the solids were transferred back to the CFB by means of the sand transfer screw conveyor. As the sand transfer screw speed was increased, the solids transfer rate to the CFB increased, which in turn increased the rate of hot solids spilling over into the overflow standpipe (z-valve). Furthermore, by continuously circulating hot solids between the two bubbling fluidised beds, the PFB reactor temperature could be easily controlled automatically, at the

desired setpoint (500 °C), by manipulating the sand transfer screw speed, as demonstrated in Figure 4.14. The excellent temperature control of the PFB reactor makes the DFB system a suitable reactor system for the fast pyrolysis of biomass on a commercial scale.

Table 4.6: Results from commissioning of PFB reactor

Operating parameter	Run 1	Run 2	Run 3	Run 4	Run 5
NCG blower speed (Hz)	40	45	50	55	60
NCG blower speed (%)	67	75	83	92	100
NCG flow (ℓ/min) [a,b]	100	110	120	130	140
SGV (m/s) [a,c]	0.35	0.42	0.45	0.5	0.55
VRT (s)	5	4.2	4.0	3.5	3.2
Avg. NCG feed temperature (°C)	47	50	60	70	75
Avg. bed temperature (°C)	500	500	500	500	500
Avg. outlet temperature (°C)	165	180	195	210	225
Avg. silica transfer rate (kg/h)	36	42	50	57	75

[a] At process conditions (i.e. temperature and pressure)

[b] Total NCG flow rate, including NCG purge

[c] Minimum fluidisation velocity calculated as 0.2 m/s

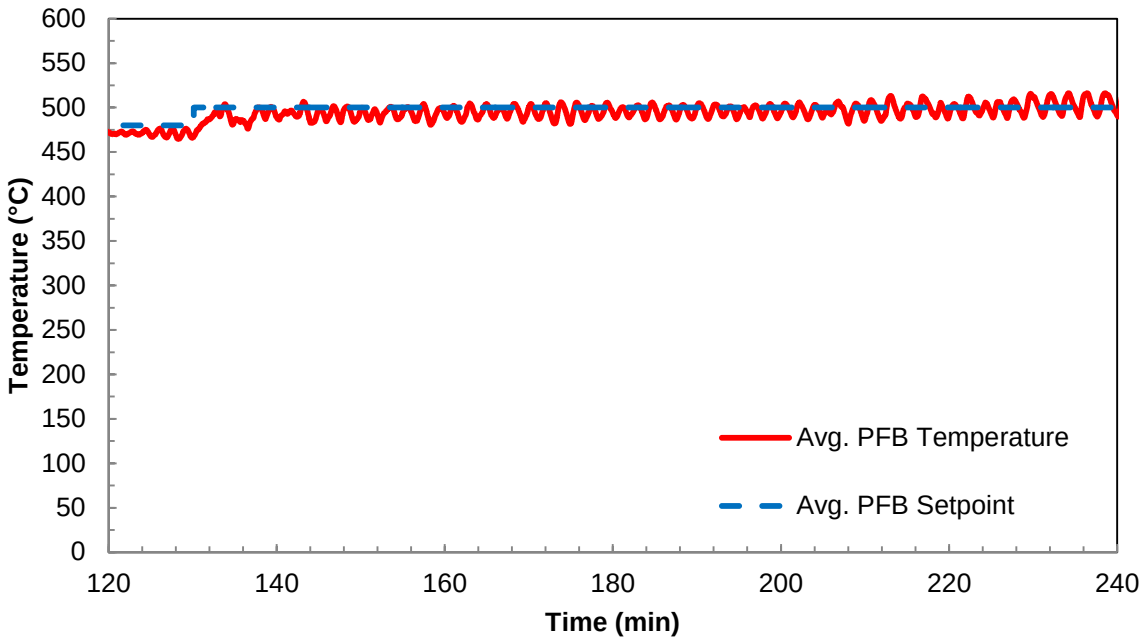

Figure 4.14: Automatic control of PFB temperature

Operation of the PFB in the bubbling fluidisation regime ensures good gas-solid contact which allows efficient heat transfer and good temperature control (Sadaka & Boateng, 2009). However, apart from fluidisation of the PFB, maintaining a sufficiently low VRT (≤ 2–3 s) is of cardinal importance to ensure optimal performance of the PFB, as stated by Bridgwater (2012). The NCG flow rate, and therefore superficial gas velocity, was increased even further to establish the minimum vapour residence time. As demonstrated in Table 4.6, by increasing the NCG blower speed from 40 to 60 Hz, in increments of 5 Hz, the SGV was increased from approximately 0.35 to 0.55 m/s as the NCG flow increased from approximately 100 to 140 ℓ/min. This resulted in a corresponding decrease in the VRT from approximately 5 to 3 s. Nonetheless, it should be noted that operation of the NCG blower at 60 Hz was not sustainable due to the high pressure drop in the NCG recirculation loop. Sustainable operation of the NCG blower, and therefore the complete PFB, could only be accomplished at an NCG blower speed of 50 to 55 Hz, which rendered an average VRT of approximately 4 s. Furthermore, as the NCG flow rate was increased from 100 to 140 ℓ/min, the NCG feed temperature increased from approximately 47 to 75 °C as the vapour outlet temperature increased from approximately 165 to 225 °C. Due to the vapour/NCG absorbing more process heat at the higher NCG flow rate, a higher hot solids transfer rate was required to maintain the PFB temperature at the desired setpoint. Table 4.6 shows that the average silica sand transfer rate increased from 36 to 75 kg/h as the NCG flow rate was increased from 100 to 140 ℓ/min.

As mentioned by Bridgwater (2012), careful control of the pyrolysis reactor temperature (≥ 450 °C), vapour phase temperature (≥ 350 °C) and vapour residence time (≤ 2–3 s) is of the utmost importance to ensure optimal performance of the fast pyrolysis reactor. The results in Table 4.6, as well as visual observation, provide sufficient evidence to conclude that the hot solids bed in the PFB reactor could be fluidised in the bubbling fluidisation regime. Furthermore, successful circulation of hot solids between the PFB and CFB enabled good temperature control of the PFB reactor temperature at the desired setpoint (500 °C). Nonetheless, due to the high pressure drop in the NCG recirculation loop a minimum VRT of only ± 4 s could be sustained, which, according to Bridgwater (2012), may lead to secondary reaction of pyrolysis tars, converting them into bio-char and NCG. Also, due to rather severe heat loss from the pyrolysis unit, a vapour phase temperature of only ± 195 °C could be sustained, which may also result in secondary reaction of pyrolysis tars.

4.4.2 Process Start-up and Operation

Upon successful start-up of the combustion unit the hot silica sand was transferred to the pyrolysis unit by means of the overflow standpipe (z-valve), which in turn started to heat the pyrolysis unit. At that point, the NCG blower was started to initiate gas/air circulation through the pyrolysis unit, bio-oil recovery system and pneumatic biomass feed system. As the pyrolysis unit started to fill up with hot sand, the NCG blower speed was increased proportionally to initiate fluidisation of the hot sand bed. The hot silica sand was continuously circulated, between the two bubbling fluidised beds, while being heated in the combustion unit, until the desired PFB reactor temperature was reached. At that point,

the PFB reactor temperature was controlled automatically, by manipulating the sand transfer screw conveyor speed. As soon as the PFB reactor temperature was controlled at the desired steady-state temperature, the biomass sawdust was introduced by starting the biomass feed screw conveyor and agitator. The first fraction of biomass sawdust that entered the PFB was combusted due to the presence of air/oxygen in the pyrolysis unit during start-up. Visual inspection of the PFB, via the top borosilicate sight-glass peephole, allowed the operator to see the onset of initial combustion as the sawdust burned with a bright orange flame, as shown in Figure 4.15. Furthermore, a sudden increase in PFB temperature was also noticed during initial combustion.

Figure 4.15: Pyrolysis unit during start-up conditions

Upon depletion of the air/oxygen in the pyrolysis unit, the combustion reaction was terminated. At that point, the biomass sawdust started to undergo the endothermic pyrolysis reaction, as was observed visually from the disappearance of the bright orange flame and the generation of thick brownish-yellow smoke. A sudden decrease in the PFB temperature was also noticed during this transition. It was therefore concluded that the required oxygen-free environment in the PFB reactor could be sustained by fluidising the PFB reactor with NCG. The operating parameters of the PFB reactor are presented in Table 4.7. These parameters, as well as other process variables, were monitored and recorded throughout the experimental runs by means of the distributed control and data acquisition system, detailed in Section 3.7. The operating parameters reported here are averages from the steady-state operation of the PFB reactor.

The PFB reactor temperatures from a typical experimental run are presented in Figure 4.16, which shows trends of the PFB temperature setpoint, average PFB, pyrolysis vapour outlet and NCG feed temperatures. The PFB temperature, as monitored and recorded on the DCS, is an average from two thermocouples within the fluidised bed. Also note that the temperature trends include the period of PFB start-up as well as steady-state operation. The initial PFB temperature spike during start-up, from ± 50 °C to ± 350–400 °C, occurred as a result of hot silica sand spilling over into the cold PFB via the overflow standpipe (z-valve). Thereafter, the PFB temperature setpoint was increased incrementally to the desired setpoint of 500 °C. The PFB temperature was controlled at ± 500 °C by manipulating the speed of the sand transfer screw conveyor. It is evident from Figure 4.16 and Table 4.7 that the pyrolysis vapour exiting the PFB reactor is significantly cooler than the actual fluidised bed temperature as a result of significant heat loss from the reactor.

Table 4.7: Pyrolysis fluidised bed operating parameters

Operating parameter	Pyrolysis reactor	Source
Bed temperature	500 °C	Measurement
Outlet temperature	195 °C	Measurement
NCG flow [a,b]	120 ℓ/min	Calculated from NCG orifice pressure drop
SGV [a]	0.45 m/s	Calculated from volumetric NCG flow and PFB cross-sectional area
Min. fluidisation velocity	0.2 m/s	Calculated from empirical formula
VRT	4 s	Calculated from SGV and PFB freeboard height
Sawdust feed rate	2.0 kg/h	Measured by weighing; also calculated from biomass screw speed
Silica transfer rate	50 kg/h	Calculated from sand screw speed
Bed height	200 mm	Calculated from PFB pressure drop

[a] At process conditions (i.e. temperature and pressure)

[b] Total NCG flow rate, including NCG purge

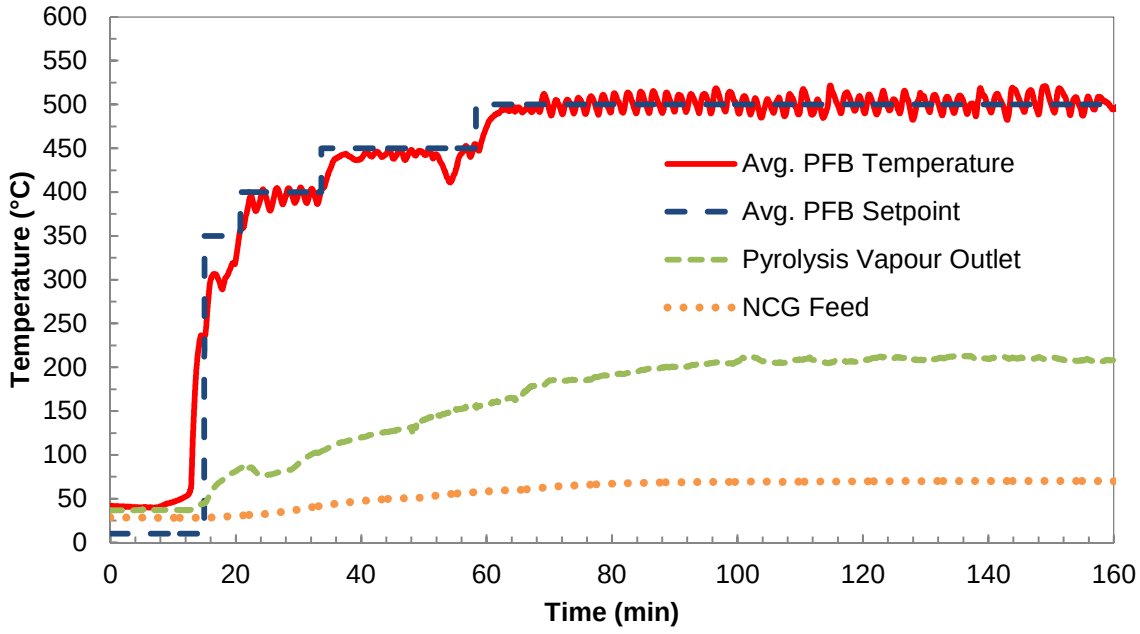

Figure 4.16: PFB reactor temperatures from a typical experimental run

Figure 4.17 presents the PFB reactor operating parameters, including NCG blower speed, NCG flow and SGV from a typical steady-state run. At the end of each experimental run, the biomass feed screw was stopped to discontinue the fast pyrolysis process. The combustion unit was taken out of operation first as described in Section 4.3.2. Thereafter the pyrolysis unit was taken out of operation by stopping the NCG blower. The biomass sawdust that remained in the biomass hopper and feed

screw was drained and collected via the feed screw by removing the distribution unit at the discharge end of the screw. The amount of biomass sawdust that remained after each experimental run was measured by weighing and recorded. The total amount of biomass consumed during each run was determined from the weight measurement data, which also allowed the estimation of an average biomass throughput. Alternatively, the amount of biomass sawdust consumed was determined from the mass indication on the biomass hopper, or calculated from the calibrated speed of the biomass screw conveyor.

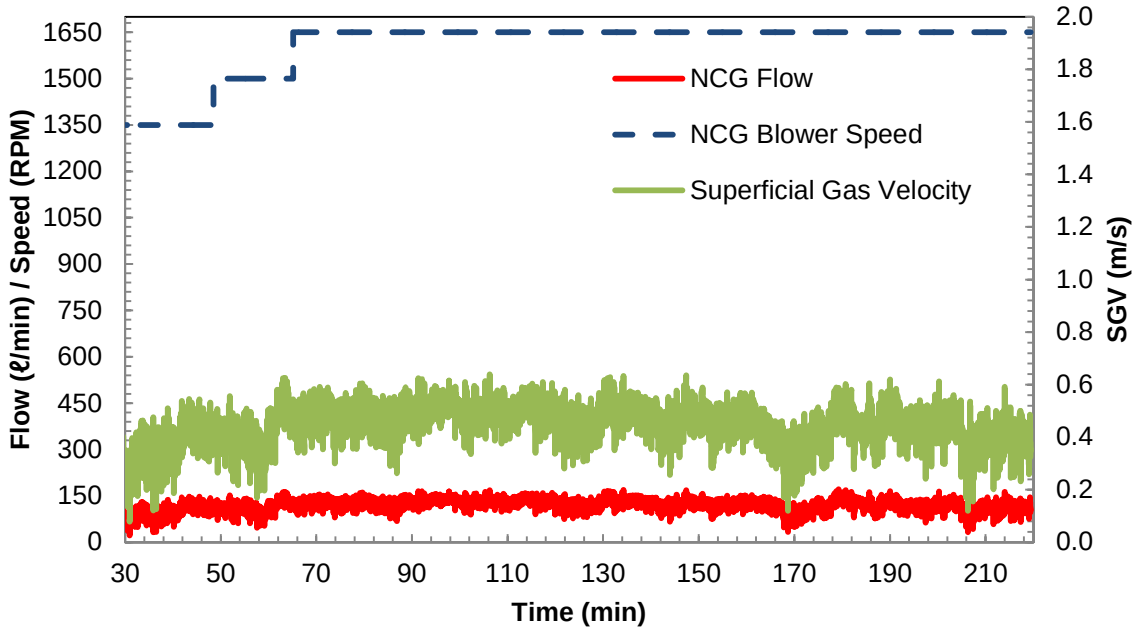

Figure 4.17: PFB reactor operating parameters from a typical steady-state experimental run

The DFB reactor system allows easy separation of bio-char from the pyrolysis vapour by means of the bio-char cyclone. After each experimental run, the bio-char collected was drained from the discharge of the bio-char cyclone. The amount of bio-char collected was measured by weighing and recorded. However, since a large fraction of the bio-char produced was transferred with the silica sand back to the combustion unit, the mass of bio-char collected does not reflect the total amount of bio-char generated. Also, a fraction of silica sand, i.e. fines, was inevitably entrained from the PFB and collected with the bio-char co-product. Since it was impractical to measure the mass of bio-char transferred to the CFB, the overall mass of bio-char produced was determined by mass balance, based on the biomass throughput, liquid product yield and NCG production rate. Figure 4.18 illustrates the combustion of bio-char particles as they enter the CFB with the silica sand. Samples of bio-char collected from the bio-char cyclone are shown in Figure 4.19.

Figure 4.18: Combustion of bio-char particles in the CFB

Figure 4.19: Bio-char samples collected from the bio-char cyclone

Physical and chemical characterisation of the bio-char co-product was conducted at the University of Pretoria, the Agricultural Research Council and the Sappi Technology Centre, South Africa. The proximate analysis of the bio-char was conducted on a PerkinElmer Thermo-gravimetric Analyser (TGA) 4000 at the University of Pretoria. The TGA method used for the proximate analysis is presented in Table 4.1 (Danje, 2011). The ultimate analysis was conducted on an elemental analyser at the Agricultural Research Council in Pretoria. The HHV of the bio-char was determined on a Leco AC-350 V1.60 Auto Calorimeter at the Sappi Technology Centre in Pretoria. Due to the presence of silica sand in the bio-char sample, the total ash content (i.e. inorganics) and hydrochloric acid (HCl) insolubles (i.e. silica) were also quantified, according to standard TAPPI methods (T211 and T244 – TAPPI, 1985a & 1999) at the Sappi Technology Centre.

The NCG produced as co-product from fast pyrolysis were purged to the CFB to maintain the freeboard pressure in the PFB reactor. A volumetric flow indicator transmitter and solenoid valve were installed on the NCG purge line to monitor and manipulate the NCG purge flow to the CFB. The NCG purge rate was used to quantify the production of NCG, based on the biomass feed rate. Samples of NCG were collected from a gas sampling point on the NCG purge line during steady-state operation. FlexiFoil® sample bags were used for NCG sampling. Samples of NCG collected from the designated NCG sampling point are presented in Figure 4.20. The NCG were characterised by gas chromatography-mass spectrometry (GC-MS) to identify the major components. The GC-MS analysis was conducted on a PerkinElmer Clarus 680 gas chromatograph connected to a

PerkinElmer Clarus SQ 8 C mass spectrometer. The GC-MS method for NCG characterisation is presented in Table 4.8. The GC column specifications are presented in Table 4.9. The peaks on the chromatograph were identified by comparing the mass spectra of each peak with the authentic mass spectra of compounds in the National Institute of Standards and Technology (NIST – Gaithersburg, MD, US) library. The HHV of the NCG was estimated from calorific value correlations developed for producer gas (i.e. syngas) by Tasma & Panait (2012).

Figure 4.20: NCG collected in FlexiFoil® sample bags

Table 4.8: GC-MS method for characterisation of NCG

Sample size	30 µℓ
Helium flow rate	1 mℓ/min
Injector temperature	150 °C
Initial oven temperature (sample hold)	35 °C (0 min)
Heating rate	15 °C/min
Final oven temperature (sample hold)	180 °C (20 min)

Table 4.9: GC column specifications for characterisation of NCG

Type	Packed column
Material	Stainless steel
Support	Porapak Q
Mesh size range	80–100 µm
Length	5 m
Outside diameter (OD)	1/8 “
Inside diameter (ID)	2 mm

4.5 Bio-oil Recovery and Collection System

The hot pyrolysis vapour from the PFB was rapidly condensed and cooled in the bio-oil recovery system in order to isolate and collect the condensable fraction known as bio-oil. However, during start-up of the DFB reactor system there was no bio-oil to condense and cool the pyrolysis vapour generated in the PFB. Ethylene glycol (EG) was used as direct cooling medium in the bio-oil recovery system during process start-up. Ethylene glycol (≥ 98%), supplied by Merck Chemicals, was selected as cooling medium based on its low volatility (i.e. high boiling point) and high polarity, which makes it miscible with water and most organic solvents. These properties are common to biomass-derived bio-oils (Boateng, 2011), which makes EG a suitable replacement during start-up conditions. The EG was charged to the bio-oil recovery system prior to every experimental run by means of the bio-oil circulation pump. A designated tie-in point to the bio-oil circulation pump suction was used for charging the EG, as demonstrated in the P&ID in Appendix A. The amount of EG charged was measured by weighing and recorded before every experimental run.

As part of the process start-up, the bio-oil recovery system was put into operation while the CFB was being heated up, as described in Section 4.3.1. This involved charging the known amount of EG and circulating the EG through all the process units in the bio-oil recovery system by means of the bio-oil pump. Thereafter, cooling water was supplied to the bio-oil cooler (brass plate heat exchanger) by opening the hand isolation valve. The hand isolation valve was used to control the flow rate of cooling water to the heat exchanger manually. Furthermore, a new 10 µm melt-blown polypropylene filter element was installed in the cartridge filter before every pyrolysis unit start-up. The mass of the cartridge filter element and bowl were measured by weighing and recorded before and after every experimental run.

As the first pyrolysis vapour entered the bio-oil quencher (brownish-yellow smoke), the EG in the bio-oil recovery system started to darken to a brownish-black colour, as seen in Figures 4.21 and 4.22. Since the quencher, hydrocyclone and demister units were manufactured from borosilicate glass, this colour transition was observed visually. The EG/bio-oil mixture continued to darken as more pyrolysis vapour was condensed. At the end of each experimental run, the liquid product (i.e. EG/bio-oil mixture) was discharged from the bio-oil container by means of the bio-oil circulation pump. A designated take-off point on the bio-oil pump delivery line was used for discharging the liquid. The liquid that remained in the bio-oil recovery system after pumping was drained out under gravity and collected with the rest of the liquid.

The liquid product (EG/bio-oil mixture) collected from a typical experimental run is shown in Figure 4.23. The cartridge filter element and bowl were also removed and weighed at the end of every experimental run to account for entrained liquid from the demister unit. Figure 4.24 shows a spent cartridge filter element after a typical experimental run. It is clear from Figure 4.24 that some condensables were entrained by the NCG and retained by the cartridge filter. However, entrainment

of pyrolysis vapour condensables would inevitably reduce the bio-oil yield as the entrained condensables would be purged to the CFB reactor. The total amount of liquid collected, i.e. from the bio-oil container, drain and NCG filter, was measured by weighing and recorded to estimate the total liquid bio-oil yield after every experimental run.

Figure 4.21: Brownish-yellow pyrolysis vapour entering the bio-oil quencher (RHS)

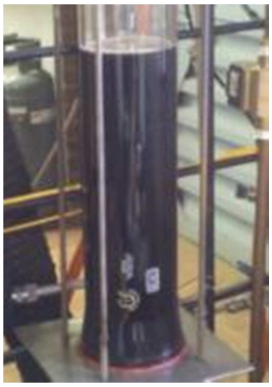

Figure 4.22: Bio-oil/ethylene glycol mixture from hydrocyclone

Figure 4.23: Bio-oil/ethylene glycol mixture in bio-oil container

Figure 4.24: Spent NCG cartridge filter element

The operating parameters of the bio-oil recovery system are presented in Table 4.10. These parameters, as well as other process variables (i.e. bio-oil temperatures), were monitored and recorded throughout the experimental runs by means of the distributed control and data acquisition system, detailed in Section 3.7. The operating parameters reported here are averages from the steady-state operation of the bio-oil recovery system. The bio-oil pump, which is also driven by a variable frequency drive, was operated at its maximum speed to ensure the maximum bio-oil circulation rate through the bio-oil recovery and collection system. Due to the physical characteristics of biomass-derived bio-oil, a flow transmitter was not installed for measuring the bio-oil circulation rate.

Table 4.10: Operating parameters of the bio-oil recovery system

Operating parameter	Bio-oil recovery system	Source
Cooling water flow rate	5 ℓ/min	Measurement
Cooling water temperature	24 °C	Measurement
Bio-oil pump speed [a]	1 500 RPM	VFD

[a] Pump motor speed

Figure 4.25 presents process trends of the bio-oil quencher operation during a typical experimental run. The hot pyrolysis vapour (± 195 °C) enters the bio-oil quencher where it is rapidly cooled and condensed with cold bio-oil (± 24 °C). The liquid bio-oil fraction (i.e. EG/bio-oil mixture) leaves the quencher at ± 25 °C, while the NCG exit the demister at ± 28 °C. At the low biomass throughput (2 kg/h), the cold bio-oil circulation rate was so much higher than the rate of the pyrolysis vapour entering the bio-oil quencher that the cold bio-oil actually functioned as a heat sink, absorbing all the process heat from the pyrolysis vapour without markedly increasing its temperature. This is evident from the process trends in Figure 4.25. However, bear in mind that none of the bio-char cyclone, quencher, demister or hydrocyclone was insulated, which would have allowed a substantial amount

of heat to be dissipated to the surrounding atmosphere. In a scaled-up DFB reactor system, these unit operations would be well insulated to ensure minimal heat loss to the environment. This would enable the cooling water in the bio-oil cooler to absorb all the process heat, which in turn could be utilised in another heating application. The gas-liquid mixture from the bio-oil quencher passes through the hydrocyclone, which allows gas-liquid disengagement. Since the bulk of the sensible and latent heat in the pyrolysis vapour was dissipated in the bio-oil quencher, at the low bio-oil production rate, the cooling duty on the countercurrent bio-oil cooler was minute. This is evident from the process trends of the bio-oil cooler shown in Figure 4.26.

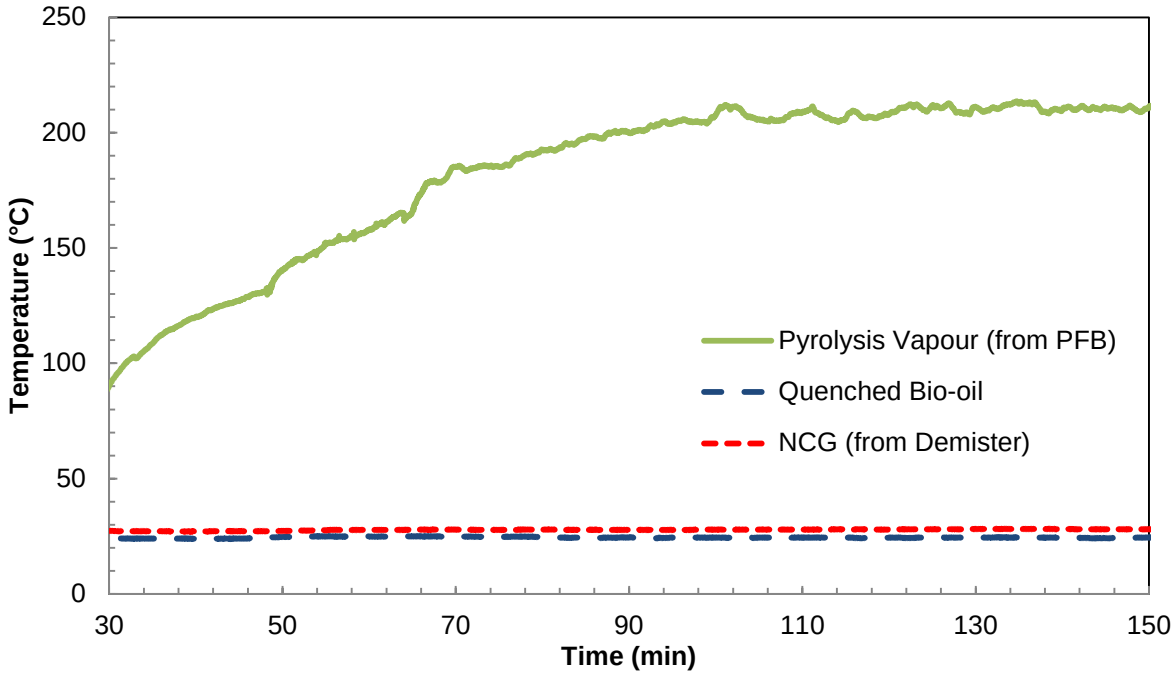

Figure 4.25: Bio-oil quencher operation from a typical experimental run

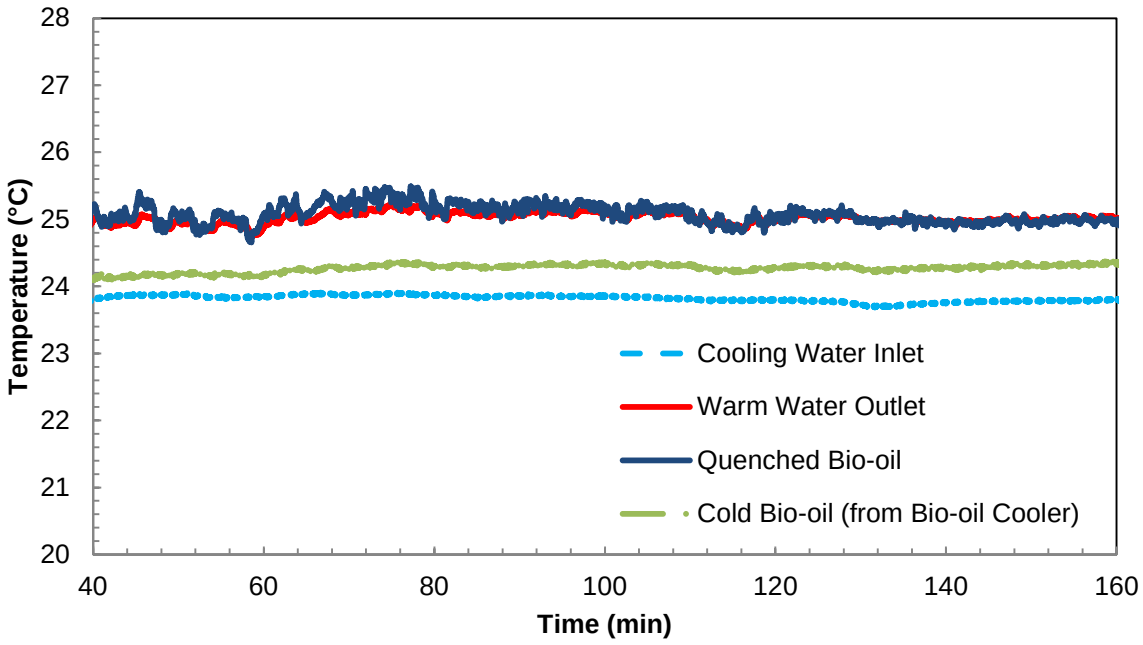

Figure 4.26: Bio-oil cooler operation from a typical experimental run

The addition of EG to the bio-oil recovery system as cooling medium and solvent during process start-up conditions made physical characterisation (i.e. water content, pH, viscosity, calorific value, etc.) of the bio-oil product impractical. Nonetheless, chemical characterisation of the bio-oil was conducted by GC-MS analysis to identify individual bio-oil constituents. Since lignocellulosic biomass is composed of cellulose, hemi-cellulose and lignin, the bio-oil produced should contain derivatives from these three major components (Kim et al., 2013). The GC-MS analysis was conducted on a PerkinElmer Clarus 680 gas chromatograph connected to a PerkinElmer Clarus SQ 8 C mass spectrometer. The GC-MS method for bio-oil characterisation is presented in Table 4.11. An MS5 column of 30 m length and 250 µm inside diameter was used on the GC. The peaks on the chromatograph were identified by comparing the mass spectra of each peak with authentic mass spectra of compounds in the National Institute of Standards and Technology (NIST – Gaithersburg, MD, US) library.

Table 4.11: GC-MS method for identification of bio-oil constituents

Sample size	30 µℓ
Helium flow rate	1 mℓ/min
Injector temperature	150 °C
Initial oven temperature (sample hold)	35 °C (0 min)
Heating rate	15 °C/min
Final oven temperature (sample hold)	180 °C (20 min)

4.6 Pyrolysis Material and Energy Balance

In order to quantify the overall performance of the PFB reactor, a total material and energy balance was conducted according to Equation 4.1. Figure 4.27 presents the PFB reactor system boundary for determining the total material and energy balance. The steady-state sawdust feed rate, total product yields and process information as provided in Tables 4.4 and 4.7 was used as the basis for the material and energy balance. The conversion of the free moisture entering with the sawdust feedstock, as well as of the chemically bound water to water vapour, was also included in the material and energy balance. Furthermore, the material and energy balance assumed complete conversion of biomass sawdust to pyrolysis products.

Biomass + NCG + Heat (hot sand) = Bio-oil + NCG + Bio-char + Heat (reaction, sand, loss) (4.1)

The total material balance was conducted according to the following procedure. Based on the biomass sawdust feed rate, the total product yields were determined as described in Sections 4.4.2 and 4.5. From the product yields, the production rate of the three main products was determined, including the rate at which bio-char was transferred to the CFB. The NCG recycle rate was determined from the online flow measurement. The material balance was then used as the basis for the total energy balance. The energy inputs from biomass sawdust, NCG recycle and hot silica sand, as well as the endothermic pyrolysis heat of reaction, heat losses and energy outputs from all the pyrolysis products, were considered in the total energy balance.

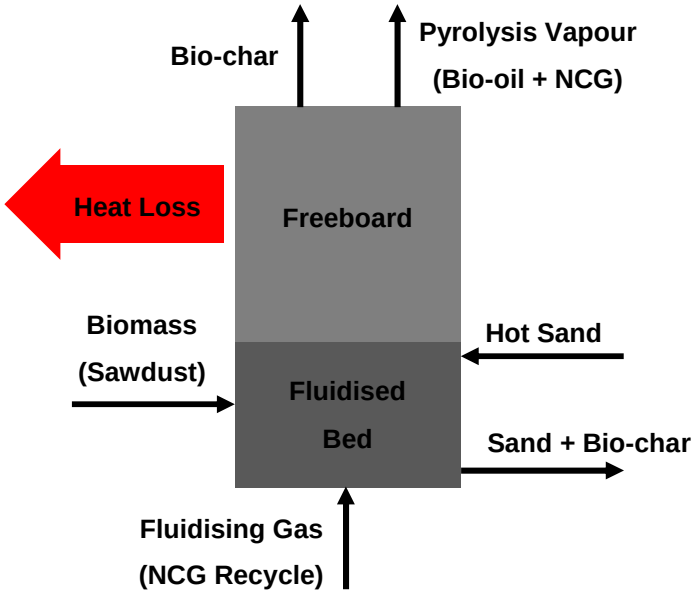

Figure 4.27: System boundary for pyrolysis reactor material and energy balance

5 RESULTS AND DISCUSSION

5.1 Introduction

Fast pyrolysis of woody biomass is the thermochemical conversion process whereby the lignocellulosic components are cracked to produce liquid bio-oil, bio-char and NCG. Although fast pyrolysis is aimed at maximising the liquid bio-oil yield, these three products are produced in varying proportions depending on the feedstock characteristics and fast pyrolysis reactor conditions (Bridgwater, 2012). Numerous investigations have demonstrated that the pyrolysis reactor temperature (i.e. fluidised bed and vapour phase), vapour residence time and feedstock particle size are the operating parameters with the largest influence on the overall product distribution (Oasmaa et al., 2010; Kim et al., 2013; DeSisto et al., 2010; Joubert, 2013; Boateng, 2011).

This chapter provides an overview of the pyrolysis product distribution, as obtained from the fast pyrolysis of *E. grandis* sawdust in the dual fluidised bed (DFB) reactor system. The material and energy balance over the pyrolysis fluidised bed (PFB) is also presented. Section 5.4 provides a summary of the physical and chemical properties of the three fast pyrolysis products. The analytical methods and instrumentation employed for the characterisation of each fast pyrolysis product were presented in Chapter 4. Also, various process benefits and shortcomings of the dual fluidised bed (DFB) reactor system are highlighted and discussed in this chapter.

5.2 Pyrolysis Product Distribution

E. grandis sawdust was pyrolysed in the scalable DFB reactor system at a pyrolysis reactor temperature of 500 °C and a VRT of approximately 4 s. At these experimental conditions, the total bio-oil yield was determined as 36.3 wt % of the dry feedstock. The liquid bio-oil yield includes the organic condensables, most of the pyrolytic water and the free moisture from the biomass feedstock. Based on the specific sawdust feed rate, the NCG yield was estimated from the steady-state NCG purge rate. The NCG yield was determined as 14.0 wt % d.b.

Quantification of the bio-char yield was made difficult by the large fraction of bio-char transported back to the CFB with the silica sand. Since it was impractical to measure this fraction, the overall bio-char yield was determined as the difference from 100%, assuming complete conversion of the biomass sawdust. The bio-char yield was estimated as 49.7 wt % d.b. Table 5.1 provides a summary of the fast pyrolysis product yields as obtained in the scalable DFB system. The expected ranges of pyrolysis product yields, according to Bridgwater (2012), are also presented for comparison. It is evident from Table 5.1 that the bio-oil yield obtained from the scalable DFB reactor system is at the lower end of the expected bio-oil yield range, while the bio-char yield is substantially higher than anticipated.

Table 5.1: Fast pyrolysis product yields

Product	Actual yield (wt % d.b.)	Expected yield (wt % d.b.) [c]
Bio-oil	36.3 [a]	30–75
NCG	14.0	13–35
Bio-char	49.7 [b]	12–35

[a] Total liquid yield

[b] By difference

[c] Typical pyrolysis product yields (Bridgwater, 2012)

Throughout the commissioning and operation of the scalable DFB reactor system, a number of process inefficiencies and/or limitations were identified that compromised the performance of the pyrolysis system at the expense of a reduced bio-oil yield. In order to favour the production of bio-oil and suppress the generation of bio-char and NCG co-products, the fast pyrolysis process has to adhere to specific process conditions.

According to Bridgwater (2012), in order to ensure maximum liquid yield, not only should the pyrolysis reactor temperature be above 450 °C, but the vapour phase temperature should also be around 350–400 °C. Even though the PFB temperature was controlled at 500 °C, the temperature of the vapour phase exiting the PFB could only be maintained at 195 °C. This severe temperature difference is a direct result of excessive heat loss, as demonstrated in the energy balance in Section 5.3. As demonstrated by Boateng (2011) in Figure 2.8, this lower temperature (< 400 °C) favours the formation of bio-char at the expense of a lower liquid bio-oil yield. This effect is exacerbated at even lower vapour-phase temperatures (< 300 °C) when near-torrefecation conditions are reached, which may result in bio-char yields as high as 80 wt % d.b. (Bridgwater, 2012). Insulating the PFB reactor more effectively would minimise the heat loss and suppress bio-char formation as a result of a low pyrolysis temperature.

The pyrolysis VRT is another vital process condition to adhere to in order to maximise the liquid bio-oil yield and prevent secondary tar reactions from forming bio-char and NCG (Joubert, 2013). According to Bridgwater (2012), the pyrolysis VRT should not exceed 2–3 s. However, due to process limitations, the minimum pyrolysis VRT that could be sustained was 4 s. Although it may not be excessively higher than the ideal VRT (< 2–3 s), it does allow secondary tar reactions to form bio-char and NCG at the expense of a lower liquid bio-oil yield. Furthermore, the longer VRT also exposes the pyrolysis vapour to bio-char and ash for a prolonged period, which has been demonstrated to have a catalytic effect on pyrolysis vapour cracking to NCG (Crocker, 2010: 151). The pyrolysis VRT may be reduced by increasing the volumetric flow rate of NCG through the PFB reactor. This subsequently increases the SGV, which in turn reduces the VRT. In this investigation,

the volumetric flow rate of NCG was limited by the high pressure drop in the NCG recirculation loop. Reducing the pressure drop in the NCG recirculation loop would therefore ensure a lower VRT and mitigate the formation of pyrolysis co-products as a result of a high pyrolysis VRT.

As mentioned, the bio-char has a catalytic effect on the pyrolysis vapour, cracking the organic condensables to NCG with a lower molecular weight and thereby reducing the bio-oil yield. The bio-char co-product must therefore be separated from the pyrolysis vapour as soon as it leaves the PFB reactor. The DFB reactor system allows easy bio-char separation by means of the bio-char cyclone. However, some residual bio-char was detected in the liquid bio-oil product after the bio-oil samples had been subjected to a centrifugal separator. The presence of residual bio-char in the final bio-oil product, together with the higher VRT, provides sufficient evidence to suggest that pyrolysis vapour cracking may also have contributed to the reduced liquid bio-oil yield. Installation of multiple bio-char cyclones in series has demonstrated enhanced separation of bio-char from the pyrolysis vapour in similar fast pyrolysis investigations (Oasmaa et al., 2010; Joubert, 2013).

Furthermore, it is believed that a few inefficiencies in the bio-oil recovery and collection system may have resulted in the entrainment of pyrolysis vapour condensables with the NCG. Since a fraction of the NCG is purged to the CFB reactor, the entrained pyrolysis vapour condensables would be lost via the purge stream, thereby reducing the bio-oil yield. During operation of the bio-oil recovery and collection system, condensable vapour leaving the demister unit was detected visually. Apart from poor liquid-gas disengagement in the bio-oil demister, improved vapour-liquid contact in the bio-oil quencher would also reduce the amount of entrained pyrolysis vapour condensables. Alternative liquid-gas disengagement units, such as an electrostatic precipitator (ESP), have proved more efficient at recovering entrained condensables in similar investigations (Oasmaa et al., 2010; Joubert, 2013; Kim et al., 2013). It was therefore concluded that the lower liquid bio-oil yield, and the consequently higher bio-char and NCG yield, resulted from the abovementioned process inefficiencies and/or limitations.

5.3 Pyrolysis Material and Energy Balance

5.3.1 Material Balance Results

A total material and energy balance was conducted in order to quantify the performance of the PFB reactor. The biomass feed rate and fast pyrolysis product yields, together with the process information from the experimental runs, were used as the basis for the steady-state material and energy balance. The results obtained from the material balance are summarised in Table 5.2.

Table 5.2: Material balance over fast pyrolysis reactor

Compound	In (g/h)	Generated (g/h)	Consumed (g/h)	Out (g/h)
Sawdust	1 893.0 [a]	-	1 893.0	-
Bio-oil	-	687.8	-	687.8
NCG	7 689.7 [b]	265.2 [c]	-	7 954.9
Bio-char	-	940.0 [d]	-	940.0
Silica sand	50 000	-	-	50 000

[a] Dry sawdust feed

[b] NCG recycle

[c] NCG purge

[d] Total bio-char, including collected and combusted

The total material balance assumed complete conversion of the biomass sawdust to fast pyrolysis products, namely bio-oil, bio-char and NCG. The yield of pyrolysis products, on a dry feedstock basis, was determined as 36.3 wt %, 14.0 wt % and 49.7 wt % for bio-oil, NCG and bio-char respectively. The bio-oil production rate was determined as 687.8 g/h and includes organic condensables, free moisture entering with the sawdust and pyrolytic water. The NCG recycle rate, as estimated from online measurement, was determined as 7 689.7 g/h, while the NCG purge or production rate was determined as 265.2 g/h. The total production rate of bio-char was determined as 940.0 g/h, of which only 13.0 g/h was collected from the bio-char cyclone. Since the PFB reactor was operated at a considerably lower SGV than the design intent (i.e. 0.4 vs. 1 m/s), the entrainment of bio-char particles was subdued, which resulted in the low proportion of bio-char collected from the bio-char cyclone. As mentioned, the PFB was operated at a lower SGV because the volumetric flow rate of NCG was limited by the high pressure drop in the NCG recirculation loop.

The balance of the bio-char, i.e. 927.0 g/h, was assumed to be transferred to the CFB reactor with the silica sand. Physical measurement of this bio-char fraction was unfortunately impractical. Nonetheless, combustion of an excessive amount of bio-char was observed visually during the pyrolysis operation, as demonstrated in Figure 4.18, Section 4.4.2. Furthermore, the collection of a substantial amount of fly ash from the ash cyclone suggests combustion of bio-char in the CFB reactor. Although some silica sand fines were entrained from the PFB reactor during process commissioning and start-up, silica sand entrainment from the PFB reactor was not included in the total material balance as it accounted for less than 0.02% of the total sand transfer rate. Therefore, it was assumed that the total amount of hot silica sand spilling into the PFB reactor, via the z-valve, left the unit through the sand transfer screw conveyor at the bottom of the PFB.

5.3.2 Energy Balance Results

The results from the total material balance were used as the basis for the energy balance. The total energy balance considered energy inputs from the sawdust feedstock, silica sand and NCG, as well as the heat of reaction, heat losses and energy outputs from the pyrolysis products. The results obtained from the energy balance are summarised in Table 5.3.

Table 5.3: Energy balance over fast pyrolysis reactor

Component	Value (W)
In	150
Generated	-
Consumed (i.e. heat of reaction)	1 000
Sand (i.e. heat carrier)	3 889
Out	344
Losses (i.e. process heat)	2 696

As seen in Table 5.3, the total energy input from the biomass feedstock and recycled NCG was determined as 150 W. The energy balance neglected any heat generated from the partial combustion of the pyrolysis feedstock or products. The amount of energy supplied to the PFB by means of the hot silica sand was determined as 3 889 W. The total energy requirement for the endothermic pyrolysis of the sawdust feedstock was determined as 1 000 W. As mentioned, the pyrolysis reactor freeboard temperature (195 °C) was much lower than the fluidised bed temperature (500 °C) as a result of severe heat loss. Therefore, the energy output from the pyrolysis products was determined as only 344 W. The overall heat loss from the PFB reactor was estimated at a huge and unanticipated 2 696 W. This implies that approximately 69% of the total energy supplied to the PFB reactor by means of the hot silica sand was dissipated to the surrounding atmosphere. The high heat loss was due to insufficient and ineffective insulation of both the fluidised bed and freeboard sections of the PFB reactor.

5.3.3 Heat Loss Evaluation

The PFB reactor was only insulated with 25 mm of ceramic fibre wool fitted to the outside of the 3 mm carbon steel shell. This resulted in a substantial heat loss as demonstrated in Table 5.3. A heat transfer resistance network, which considers convective and conductive heat transfer, was developed for the PFB reactor to illustrate the heat transfer through the various layers of material surrounding the pyrolysis reaction zone, as presented in Figure 5.1. Due to the lack of insulating material, the total resistance to heat transfer from the pyrolysis reaction zone was determined as only 0.4 $K.m^2/W$, which yields a total heat flux of 1 371 W/m^2 from the PFB reactor. As a result of the high heat flux, the

PFB reactor surface temperature was estimated as 157 °C, as presented in Figure 5.2. The high PFB reactor surface temperature results in a high temperature driving force (± 130–140 °C) for heat transfer, which explains the severe heat loss to the surrounding atmosphere. As one would expect, the severe heat loss has a huge effect on the throughput and overall performance of the PFB reactor as less energy is available to drive the endothermic pyrolysis reaction. From the energy balance results in Table 5.3 it is evident that if sufficient insulation could be supplied to the PFB reactor, the biomass throughput could be expected to increase by as much as 2.5 to 3 times the recorded throughput, at the same hot silica transfer rate. Furthermore, since the solids transfer mechanism is capable of sustaining a transfer rate double that of the recorded rate (i.e. 100 kg/h), the biomass throughput could be expected to increase by as much as 5.5 to 6 times the recorded throughput.

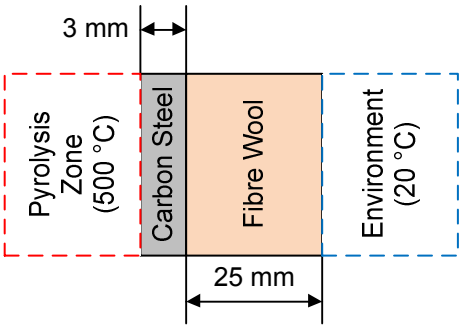

Figure 5.1: Pyrolysis reactor heat transfer resistance network

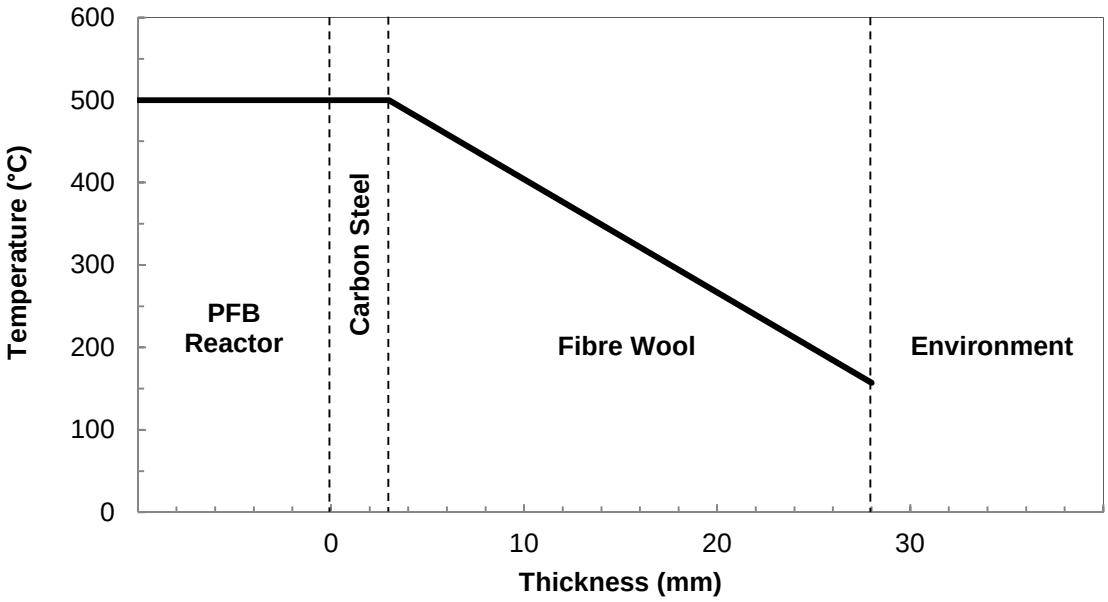

Figure 5.2: Pyrolysis reactor surface temperature profile

The heat loss problem in the DFB reactor system was not limited only to the PFB reactor, but also included the CFB reactor to a lesser extent. Heat loss from the CFB was more subdued due to several layers of insulating material. The CFB reactor was insulated with 25 mm castable refractory on the inside, a 15 mm layer of Vermiculite insulating material between the castable refractory and the outer shell, and a 25 mm layer of ceramic fibre wool fitted to the outside of the shell. A heat transfer resistance network, which considers convective and conductive heat transfer, was developed for the CFB reactor to illustrate the heat transfer through the various layers of material surrounding the combustion reaction zone, as presented in Figure 5.3.

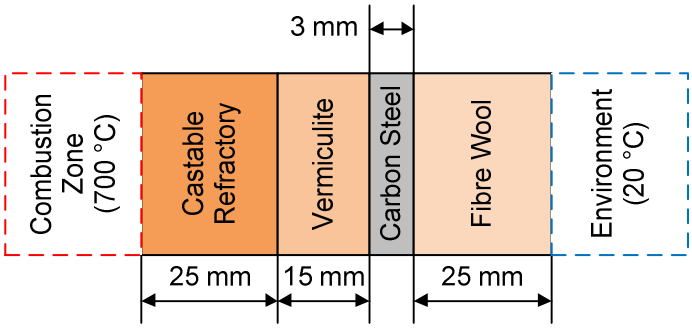

Figure 5.3: Combustion reactor heat transfer resistance network

Even though the CFB reactor was insulated with a number of insulating materials, the total resistance to heat transfer from the combustion reaction zone was determined as only 0.5 K.m^2/W, which yields a total heat flux of 1 339 W/m^2 from the CFB reactor. As a result of the high heat flux, the CFB reactor surface temperature was estimated as 154 °C, as shown in Figure 5.4. The high CFB reactor surface temperature results in a high temperature driving force (± 130–140 °C) for heat transfer, which would also lead to severe heat loss to the surrounding atmosphere.

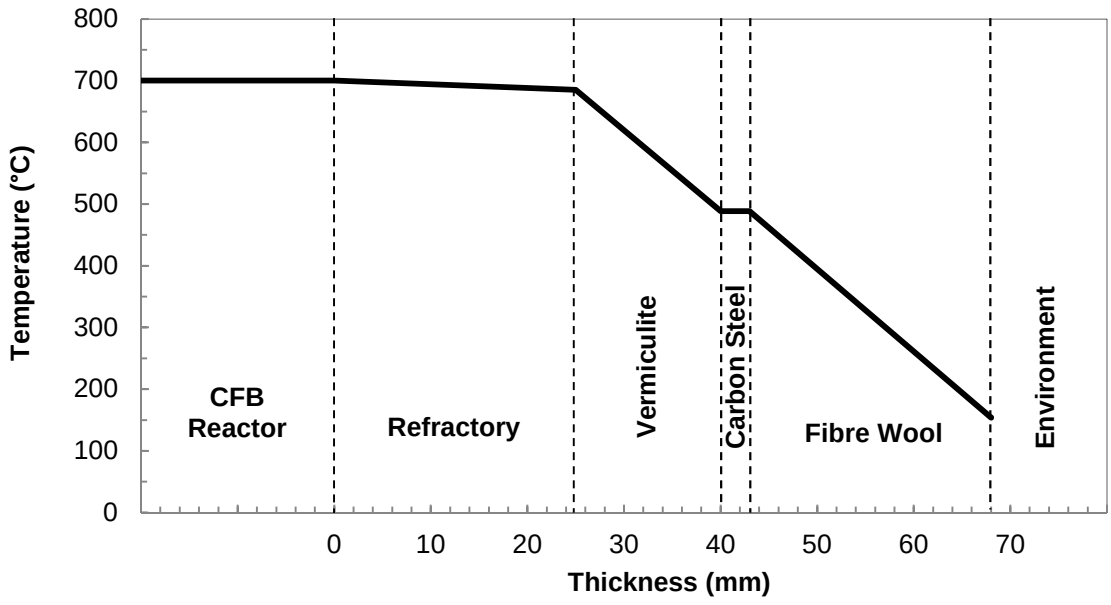

Figure 5.4: Combustion reactor surface temperature profile

It is clear from Figures 5.2 and 5.4 that even though the CFB reactor has more layers of insulating material, the anticipated resultant reactor surface temperature (indicated as fibre wool) is very similar to that of the PFB reactor. This is because the CFB reactor operates at a much higher temperature than the PFB reactor. Nevertheless, heat loss from the CFB reactor also influenced the operation of the PFB reactor. As shown previously in Table 4.4, Section 4.3.2, the CFB reactor was operated at only 700 °C, compared with the predicted 900 °C, as a result of excessive heat loss. As the silica sand heat-carrier was cooler than predicted, the sand transfer screw conveyor had to work harder to supply sufficient heat to the PFB reactor in order to sustain the temperature and the biomass throughput. As seen in Table 5.2, an average silica sand transfer rate of 50 kg/h was used in order to maintain the PFB reactor temperature at 500 °C, while sustaining the sawdust throughput at 2 kg/h. However, from the total energy balance it was determined that the PFB reactor temperature and biomass throughput could have been sustained at an average silica sand transfer rate of only 25 kg/h if the CFB reactor had been operated at the design temperature of 900 °C.

It is therefore evident that excessive heat loss from the PFB and CFB reactors compromised the performance of the DFB reactor system. According to initial process modelling of the DFB reactor system conducted by Swart (2012), the projected heat losses were somewhat underestimated. This resulted in a much higher anticipated biomass throughput in the DFB reactor system than what was actually achieved in this investigation. Table 5.4 provides a comparison of the predicted versus actually attained PFB reactor heat loss and the subsequent biomass throughput capability.

Table 5.4: Comparison of actual vs. predicted pyrolysis unit heat loss and biomass throughput

Parameter	Model prediction	Actual attained
Biomass throughput (kg/h)	20	2
Heat of reaction requirement (kW)	10	1
Heat supplied by silica sand (kW)	13.2 [b]	3.9 [c]
Heat loss	1	2.7
Loss of heat supply (%) [a]	± 7.6	± 69.2

[a] Expressed as the percentage heat loss based on heat supply from silica sand

[b] Silica sand at 900 °C, according to model prediction

[c] Silica sand at 700 °C, according to actual process data

It is clear from Table 5.4 that the actual process heat loss from the PFB reactor was greatly underestimated in the initial process model prediction. The model accounted for only approximately 7.6% of the total energy input by hot silica sand to be dissipated due to process inefficiencies. The actual heat loss determined from the process operation was almost 10 times higher at approximately 69.2%. The low sustainable biomass throughput attained (i.e. 2 kg/h), approximately 10 times less

than the predicted throughput (i.e. 20 kg/h), therefore comes as no surprise. These numbers surely justify the installation of adequate insulating materials on both the PFB and CFB reactors before the commencement of any further investigations as heat loss from these two units severely compromises the performance of the DFB reactor system.

5.4 Pyrolysis Product Characterisation

5.4.1 Bio-oil

Liquid bio-oil, also known as pyrolysis oil, is produced as the main product from the fast pyrolysis of lignocellulosic biomass. Since this biomass is composed of cellulose, hemi-cellulose and lignin, the bio-oil produced contains derivatives from these three major components (Kim et al., 2013). Pyrolysis liquid consists of a complex mixture of oxygenated hydrocarbons with a substantial amount of water from the pyrolysis reaction, known as pyrolytic water, as well as from the biomass feedstock (Crocker, 2010: 164). The liquid bio-oil product was obtained, by means of rapid quenching and cooling, from the bio-oil recovery and collection system, as detailed in Section 4.5. The tars produced during fast pyrolysis, i.e. organic condensables, are collected with the pyrolytic water and the majority of the free moisture entering with the sawdust raw material.

The addition of ethylene glycol to the bio-oil recovery system as cooling medium and solvent during process start-up conditions made physical characterisation (i.e. water content, pH, viscosity, calorific value, etc.) of the bio-oil product impractical. Nonetheless, chemical characterisation of the *E. grandis* bio-oil, as produced in the scalable DFB reactor system, was conducted by GC-MS analysis to identify individual bio-oil components. However, due to the inherent complexity of bio-oil, complete identification of all bio-oil components by GC-MS is impractical as more than 300 chemical components have been reported in biomass-derived bio-oils (Lu, Li, & Zhu, 2009). Furthermore, the ethylene glycol appeared broadly at retention times between 4 and 8 min and unfortunately overlapped with several other signals, which made the identification of numerous other components inconclusive.

Approximately 60 peaks appeared on the chromatograph, of which 20 were identified. The most prominent peaks on the chromatograph were identified by comparison of the mass spectra of each peak with authentic mass spectra of compounds in the National Institute of Standards and Technology (NIST – Gaithersburg, MD, US) library. Several compounds from the pyrolysis of carbohydrates and lignin were identified in the bio-oil derived from *E. grandis*, as demonstrated in Table 5.5. These include organic acids, alcohols, esters, sugars, aldehydes, ketones, furans, pyrans and phenolics. The identified components are consistent with hardwood-derived bio-oils from similar pyrolysis investigations (Azeez et al., 2010; Kim et al., 2013).

Table 5.5: Identification of *E. grandis* bio-oil components by GC-MS analysis

Group	Components
	Water
Solvent	Ethylene glycol
Acids	Formic acid
	Acetic acid
Carbohydrates	2-furaldehyde (furfural)
	1-hydroxy-2-propanone (acetol)
	2(5H)-furanone
	1-hydroxy-2-butanone
	2-hydroxy-3-methyl-2-cyclopenten-1-one
	1,6-anhydro-β-D-glucopyranose (levoglucosan)
Lignin	phenol
	2-methyl-phenol (o-cresol)
	4-methyl-phenol (p-cresol)
	3-methyl-phenol (m-cresol)
	2,6-dimethoxy-phenol
	2,4-dimethylphenol (m-xylenol)
	4-hydroxy-3,5-dimethoxy-benzaldehyde
	3,5-dimethoxy-4-hydroxycinnamaldehyde
	2,6-dimethoxy-4-(2-propenyl)-phenol
	1-hydroxy-2-ethylbenzene (2-ethyl-phenol)

As one would expect, a prominent peak was identified for ethylene glycol. As mentioned, for the purpose of this investigation ethylene glycol was used as direct cooling medium in the scalable DFB reactor system for recovering bio-oil from the pyrolysis vapour. However, in practice, the ethylene glycol would be replaced with pyrolysis-derived bio-oil to quench and cool the hot pyrolysis vapour in the bio-oil recovery and collection system. A prominent peak for water was also identified due to the presence of inherent and pyrolytic water. Several organic acids, including acetic and formic acid, were identified, which would contribute to the characteristic low pH of biomass-derived bio-oils (Oasmaa et al., 2010; Sadaka & Boateng, 2009).

The degradation products identified from the pyrolysis of carbohydrates include furfural, 1-hydroxy-2-propanone (acetol), 2(5h)-furanone, 1-hydroxy-2-butanone, 2-hydroxy-3-methyl-2-cyclopenten-1-one, and 1,6-anhydro-β-d-glucopyranose (levoglucosan). According to Kim et al. (2013), hemi-cellulose is the most susceptible to thermal degradation, and degrades to form water and furfural. Furthermore, the prominent levoglucosan peak identified results from the pyrolysis of cellulose (Kim et al., 2013). Due to the phenolic nature of lignin, most lignin degradation products are also of a phenolic nature. Table 5.5 lists a few phenolic compounds, characteristic of lignin pyrolysis, that were identified by GC-MS analysis.

The results in Table 5.5, as well as the results from similar fast pyrolysis investigations (Azeez et al., 2010; Oasmaa et al., 2010; DeSisto et al., 2010; Kim et al., 2013), illustrate the presence of highly oxygenated compounds in bio-oil derived from fast pyrolysis of lignocellulosic biomass. According to Bridgwater (2012), the high bio-oil oxygen content adversely affects bio-oil fuel quality and renders the crude bio-oil incompatible with conventional transportation-grade fuels. Despite this shortcoming, the bio-oil produced from the fast pyrolysis of *E. grandis* sawdust in the DFB reactor system may still be utilised in its crude form for heat generation when co-fired with conventional fossil fuels, including heavy furnace oil, etc. (Crocker, 2010: 174–177).

In order to enhance the quality of crude bio-oil fuel, and ultimately its value, deoxygenation of the bio-oil compounds is essential. According to Bridgwater (2012) and Butler et al. (2011), bio-oil deoxygenation can be accomplished either by integrated catalytic (in situ) pyrolysis or by a close decoupled operation employing one of many available upgrading technologies. These upgrading technologies are aimed at deoxygenating the crude liquid bio-oil, thereby increasing its HHV and hydrocarbon fuel miscibility, resulting in a bio-oil product that is compatible with conventional petroleum refinery streams for conversion to transportation-grade fuels (Bridgwater, 2012). The scalable DFB reactor system allows for in situ catalytic fast pyrolysis by replacing the silica sand fluidised bed material with a viable solid catalyst (e.g. ZSM-5) as heat carrier. As stated by Bridgwater (2012), this practice is not uncommon as a number of combined pyrolysis-catalysis reaction systems have been investigated with positive outcomes. In situ catalytic fast pyrolysis enables catalytic cracking of the biomass feedstock and the subsequent pyrolysis vapours to selectively produce deoxygenated bio-oil compounds, with the rejection of oxygen as H_2O and/or CO_2 depending on the catalyst employed (Butler et al., 2011). Although catalysts employed for in situ catalytic fast pyrolysis are prone to coking, the scalable DFB reactor system allows for catalyst regeneration by combustion of the coke in the CFB reactor.

5.4.2 Bio-char

Solid bio-char is produced as co-product from the fast pyrolysis of lignocellulosic biomass. According to Kim et al. (2013), the bio-char consists primarily of carbon, hydrogen and inorganics. The presence of carbon and hydrogen makes bio-char an attractive solid fuel with a high heating value comparable to that of high-grade coals. The inorganic proportion is strongly dependent on the ash content of the biomass feedstock from which it is derived (Crocker, 2010: 151). A fraction of the bio-char produced in the DFB reactor system was collected from the bio-char cyclone. As mentioned, most of the bio-char produced was transported back to the CFB with the silica sand heat carrier. Physical and chemical characterisation of the bio-char collected was conducted according to the analysis methods detailed in Section 4.4.2. The results from the physical and chemical characterisation of the bio-char produced from the fast pyrolysis of *E. grandis* sawdust are presented in Table 5.6.

It is evident from the results in Table 5.6 that the total inorganic portion of the bio-char is much higher than anticipated, based on the low ash content (3.5 wt % d.b.) of the biomass feedstock. Due to the impractically high proportion of inorganics, the bio-char samples were further analysed for hydrochloric acid (HCl) insolubles, i.e. for silica content, in order to differentiate the ash fraction from the entrained silica sand fraction. As demonstrated in Figure 4.19, Section 4.4.2, entrained silica sand fluidised bed material was observed visually in the bio-char samples collected. The results from the bio-char inorganics fractionation analysis are also presented in Table 5.6. The total amount of entrained silica bed material accounted for approximately 77.0 wt % of the total inorganic fraction, with the balance being ash from the biomass feedstock. As one would expect, the ash entering with the biomass feedstock will inevitably be concentrated in the bio-char co-product as it is also removed from the pyrolysis vapours in the bio-char cyclone. Due to the high amount of entrained silica sand in the bio-char, the HHV, as determined by bomb calorimeter, was recorded as only 17.0 MJ/kg. This comes as no surprise as approximately 54.4 wt % d.b. of the bio-char material consists of incombustible material.

It is clear from the results in Table 5.6 that the entrainment of silica sand from the DFB reactor system compromised the bio-char quality, as it is collected with the bio-char co-product from the bio-char cyclone. However, it should be noted that although the silica sand bed material may be subjected to some attrition and abrasion in the bubbling fluidised beds, the silica sand used in this investigation was utilised as received from the supplier and contained a fair amount of fines. The sand fines would inevitably be entrained with the pyrolysis vapour and collected with the bio-char, especially during start-up conditions or during short periods of operation. A large fraction of silica sand fines (± 2.0 kg) collected from the ash cyclone at the end of every experimental run provided conclusive evidence of the presence of a large amount of fines in the starting fluidised bed material. However, operation of the DFB reactor system for prolonged periods would ultimately allow thorough particle classification of the fluidised bed material, thereby significantly reducing the amount of fines entrained and collected with the bio-char co-product. This would eventually result in better-quality

bio-char from the DFB reactor system. Judging from the results in Table 5.6, if the bulk of entrained silica sand were to be excluded from the bio-char collected, the carbon content would increase to approximately 55 wt % on a dry basis, which would result in an HHV of approximately 29 MJ/kg.

Table 5.6: Properties and composition of bio-char co-product

	Bio-char
Proximate analysis	
Moisture	1.6 wt %
Total inorganics	54.4 wt % d.b.
Ash	12.5. wt % d.b.
HCl insolubles (i.e. silica)	41.9 wt % d.b.
Volatiles	12.2 wt % d.b.
Fixed carbon	32.0 wt % d.b.
Ultimate analysis	
Carbon	31.2 wt % d.b.
Hydrogen	1.2 wt % d.b.
Nitrogen	0.7 wt % d.b.
Sulphur	BDL [a]
Other [b]	67.0 wt % d.b.
Inorganics	54.4 wt % d.b.
Oxygen [b]	12.6 wt % d.b.
HHV	17.0 MJ/kg

[a] Below detection limit

[b] By difference

The high amount of volatiles (12.2 wt % d.b.) detected in the bio-char is also uncommon. Due to the low bio-char moisture content (1.6 wt %), most of the volatiles may actually be organic condensables reporting to the bio-char component. This could be the result of insufficient or ineffective bio-char and pyrolysis vapour separation in the bio-char cyclone, which could result in condensables entraining at the bottom of the bio-char cyclone. Furthermore, recalling that the pyrolysis vapour temperature was only 195 °C when it left the PFB reactor, condensation of some organic condensables is not entirely unlikely, seeing that the bio-char cyclone and connecting pipework are not insulated.

Despite the entrained silica sand in the collected bio-char, the bio-char co-product produced from the fast pyrolysis of *E. grandis* sawdust in the DFB reactor system finds widespread application. Due to the presence of biomass-derived inorganics (i.e. ash), which tend to be rich in important plant mineral nutrients, the bio-char can be utilised as a fertiliser in soil amendment and nutrient replacement applications to enhance soil quality (Kim et al., 2013). The bio-char is also an attractive solid fuel, which may be used to supplement or substitute other fuel sources in various applications. As demonstrated in this investigation, the bio-char may also be combusted in the DFB reactor system to supplement the energy demand in the CFB reactor. Furthermore, the high carbon content in the bio-char co-product indicates that it may be utilised as a carbon-sequestering agent, which removes carbon from the atmosphere, as detailed in Section 2.3.2.

5.4.3 Non-condensable Gases

Non-condensable gases (NCG) of low molecular weight are produced as a co-product from the fast pyrolysis of biomass. These NCG contain a mixture of combustible and incombustible gases. The NCG generated in the dual fluidised bed reactor system were characterised by GC-MS analysis to identify individual chemical components. The peaks on the chromatograph were identified by comparison of the mass spectra of each peak with authentic mass spectra of compounds in the National Institute of Standards and Technology (NIST – Gaithersburg, MD, US) library. A semi-quantitative analysis was conducted by comparing relative peak areas for the different components.

Carbon monoxide (CO), methane (CH_4), ethane (C_2H_6), ethylene (C_2H_4), acetylene (C_2H_2) and propene (C_3H_6) were the combustible gases identified and they constitute approximately 65.7 v/V % d.b. of the NCG. Incombustible components that were identified include carbon dioxide (CO_2) and water vapour (H_2O). The approximated NCG composition is presented in Table 5.6. The quality of the NCG was quantified by estimation of the high heating value – HHV (i.e. the calorific value). Correlations developed for the estimation of the calorific value of biomass-derived producer gas by Tasma & Panait (2012) were used for NCG HHV estimation. The NCG had an average HHV of 7.3 MJ/kg or 8.3 MJ/Nm^3, as presented in Table 5.7. The low calorific value of the NCG is due to the presence of a large amount of water vapour (± 34.7 v/V %) and CO_2 (± 34.3 v/V % d.b).

Varying proportions of CO_2 are generated during the thermal degradation and partial oxidation of woody biomass, which would inevitably report to the NCG. However, the amount of water vapour in the final NCG stream should be considerably lower. The bulk of water entering the PFB reactor via the sawdust feedstock, as well as the pyrolytic water generated during pyrolysis, should be condensed and collected in the bio-oil recovery system. However, it appeared through visual inspection of the operation of the bio-oil recovery system that poor liquid-vapour contact in the bio-oil quencher, as well as poor liquid-gas disengagement in the hydrocyclone and demister units, all contributed to vapours entraining from the liquid recovery system, as demonstrated in Figure 5.5.

Table 5.7: Properties and composition of NCG co-product

Component	
H_2O	34.7 v/V %
CO	52.7 v/V % d.b.
CO_2	34.3 v/V % d.b.
CH_4	5.3 v/V % d.b.
C_2H_2	1.8 v/V % d.b.
C_2H_4	3.7 v/V % d.b.
C_2H_6	0.7 v/V % d.b.
C_3H_6	1.4 v/V % d.b.
HHV	7.3 MJ/kg [a]

[a] Estimated from calorific value correlations by Tasma & Panait (2012)

Figure 5.5: Vapour entraining from liquid recovery system (LHS)

Furthermore, the cartridge filter installed for protection of the NCG blower is intended to remove only particulate matter (i.e. bio-char and/or silica sand fines) and viscous (i.e. sticky) organic condensables from the NCG before they pass through the blower. Alternative liquid-gas disengagement units, such as an electrostatic precipitator (ESP), have proved more efficient at recovering entrained condensables in similar investigations (Oasmaa et al., 2010; Joubert, 2013; Kim et al., 2013). Nonetheless, valuable NCG are produced as co-product from the fast pyrolysis of *E. grandis* sawdust in the DFB reactor system. The combustible NCG may be utilised as a viable source of energy to supplement or substitute other fuel sources in various applications. As demonstrated in this investigation, the NCG may also be combusted in the DFB reactor system to supplement the energy demand in the CFB reactor. Due to the absence of hydrogen (H_2) in the NCG, it is rather unlikely that the NCG would be refined for other applications, as mentioned in Section 2.3.3.

5.5 Summary of Pyrolysis Experimental Runs

As part of the hot commissioning and performance testing of the DFB reactor system, as detailed in Section 4.4, a total of five experimental runs were performed to provide an indication of the degree of repeatability in the operation of the apparatus. However, experimental run 1 was excluded from the evaluation since all the necessary data were not collected and recorded. Furthermore, as mentioned in Section 4.4.1, operation of the NCG blower speed in excess of 50 Hz was not sustainable due to the high pressure drop in the NCG recirculation loop. Experimental run 3 was recorded as the most sustainable and successful experimental run, due to the overall process stability during the particular run. Experimental run 3 was therefore used as the process baseline for quantification and elaboration of the overall DFB reactor system performance as detailed in Section 4.4, 5.2 and 5.3. Table 5.8 summarises the process parameters, and material and energy balance of the four recorded pyrolysis experimental runs.

It should be noted in Table 5.8 that all four recorded experimental runs were conducted at a PFB reactor temperature of 500 °C and CFB temperature of 670–700 °C. It again highlights the ability of the apparatus to easily achieve and sustain the pyrolysis temperature by means of the novel solids (heat carrier) transport system detailed in Section 3.2 and 4.4. As discussed in Section 4.4.1, and demonstrated in Table 5.8, as the NCG flow rate was increased from 110 to 140 ℓ/min, the NCG feed temperature increased from approximately 50 to 75 °C as the pyrolysis vapour outlet temperature increased from approximately 180 to 225 °C. Due to the vapour/NCG absorbing more process heat at the higher NCG flow rate, a higher hot solids transfer rate (42 to 75 kg/h) was required to maintain the PFB temperature at the desired setpoint.

Since the biomass sawdust feed rate to the PFB reactor was kept constant at 2.0 kg/h, the heat of pyrolysis reaction (1 000 W) was subsequently consistent throughout all the experimental runs. However, since a higher hot solids transfer rate was required to maintain the PFB reactor temperature, at the higher NCG flow rate, the subsequent energy input to the PFB reactor (from the hot solids) was substantially increased as presented in Table 5.8. This inevitably resulted in a substantial increase in PFB reactor heat loss (2 076 to 4 661 W), as discussed in Section 5.3.2 and 5.3.3, as the pyrolysis vapour temperature increased from approximately 180 to 225 °C. Interestingly enough, as demonstrated in Table 5.8, the liquid bio-oil yield decreased from 41.6 to 31.0 wt % d.b. as the pyrolysis vapour temperature increased from 180 to 225 °C and VRT decreased from approximately 4.2 to 3.2 s. Since this is in contradiction to findings from similar pyrolysis investigations (Boateng, 2011; Bridgwater, 2012), it is anticipated that the decreased bio-oil yield resulted from the aggravation of the process shortfalls as discussed in Section 5.2, especially within the bio-oil recovery and collection system.

Table 5.8: Operating parameters, and material and energy balance of fast pyrolysis runs

Experimental Run	Run 2	Run 3	Run 4	Run 5
PFB temperature (°C)	500	500	500	500
PFB vapour temperature (°C)	180	195	210	225
NCG temperature (°C)	50	60	70	75
NCG flow [a,b] (ℓ/min)	110	120	130	140
SGV [a] (m/s)	0.42	0.45	0.5	0.55
VRT (s)	4.2	4.0	3.5	3.2
Sawdust feed rate (kg/h)	2.0	2.0	2.0	2.0
Silica transfer rate (kg/h)	42	50	57	75
CFB temperature (°C)	670–700 °C	670–700 °C	670–700 °C	670–700 °C
LPG flow (ℓ/min)	15	15	15	15
NCG purge flow (ℓ/min)	4	4	4	4
Bio-oil yield [c] (wt % d.b.)	41.6	36.3	32.2	31.0
NCG yield [d] (wt % d.b.)	14.4	14.0	13.6	13.4
Bio-char yield [e] (wt % d.b.)	43.9	49.7	54.2	55.0
Energy in [f] (W)	3 390	4 039	4 613	6 035
Heat of reaction (W)	1 000	1 000	1 000	1 000
Energy out [g] (W)	314	344	364	375
Heat losses (W)	2 076	2 696	3 249	4 661

[a] At process conditions (i.e. temperature and pressure)

[b] Total NCG flow rate, including NCG purge

[c] Total liquid yield

[d] From NCG purge flow rate

[e] By difference

[f] Energy in = biomass + NCG + sand (heat carrier)

[g] Energy out = pyrolysis vapour + NCG + bio-char

6 CONCLUSIONS AND RECOMMENDATIONS

E. grandis sawdust was successfully converted to bio-oil, bio-char and non-condensable gases (NCG), through the process of fast pyrolysis, in the scalable dual fluidised bed (DFB) reactor system designed and constructed at the University of Pretoria. Fast pyrolysis was conducted at a pyrolysis fluidised bed (PFB) reactor temperature of 500 °C, a pyrolysis vapour residence time (VRT) of 4 s and a continuous *E. grandis* sawdust feed rate of 2.0 kg/h. The yield of fast pyrolysis products, on a dry feedstock basis, was determined as 36.3 wt %, 14.0 wt % and 49.7 wt % for bio-oil, NCG and bio-char respectively. High-value process heat in the form of hot flue gas (450–500 °C) was produced in the combustion fluidised bed (CFB) reactor as co-product from the DFB reactor system. Therefore, it can be concluded that the conversion of lignocellulosic biomass, through the process of fast pyrolysis, is technically feasible in the scalable DFB reactor system.

This chapter provides an overview of the most important results and findings obtained during this investigation. Also, various process inefficiencies and shortcomings of the DFB reactor system are highlighted in this section and recommendations are made for alleviating these inadequacies.

6.1 Biomass Feedstock Handling

E. grandis woodchips from Sappi Southern Africa's Ngodwana mill were utilised in this investigation. However, since the particle size and moisture content (7.6–16.6 wt % d.b.) of the biomass raw material, as received was extremely variable, extensive pre-treatment was necessary. Before conversion in the DFB reactor system, the *E. grandis* biomass raw material was air/sun dried, pulverised and screened in order to obtain a homogeneous biomass feedstock suitable for the fast pyrolysis process. Air/sun drying the biomass woodchips for 6 h ensured a homogeneous feedstock moisture content before further pre-treatment. Subsequent grinding and screening of the biomass feedstock enabled the isolation and collection of a biomass sawdust feedstock compatible with the fast pyrolysis process, as detailed in Section 2.2.3. *E. grandis* sawdust with a particle size of 0.5–1.0 mm and a moisture content of 5.4 wt % was utilised as fast pyrolysis feedstock in the DFB reactor system. Successful commissioning of the biomass feed system, as detailed in Sections 3.4 and 4.2.3, ensured satisfactory operation of the biomass hopper, agitator, screw conveyor and pneumatic feeder.

6.2 Process Commissioning

Successful commissioning of the solids transport system, electrical heating elements, liquefied petroleum gas (LPG) combustion system, air system and flue gas extraction system, as detailed in Section 4.3, enabled satisfactory operation of the CFB reactor. The electrical heating elements ensured a safe and convenient CFB reactor start-up before the introduction of LPG. Combustion of

LPG in the CFB reactor enabled sufficient heating of the solid heat carrier (i.e. silica sand). The hot solids transfer system, detailed in Section 3.3, performed effectively and ensured continuous transfer of hot silica sand between the two bubbling fluidised bed reactors, while maintaining the CFB reactor temperature at ± 700 °C. Due to excessive heat loss from the CFB reactor, the maximum sustainable flue gas temperature was only ± 450–500 °C. As a result of the negative influence of excessive heat loss on the overall system performance, as detailed in Section 5.3.3, it is recommended that the insulation installed on the CFB reactor, as detailed in Section 3.3, be enhanced to reduce heat loss. Nonetheless, the hot flue gases generated in the CFB reactor are still a viable source of heat that could be utilised in various applications, including drying/pre-heating the biomass feedstock, and/or pre-heating of combustion air or recycled NCG. It is recommended that these heat integration synergies be evaluated and implemented where practical, since the energy efficiency of the DFB reactor system would be improved as a result.

The hot commissioning of the NCG blower and recirculation system, as detailed in Section 4.4, ensured satisfactory operation of the PFB reactor. Furthermore, successful operation of the hot solids transfer system and the NCG recirculation system enabled operation of the PFB reactor in the bubbling fluidisation regime, while maintaining an oxygen-free environment, a PFB temperature of 500 °C and a pyrolysis VRT of 4 s. Successful control of the PFB temperature at 500 °C was made possible by manipulation of the sand screw conveyor in the hot solids transfer system, as discussed in Section 4.4.1. The excellent temperature control of the PFB reactor makes the DFB system a suitable reactor system for the fast pyrolysis of biomass on a commercial scale.

Although these process conditions were suitable for fast pyrolysis, a lower VRT would have been preferred, as suggested by Bridgwater (2012). However, due to the high pressure drop in the NCG recirculation loop, a higher volumetric NCG flow rate and subsequent lower VRT could not be sustained. It is therefore recommended to reduce the pressure drop in the NCG recirculation loop, by redesigning the bio-oil recovery and collection system, to establish the influence of a lower VRT (i.e. < 3 s) on the PFB reactor performance. According to Bridgwater (2012), the liquid bio-oil yield would be increased at a lower VRT due to the suppression of secondary pyrolysis vapour reactions.

At the abovementioned PFB reactor process conditions, the maximum sustainable pyrolysis vapour temperature was only ± 195 °C due to excessive heat loss from the PFB reactor. As a result of the negative influence of excessive heat loss on the overall system performance, as detailed in Section 5.3.3, it is recommended that the insulation installed on the PFB reactor, as detailed in Section 3.5, be enhanced considerably to minimise heat loss. The bio-char cyclone allowed easy separation and collection of bio-char as co-product from the DFB reactor system. Separation of the bio-char co-product enables its utilisation in various attractive applications, as detailed in Section 2.3.2.

Successful commissioning of the bio-oil recovery and collection system, as detailed in Sections 3.6 and 4.5, allowed the quenching, cooling and separation of the pyrolysis vapour condensables. Furthermore, the bio-oil hydrocyclone and demister enabled the disengagement of bio-oil and NCG, while the NCG cartridge filter facilitated NCG clean-up. However, through visual inspection of the cartridge filter element, it was found that some condensables were entrained from the bio-oil recovery and collection system, by means of the NCG recirculation and purge, which would ultimately reduce the liquid bio-oil yield. It is therefore apparent that optimisation of the bio-oil hydrocyclone and demister, for enhanced liquid-gas disengagement, should be investigated since reduced vapour entrainment would result in a higher liquid bio-oil yield. Furthermore, to increase the liquid bio-oil yield, it is recommended that an alternative to the NCG cartridge filter be investigated and installed for NCG clean-up and recovery of entrained condensables. Installation of an electrostatic precipitator (ESP) has been demonstrated in similar investigations to be more viable for the recovery of entrained condensables (Oasmaa et al., 2010; Joubert, 2013; Kim et al., 2013). Nevertheless, the NCG purge permitted control of the PFB freeboard pressure, as well as enabling either collection or combustion of the NCG.

The use of ethylene glycol (EG) as direct cooling medium in the bio-oil recovery system enabled pyrolysis vapour quenching and cooling during process start-up conditions. However, the addition of ethylene glycol to the liquid bio-oil product made physical characterisation in this investigation impractical. Nevertheless, in practice, the ethylene glycol would be replaced with pyrolysis-derived bio-oil to quench and cool the hot pyrolysis vapour in the bio-oil recovery and collection system. Successful commissioning of the bio-oil circulation pump, as detailed in Section 4.5, enabled a sufficient supply of cold EG/bio-oil mixture (at ± 24 °C) to the bio-oil quencher. At the low biomass throughput (± 2 kg/h), the cold EG/bio-oil circulation rate was so much higher than the rate of pyrolysis vapour entering the bio-oil quencher that the cold bio-oil actually functioned as a heat sink, absorbing all the process heat from the pyrolysis vapour without markedly increasing its temperature (which was ± 24–25 °C).

However, since none of the unit operations in the bio-oil collection and recovery system was insulated, excessive heat loss may have enhanced pyrolysis vapour quenching and cooling. Furthermore, since the bulk of the sensible and latent heat in the pyrolysis vapour was dissipated in the bio-oil quencher, at the low bio-oil production rate, the cooling duty on the countercurrent bio-oil cooler was insignificant. Although construction of the bio-oil quencher, demister and container from borosilicate sight-glass enables visual monitoring of their operation, it is recommended that these unit operations be insulated to minimise process heat loss. Reducing the heat loss from the bio-oil recovery and collection system would allow recovery of process heat in the brass-plate heat exchanger (bio-oil cooler), thereby increasing the overall energy efficiency of the system.

The scalable DFB reactor system allowed online sampling of the fast pyrolysis products in order to analyse the physical and chemical properties of each individual fast pyrolysis product. The DFB reactor system also allowed separation and collection of the fast pyrolysis products so that a total material and energy balance over the PFB reactor could be conducted.

6.3 Process Operation and Performance

Fast pyrolysis of *E. grandis* sawdust was conducted in a scalable DFB reactor system at a pyrolysis temperature of 500 °C, a VRT of 4 s and a biomass feed rate of 2.0 kg/h. The yield of pyrolysis products, on a dry feedstock basis, was determined as 36.3 wt %, 14.0 wt % and 49.7 wt % for bio-oil, NCG and bio-char respectively. It is understood that the low liquid bio-oil yield, and subsequent higher yield of bio-char, resulted from a number of process inefficiencies, including a low pyrolysis vapour temperature and a high VRT. These conditions have been reported to result in secondary tar reactions which favour bio-char formation, at the expense of a lower bio-oil yield (Boateng, 2011; Bridgwater, 2012).

Furthermore, evidence of pyrolysis vapour entrainment with NCG from the bio-oil recovery and collection system, followed by subsequent purging to the CFB, may have contributed to the lower bio-oil yield. The presence of residual bio-char in the final bio-oil product, together with the higher VRT, provided evidence to suggest that pyrolysis vapour cracking to NCG may also have contributed to the reduced liquid bio-oil yield.

A total material and energy balance over the PFB reactor was conducted to quantify its performance. The biomass feed rate and pyrolysis product yields were used as the basis for the material and energy balance. At the biomass feed rate of 2 000 g/h, the production rate of pyrolysis products was estimated at 687.8 g/h, 265.2 g/h and 940.0 g/h for bio-oil, NCG and bio-char respectively. Although the bio-char generation rate was estimated at 940.0 g/h, only 13.0 g/h was collected from the bio-char cyclone, with the balance understood to have been transferred to the CFB with the silica sand. Evidence of excessive bio-char combustion in the CFB reactor includes visual detection through the borosilicate sight-glass peephole at the top of the CFB, as well as the collection of fly ash from the ash cyclone.

The low superficial gas velocity (SGV) in the PFB reactor is understood to have subdued bio-char entrainment, resulting in the low bio-char collection rate from the bio-char cyclone. The PFB was operated at a lower SGV because the volumetric flow rate of NCG was limited by the high pressure drop in the NCG recirculation loop. It is therefore recommended to reduce the pressure drop in the NCG recirculation loop, by redesigning the bio-oil recovery and collection system, in order to increase the SGV in the PFB reactor, and subsequently the bio-char entrainment rate. The NCG recycle rate used for the fluidisation of the PFB reactor was determined as 7 689.7 g/h.

The results from the total material balance were used as the basis for the energy balance. The total energy balance considered energy inputs from the sawdust feedstock, silica sand and NCG, as well as the heat of reaction, heat losses and energy outputs from the pyrolysis products. The total energy input from the biomass feedstock and recycled NCG was determined as 150 W, while the total amount of energy supplied to the PFB by means of the hot silica sand was determined as 3 889 W. As mentioned in Section 6.2, it is recommended that the use of hot flue gases (i.e. high-value heat) generated in the CFB reactor to dry or pre-heat the biomass feedstock and/or recycled NCG be investigated to increase the energy efficiency of the overall process. The total energy requirement for the endothermic pyrolysis of the sawdust feedstock, at the feed rate of 2 000 g/h, was determined as 1 000 W.

The pyrolysis reactor freeboard temperature was found to be much lower than the fluidised bed temperature (± 195 °C vs. ± 500 °C) as a result of severe heat loss. Therefore, the energy output from the pyrolysis products was determined as only 344 W. The overall heat loss from the PFB reactor was estimated at a very high 2 696 W, which implies that approximately 69% of the total energy supplied to this reactor by means of the hot silica sand was dissipated to the surrounding atmosphere. This severe heat loss was due to insufficient and ineffective insulation of both the fluidised bed and freeboard sections of the PFB reactor. As detailed in Section 4.3.2, the CFB reactor also suffered severe heat loss as a result of inadequate insulation. Furthermore, it was demonstrated that the performance of the DFB reactor system was severely compromised as a result of the high heat loss from the CFB and PFB reactor. More specifically, with the use of the total energy balance, the severe heat loss was demonstrated to have huge consequences for the throughput and overall performance of the PFB reactor as less energy is available to drive the endothermic pyrolysis reaction.

It is believed that sufficient insulation of the two bubbling fluidised bed reactors, to inhibit heat loss to the surrounding atmosphere, could increase the biomass throughput capacity by as much as five to ten times the recorded throughput of 2 000 g/h, as illustrated in Section 5.3.3. The negative impact on the biomass throughput and overall performance of the PFB reactor as a result of excessive heat loss is evident from these conclusions. Installation of adequate insulating material on the PFB reactor is therefore recommended to enhance the energy efficiency, biomass throughput and subsequently the overall performance of the PFB reactor.

6.4 Fast Pyrolysis Product Characterisation

The crude liquid bio-oil product produced from the fast pyrolysis of *E. grandis* in the DFB reactor system was collected from the bio-oil recovery and collection system. The addition of ethylene glycol (EG) to the bio-oil recovery system, as cooling medium and solvent during process start-up conditions, made physical characterisation of the bio-oil product in this investigation impractical.

Chemical characterisation was conducted by gas chromatography-mass spectrometry (GC-MS) analysis to identify individual bio-oil components. However, the EG appeared broadly at retention times between 4 to 8 min and unfortunately overlapped with several other signals, which made identification of numerous other components inconclusive. Due to the interference of EG with the characterisation of the liquid bio-oil, the use of an alternative bio-oil solvent is recommended. According to Bridgwater (2012), the addition of methanol as bio-oil solvent has been demonstrated to be beneficial to bio-oil stability. Nonetheless, the most prominent peaks on the chromatograph were identified by comparison of the mass spectra of each peak with authentic mass spectra of compounds in the US National Institute of Standards and Technology (NIST) library.

The crude liquid bio-oil contained highly oxygenated compounds, including organic acids, water, alcohols, esters, sugars, aldehydes, ketones, furans, pyrans and phenolics, which are consistent with the degradation of lignocellulosic biomass (Azeez et al., 2010; DeSisto et al., 2010; Kim et al., 2013). According to Bridgwater (2012), the high bio-oil oxygen content influences bio-oil fuel quality unfavourably and renders the crude bio-oil incompatible with conventional transportation-grade fuels. Despite this shortcoming, the bio-oil produced from the fast pyrolysis of *E. grandis* sawdust in the DFB reactor system may still be utilised in its crude form for heat generation when co-fired with conventional fossil fuels, including heavy furnace oil, etc. (Crocker, 2010: 174–177).

However, the scalable DFB reactor system allows for integrated catalytic fast pyrolysis, which would enable catalytic cracking of the biomass feedstock and the subsequent pyrolysis vapours to selectively produce deoxygenated bio-oil compounds of higher quality and value. It is understood that a deoxygenated bio-oil product would be compatible with fossil fuel refinery streams and could be refined to transportation-grade fuels in a conventional petroleum refinery (Bridgwater, 2012). The scalable DFB reactor system would allow in situ catalytic fast pyrolysis by replacement of the silica sand fluidised bed material with a viable solid catalyst (e.g. ZSM-5) as heat carrier. Furthermore, the system would also permit catalyst regeneration in the CFB reactor by combustion of the coke formed on the catalyst structure during catalysis. It is therefore recommended that integrated catalytic fast pyrolysis of lignocellulosic biomass in the scalable DFB reactor system be investigated to produce a deoxygenated bio-oil product, compatible with conventional transportation fuel refining.

The DFB reactor system allowed easy separation of bio-char from the pyrolysis vapour by means of the bio-char cyclone. The bio-char had a high heating value (HHV) of only 17.0 MJ/kg because of an unexpectedly high inorganic content of 54.4 wt % d.b. However, approximately 77.0 wt % of the inorganics were identified as entrained silica sand fines from the PFB reactor. It was concluded that the starting silica sand fluidised bed material, utilised as received from the supplier, contained a large amount of fines, which inevitably reported to the solid bio-char fraction. Because the entrainment of silica sand fines was more prominent during start-up conditions and short periods of operation, it is believed that prolonged periods of operation would allow thorough particle classification of the

fluidised bed material, resulting in bio-char of higher purity or quality. In addition, for any further experimental investigations on the DFB reactor system, it is suggested that the fluidised bed material be screened to remove most of the undersized material.

Notwithstanding the entrained silica fines, the bio-char carbon content was determined as approximately 55 wt % d.b., which would result in an HHV of approximately 29 MJ/kg. The high calorific value of biomass pyrolysis-derived bio-char makes it an attractive solid fuel source, suitable for supplementing or substituting other fuel sources in various applications. It was demonstrated in this investigation that the solid bio-char residue could be combusted in the CFB reactor to supplement the energy requirement in the DFB reactor system. Due to the high proportion of biomass-derived ash in the bio-char product (12.5 wt % d.b.), which tends to be rich in important plant mineral nutrients according to Kim et al. (2013), the bio-char can be utilised as a fertiliser in soil amendment and nutrient replacement applications, particularly in the forestry sector.

NCG, containing a mixture of combustible and incombustible compounds, was produced as co-product from the fast pyrolysis of *E. grandis* sawdust in the DFB reactor system. The combustible components, identified by GC-MS analysis, included carbon monoxide (CO), methane (CH_4), ethane (C_2H_6), ethylene (C_2H_4), acetylene (C_2H_2) and propene (C_3H_6). The NCG HHV was estimated at 7.3 MJ/kg or 8.3 MJ/Nm^3, based on calorific value correlations developed by Tasma & Panait (2012) for biomass-derived producer gas. The low calorific value of the NCG was due to the presence of a large amount of water vapour (± 34.7 % v/V) and CO_2 (± 34.3 % v/V d.b). It is concluded that the large proportion of water vapour in the NCG resulted from the entrainment of pyrolysis vapour, especially water vapour, from the bio-oil recovery and collection system.

As mentioned in Section 6.2, an alternative to the NCG cartridge filter is recommended for NCG clean-up and the recovery of entrained condensables. It is believed that a lower NCG water vapour content would result in a higher NCG calorific value, and therefore higher-quality NCG. Replacement of the NCG cartridge filter with an ESP has been demonstrated to be more efficient at recovering entrained condensables in similar investigations (Oasmaa et al., 2010; Joubert, 2013; Kim et al., 2013). Nonetheless, the NCG may be utilised as a viable source of energy to supplement or substitute other fuel sources in various applications, as detailed in Section 2.3.3. As demonstrated in this investigation, the NCG may be combusted in the DFB reactor system to supplement the energy demand in the CFB reactor.

6.5 Recommendations for Future Work

This dissertation provides an overview of the commissioning and operation of the scalable DFB reactor system for the fast pyrolysis of lignocellulosic biomass. A summary of the production and characterisation of the fast pyrolysis products, as well as the quantification of the pyrolysis reactor

performance, is also presented. Although it has been demonstrated that the conversion of lignocellulosic biomass through the process of fast pyrolysis is technically feasible in the scalable DFB reactor system, several process inefficiencies and limitations were identified during its commissioning and operation, which compromised the overall performance. In order to mitigate or eliminate these inefficiencies and limitations, the following future work is recommended:

- Installation of adequate insulation material on a number of unit operations in the DFB reactor system, including the PFB and CFB reactors, bio-oil container, quencher and demister. As discussed in Sections 6.2 and 6.3, excessive heat loss from these unit operations hindered the capacity and overall performance severely.
- Redesigning the bio-oil recovery and collection system to reduce the pressure drop in the NCG recirculation loop, thereby increasing the SGV of the PFB reactor and subsequently reducing the VRT to < 3 s. According to Bridgwater (2012), the liquid bio-oil yield would be increased at a lower VRT, due to the suppression of secondary pyrolysis vapour reactions. Furthermore, a higher SGV would also increase the bio-char entrainment rate, thereby increasing the bio-char collection rate.
- Investigation of the performance of the scalable DFB reactor system at a higher biomass sawdust throughput. As discussed in Section 6.3, if the heat loss can be mitigated or eliminated, the system is capable of a biomass throughput approximately five to ten times the rate operated in this investigation.
- Investigation and implementation of heat integration synergies, especially the use of hot flue gases generated in the CFB reactor, to dry and/or pre-heat the biomass feedstock, pre-heat the combustion air or pre-heat the recycled NCG used to fluidise the PFB reactor. It is believed that these synergies would improve the overall energy efficiency of the DFB reactor system.
- Installation and commissioning of an ESP for recovery of entrained pyrolysis condensables from the bio-oil recovery and collection system, and subsequent clean-up of the NCG. It is believed that enhanced recovery of pyrolysis condensables would not only increase the liquid bio-oil yield, but also improve the quality of the NCG.
- Utilisation of an alternative solvent for bio-oil recovery and collection during process operation. As discussed in Section 6.4, the ethylene glycol utilised in this investigation interfered with the characterisation of the liquid bio-oil. According to Bridgwater (2012), the addition of methanol as bio-oil solvent has been demonstrated to be beneficial to bio-oil stability.
- Investigation of integrated catalytic fast pyrolysis in the scalable DFB reactor system, by replacing the silica sand fluidised bed material with a viable solid catalyst (e.g. ZSM-5) as heat carrier. According to Bridgwater (2012), integrated catalytic fast pyrolysis has the potential to render a bio-oil product compatible with a conventional refinery stream, which would enable conversion into transportation-grade fuels.
- Although this investigation was limited to the fast pyrolysis of *E. grandis* sawdust, pyrolysis has been demonstrated to be quite robust due to its capability of processing various feedstocks. The pyrolysis of alternative biomass resources available within South Africa,

including forestry slash, sawmill residue, bark, municipal waste, sugarcane bagasse, etc., should be investigated in the DFB reactor system.

- As mentioned by Swart (2012), the main purpose of the modelling, design, construction, commissioning and performance testing of the scalable DFB reactor system is to develop a commercial-scale system for the fast pyrolysis of biomass. A commercial-scale system should be designed to evaluate its technical feasibility and economic viability.

It is recommended that a thorough economic evaluation and sensitivity analysis be conducted to determine the financial viability of a commercial-scale DFB fast pyrolysis system. The economic evaluation should consider the feasibility of a stationary, pulp and paper mill integrated system, as well as a modular, decentralised system which would typically be located in forestry plantations near the biomass feedstock. Although both of these options have their advantages and disadvantages, the more technically feasible and economically viable option would depend on numerous factors specific to each individual scenario. According to Palma, Richardson, Robertson et al. (2011), a stationary biomass conversion system, i.e. based in a forestry plantation or pulp and paper mill, is more likely to be economically viable due to the on-site availability of biomass raw material, which could reduce or eliminate the substantial cost of transporting biomass. However, according to Miller (2012), significantly more value could be realised from a pulp and paper mill integrated system due to the availability of existing infrastructure, utilities and potential integration synergies. Potential integration synergies include combined heat and power generation, as well as the on-site utilisation of fast pyrolysis products, including boiler feeds, lime kiln firing, etc. Furthermore, depending on commercial markets, the viability of upgrading crude fast pyrolysis bio-oil to drop-in liquid transportation fuels, as opposed to application in its crude form, should also be considered.

While fast pyrolysis is aimed at maximising the yield of liquid bio-oil as the main product, the co-products from fast pyrolysis, i.e. bio-char and NCG, should also be considered in such an evaluation as they have the potential to influence the overall technical feasibility and economic viability of a commercial-scale system dramatically (Palma et al., 2011; Miller et al., 2012; Wright et al., 2010). Although bio-char contains the bulk of the feedstock inorganics, making it suitable for soil amendment applications, it also has the potential to be utilised for its energy content. Assuming the biomass feedstock does not originate from forestry slash, the bio-char could be burnt in the CFB reactor in order to utilise its heat of combustion. Also, since the bio-char obtained from the scalable DFB reactor system contained a lot of inorganics, especially fluidised bed material, it is recommended that the use of a fast or circulating pyrolysis fluidised bed be investigated in the commercial-scale design. In that way, there would be no need to separate the bio-char co-product from the system, and all the bio-char could be transported back to the CFB reactor with the entrained fluidised bed material.

It has been demonstrated that more than enough bio-char is produced during fast pyrolysis to sustain the energy requirement in the PFB reactor, which would enable self-sufficient operation and eliminate the need for external fuel sources in the DFB reactor system (Wright et al., 2010). Furthermore, according to Wright et al. (2010), the surplus bio-char could be combusted in the CFB reactor to generate steam and electricity. Also, due to the lack of hydrogen (H_2) in the combustible NCG, it is recommended that the NCG be utilised for their energy content by means of combustion in the CFB reactor. According to Göransson, Söderlind, He et al. (2011), in order to utilise producer gas for synthetic fuels, such as Fischer-Tropsch fuels, an H_2/CO ratio of between 0.6 and 2.0 is necessary, which has not been obtained on the scalable DFB reactor system.

REFERENCES

Azeez, AM, Meier, D, Odermatt, J and Willner, T (2010) Fast pyrolysis of African and European lignocellulosic biomasses using Py-GC/MS and fluidized bed reactor. *Energy Fuels*, 24, 2078–2085.

Boateng, AA (2011) Pyrolysis oil – *Overview of characterization and utilization.* Report published on Sun Grant BioWeb. Available at: http://www.bioweb.sungrant.org/Technical/Biopower/Technologies/Pyrolysis/Pyrolysis+Oil/Pyrolysis+Oil.htm [accessed 29 June 2011].

Brent, S (2011) Introduction to pyrolysis and our students. Talk presented at the *Pyrolysis Research Feedback* session, 14 October 2011, Pretoria, South Africa.

Bridgwater, AV (2012) Review of fast pyrolysis of biomass and product upgrading. *Biomass and Bioenergy*, 38, 68–94.

Butler, E, Devlin, G, Meier, D and McDonnell, K (2011) A review of recent laboratory research and commercial developments in fast pyrolysis and upgrading. *Renewable and Sustainable Energy Reviews*, 15, 4171–4186.

Crocker, M (2010) *Thermochemical conversion of biomass to liquid fuels and chemicals*. The Royal Society of Chemistry, Cambridge, UK.

Danje, S (2011) *Fast pyrolysis of corn residues for energy production*. MSc dissertation, Department of Process Engineering, University of Stellenbosch, Stellenbosch, South Africa.

Demirbas, MF (2006) Current technologies for biomass conversion into chemicals and fuels. *Energy Sources, Part A: Recovery, Utilization, and Environmental Effects*, 28(13), 1181–1188.

DeSisto, WJ, Hill, II, N, Beis, SH, Mukkamala, S, Joseph, J, Baker, C, Ong, T, Stemmler, EA, Wheeler, MC, Frederick, BG and Van Heiningen, A (2010) Fast pyrolysis of pine sawdust in a fluidized-bed reactor. *Energy Fuels,* 24, 2642–2651.

Faaij, A (2006) Modern biomass conversion technologies. *Mitigation and Adaptation Strategies for Global Change*, 11 (2), 343–375.

Fengel, D and Wegener, G (2003) *Wood: Chemistry, Ultrastructure, Reactions*. Kessel Verlag, Remagen, Germany.

Göransson, K, Söderlind, U, He, J and Zhang, W (2011) Review of syngas production via biomass DFBGs. *Renewable and Sustainable Energy Review*, 15, 482–492.

Joubert, J (2013) *Fast pyrolysis of* Eucalyptus grandis. MSc dissertation, Department of Process Engineering, University of Stellenbosch, Stellenbosch, South Africa.

Kim, KH, Kim, T, Lee, S, Choi, D, Yeo, H, Choi, I and Choi, JW (2013) Comparison of physicochemical features of bio-oils and bio-chars produced from various woody biomasses by fast pyrolysis. *Renewable Energy*, 50, 188–195.

Lin, YC and Huber, GW (2009) The critical role of heterogeneous catalysis in lignocellulosic biomass conversion. *Energy & Environmental Science*, 2, 68–80.

Lu, Q, Li, WZ and Zhu, XF (2009) Overview of fuel properties of biomass fast pyrolysis oils. *Energy Conversion Management*, 50(5), 1376–1383.

Meincken, M (2011) Converting biomass to energy – A South African perspective. *Quest*, 7(4), 4–7.

Miller, B (2012) Forestry to fuels: Biodiesel via Fischer Tropsch. Paper presented at the *66^{t}h Appita Annual Conference and Exhibition*, April 2012, Melbourne, Australia.

Oasmaa, A, Solantausta, Y, Arpiainen, V, Kuoppala, E and Sipila, K (2010) Fast pyrolysis bio-oils from wood and agricultural residues. *Energy Fuels*, 24, 1380–1388.

Palma, M, Richardson, J, Robertson, B, Ribera, L, Outlaw, J and Munster, C (2011) Economic feasibility study of a mobile fast pyrolysis system for sustainable bio-crude oil production. *International Food and Agribusiness Management Review*, 14(3), 1–16.

Papadikis, K, Gu, S and Bridgwater, AV (2009) CFD modelling of the fast pyrolysis of biomass in fluidised bed reactors: Modelling the impact of biomass shrinkage. *Chemical Engineering Journal,* 149(1-3), 417–427.

Postma, U (2012) Pyrolysis as a new resource for energy. Paper presented at the *SAIChE Conference 2012*, 17– 9 September, 2012, Champagne Sports Resort, KwaZulu-Natal, South Africa.

Raveendran, K, Ganesh, A and Khilar, KC (1996) Pyrolysis characterisation of biomass and biomass components. *Fuel*, 75(8), 987–998.

Sadaka, S and Boateng, AA (2009) *Pyrolysis and bio-oil.* Report issued in furtherance of the Cooperative Extension Service, University of Arkansas publication – FSA1052. Available at: http://www.uaex.edu/Other_Areas/publications/PDF/FSA-1052.pdf

Shen, J, Wang, X, Garcia-Perez, M, Mourant, D, Rhodes, MJ and Li, C (2009) Effect of particle size on the fast pyrolysis of oil mallee woody biomass. *Fuel*, 88, 1810–1817.

Swart, SD (2012) *Design, modelling and construction of a scalable dual fluidised bed reactor for the pyrolysis of biomass.* MEng dissertation, Department of Chemical Engineering, University of Pretoria, Pretoria, South Africa.

TAPPI (Technological Association of the Pulp and Paper Industry) (1985a) *Test Method T211 om-85: Ash in wood and pulp: Combustion at 525 °C.* Atlanta, GA, US, TAPPI.

TAPPI (Technological Association of the Pulp and Paper Industry) (1985b) *Test Method T249 cm-85: Carbohydrate composition of extractive-free wood and wood pulp by gas-liquid chromatography.* Atlanta, GA, US, TAPPI.

TAPPI (Technological Association of the Pulp and Paper Industry) (1988a) *Test Method T222 om-88: Acid-insoluble lignin in wood and pulp.* Atlanta, GA, US, TAPPI.

TAPPI (Technological Association of the Pulp and Paper Industry) (1988b) *Test Method T264 om-88: Preparation of wood for chemical analysis.* Atlanta, GA, US, TAPPI.

TAPPI (Technological Association of the Pulp and Paper Industry) (1999) *Test Method T244 cm-99: Acid–insoluble ash in wood and pulp.* Atlanta, GA, US, TAPPI.

Tasma, D and Panait, T (2012) The quality of syngas produced by fluidised bed gasification using sunflower husks. *Annals of "Dunarea de Jos",* University of Galati, Fascicle V, Technologies in Machine Building, University of Galati, Romania.

Wright, MM, Daugaard, DE, Satrio, JA and Brown, RC (2010) Techno-economic analysis of biomass fast pyrolysis to transportation fuels. *Fuel*, 89, 2–10.

Zhang, L, Xu, CC and Champagne, P (2010) Overview of recent advances in thermo-chemical conversion of biomass. *Energy Conversion and Management*, 51(5), 969–982.

APPENDIX A PIPING AND INSTRUMENTATION DIAGRAM

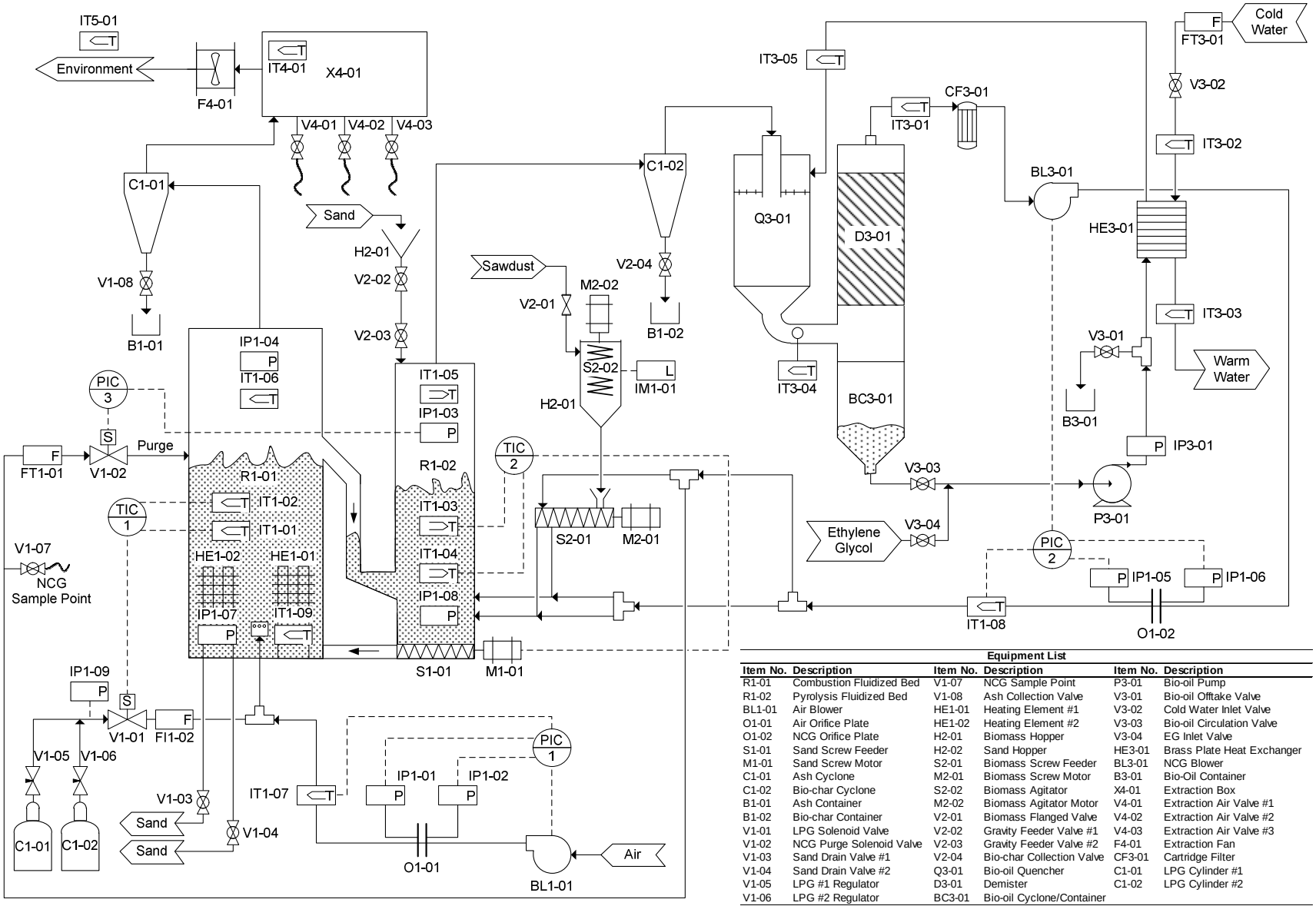

Equipment List

Item No.	Description	Item No.	Description	Item No.	Description
R1-01	Combustion Fluidized Bed	V1-07	NCG Sample Point	P3-01	Bio-oil Pump
R1-02	Pyrolysis Fluidized Bed	V1-08	Ash Collection Valve	V3-01	Bio-oil Offtake Valve
BL1-01	Air Blower	HE1-01	Heating Element #1	V3-02	Cold Water Inlet Valve
O1-01	Air Orifice Plate	HE1-02	Heating Element #2	V3-03	Bio-oil Circulation Valve
O1-02	NCG Orifice Plate	H2-01	Biomass Hopper	V3-04	EG Inlet Valve
S1-01	Sand Screw Feeder	H2-02	Sand Hopper	HE3-01	Brass Plate Heat Exchanger
M1-01	Sand Screw Motor	S2-01	Biomass Screw Feeder	BL3-01	NCG Blower
C1-01	Ash Cyclone	M2-01	Biomass Screw Motor	B3-01	Bio-Oil Container
C1-02	Bio-char Cyclone	S2-02	Biomass Agitator	X4-01	Extraction Box
B1-01	Ash Container	M2-02	Biomass Agitator Motor	V4-01	Extraction Air Valve #1
B1-02	Bio-char Container	V2-01	Biomass Flanged Valve	V4-02	Extraction Air Valve #2
V1-01	LPG Solenoid Valve	V2-02	Gravity Feeder Valve #1	V4-03	Extraction Air Valve #3
V1-02	NCG Purge Solenoid Valve	V2-03	Gravity Feeder Valve #2	F4-01	Extraction Fan
V1-03	Sand Drain Valve #1	V2-04	Bio-char Collection Valve	CF3-01	Cartridge Filter
V1-04	Sand Drain Valve #2	Q3-01	Bio-oil Quencher	C1-01	LPG Cylinder #1
V1-05	LPG #1 Regulator	D3-01	Demister	C1-02	LPG Cylinder #2
V1-06	LPG #2 Regulator	BC3-01	Bio-oil Cyclone/Container		

APPENDIX B DISTRIBUTED CONTROL SYSTEM